RCA

Tunnel Diodes

**for
Switching and
Microwave Applications**

TECHNICAL MANUAL TD-30

CONTENTS

RCA Tunnel Diode Manual

WHEN the phenomenon of tunneling in a p-n junction semiconductor diode was first reported, RCA scientists immediately recognized the importance of this effect for potential use in high-speed semiconductor devices. Since then, great strides have been made both in the theoretical understanding of the tunnel effect in semiconductors and in its utilization in circuit elements. Today, tunnel diodes are finding increasing uses in high-speed switching circuits for computers, in microwave equipment, and in electronic instrumentation.

THIS manual has been prepared to assist design engineers in the practical use of tunnel diodes. It includes basic theory, construction, and other general information describing the tunnel diode. The switching capability of the tunnel diode is explained in detail, and several representative circuits are given. Design considerations for the use of the tunnel diode as a microwave amplifier, converter, and oscillator device are explained in detail. High-current applications and several unusual tunnel-diode circuits are also included, as well as practical circuits for the measurement of important tunnel-diode parameters. The manual also includes a data section giving ratings and characteristics for RCA tunnel diodes.

RCA SEMICONDUCTOR AND MATERIALS DIVISION

SOMERVILLE   NEW JERSEY
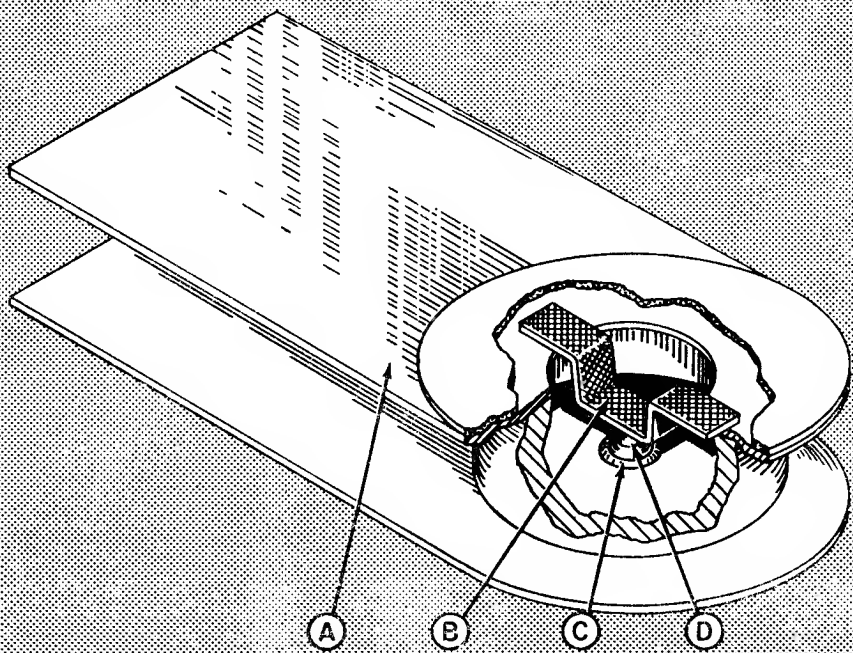
TYPICAL
RCA TUNNEL
DIODE

A. Gold-plated five-mil Kovar leads for ruggedness and thermal dissipation.

B. Low-inductance screen connector minimizes pressure sensitivity and improves ruggedness.

C. Rugged junction structure for extra mechanical reliability.

D. Expitaxial area for low saturation resistance, high speed and low capacitance.

- switching times to 75 picoseconds
- peak currents from 1 milliampere to 220 amperes
- broad application capability
- gigacycle switching speeds
- over 40 germanium and gallium arsenide types available in production quantities

ACTUAL SIZE
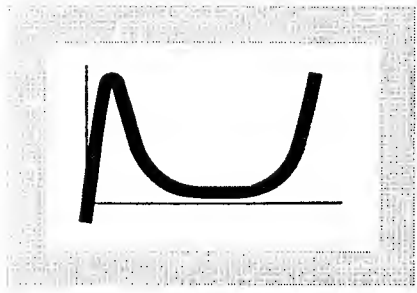
THEORY

THE tunnel diode is one of the most significant electron devices to emerge from the research laboratory since the transistor. Essentially smaller and faster than either the transistor or the electron tube, it offers design engineers a host of outstanding features. The high switching speed of tunnel diodes, coupled with their simplicity and stability, makes them particularly suitable for high-speed computer applications. They can also operate effectively as amplifiers, oscillators, and converters even at microwave frequencies. In addition, tunnel diodes have extremely low power consumption and are relatively unaffected by radiation, surface effects, or temperature.

The two-terminal nature of the tunnel diode is an important consideration in circuit design. On the one hand, this feature permits the design of circuits which are extremely simple, and thus provides significant savings in size and weight as well as substantial improvements in reliability. On the other hand, the lack of inherent isolation between input and output can be a serious design problem in some applications. Generally, at frequencies below the microwave region transistors are a more practical and economical choice than tunnel diodes. At microwave frequencies, however, tunnel diodes have several important advantages over transistors, and are highly competitive with other high-frequency devices such as microwave tubes, parametric diodes, and masers.

GENERAL DESCRIPTION

A **tunnel diode** is a small two-terminal device containing a single junction formed by heavily doped semiconductor materials. It differs from other p-n junction diodes primarily

3

because the doping levels are from a hundred to several thousand times as high. For example, the doping level in conventional microwave detector diodes is in the order of 10^{16} to 10^{17} atoms per cubic centimeter, whereas the doping level in tunnel diodes is in the order of 10^{19} to 10^{20} atoms per cubic centimeter. The high impurity concentrations in both the n-type and p-type materials of tunnel diodes result in an extremely thin depletion region at the junction (approximately 0.000001 centimeter). The tunneling effect which occurs at this junction produces the unusual current-voltage relationship and high frequency capability of the tunnel diode.

Fig. 1 compares the current-voltage characteristic of a tunnel diode with that of a conventional rectifier diode. In
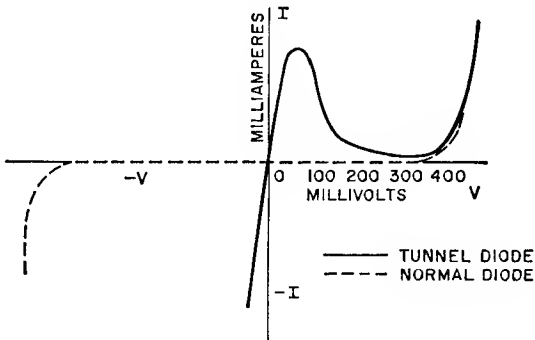

Fig. 1.   Current-voltage characteristics for tunnel diode and conventional rectifier diode.

the rectifier diode, forward current does not begin to flow freely until a forward-bias voltage in the order of half a volt to a volt (depending on the semiconductor material) is applied. For conventional diodes, this forward voltage is sometimes referred to as the "offset" voltage. In the reverse-bias direction, the conventional diode has high resistance to current flow until the "breakdown" region is reached. The tunnel diode, on the other hand, is much more conductive near zero bias; appreciable current flows when small bias is applied in either the forward or reverse direction. Because the active region of tunnel diodes is at a much lower voltage than conventional devices, tunnel diodes are extremely low power devices.

As forward bias on the tunnel diode is increased, the current reaches a sharp maximum (peak), then drops to a deep minimum (valley), and finally increases exponentially with voltage as in the rectifier diode. The drop in current with increasing positive bias results in the negative-resistance characteristic of the tunnel diode. This property enables the

tunnel diode to convert dc power-supply energy into an ac circuit energy, and thus permits its use as an amplifier or oscillator.

The differences in operating characteristics of conventional diodes and tunnel diodes can only be clearly explained in terms of the energy-band concept in semiconductors. The following sections describe qualitatively the theory of energy bands in semiconductors, conventional n-p junctions, and tunnel n-p junctions.

ENERGY BANDS IN SEMICONDUCTORS

According to atomic theory, a single isolated atom consists of a positively charged nucleus surrounded by one or more electrons. These electrons can have only certain discrete energies. The number of electrons and the energy levels they occupy depend on the particular element, e.g., germanium has thirty-two electrons occupying four specific levels. The first three levels contain, respectively, two, eight, and eighteen electrons, all of which are tightly bound to the nucleus. The fourth, and highest, energy level contains four electrons which, because of their high energy and the shielding action of the first three levels, are only loosely bound to the nucleus. In the case of germanium, it is these four electrons which generally enter into chemical reactions and which interact with other germanium atoms to form covalent bonds with adjacent atoms. These four electrons are called the valence electrons.

A semiconductor is a crystalline solid in which the individual atoms occupy fixed positions in a regular pattern. Because the atoms are so closely spaced, the discrete energy levels associated with each atom merge into "bands" of allowed energies, separated by "forbidden" regions. This energy-band configuration actually determines whether a material is a semiconductor, conductor, or insulator.

The energy band which contains the valence electrons is called the **valence band.** Electrons in this valence band, as well as in the higher energy bands, are not confined to any particular atom but are free to wander through the valence bands within the entire crystal. In the absence of any outside sources of energy such as thermal excitations, the valence electrons exactly fill all the possible states in the valence band. Under this idealized condition, no net current can flow, and the crystal is a perfect insulator.

The valence band is separated from the next higher band of allowed energies (the **conduction band**) by a **forbidden region;** this region is so called because it has no states for free

electrons. The forbidden region between the valence band and the conduction band is called the **energy gap.** This gap represents the minimum excitation energy necessary to move an electron from the valence to the conduction band. When an electron is moved from the valence to the conduction band (e.g., through thermal excitation), the crystal is no longer an insulator. Because the conduction band has many empty states available to the free electron, the electron can now be accelerated readily by an applied field. This energy-level condition represents the basis of conduction by electrons.

At the same time, the empty state left in the valence band (as a result of the removal of an electron) permits acceleration of the valence electrons. This empty state can be considered to be a "hole", or an absence of an electron in the valence band, and its effect is equivalent to that of a single positive charge. This acceleration of electrons within the valence band is called hole conduction. In general, current in a solid can be conveniently treated as motion of electrons in the conduction band and of positively charged holes in the valence band.

The width of the energy gap determines whether the solid is a semiconductor, conductor, or insulator. The energy-band diagrams shown in Fig. 2 indicate the difference in band gap
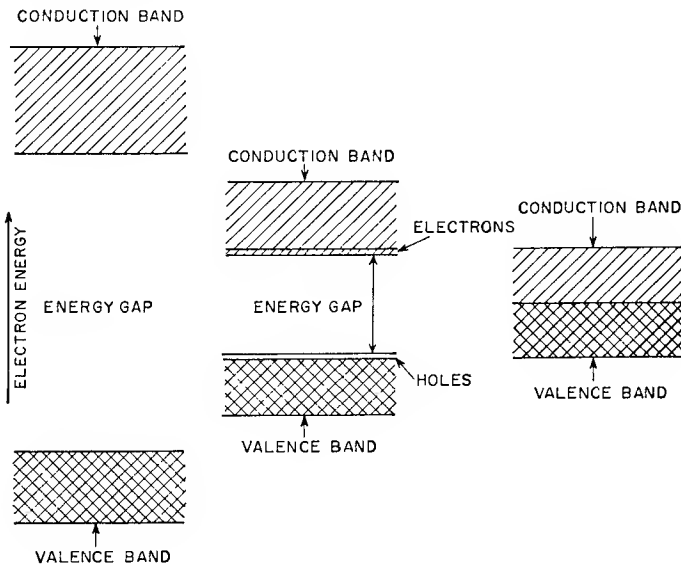
Fig. 2.   Energy-band diagrams for (a) an insulator, (b) a semiconductor, and (c) a conductor.

and free carrier concentration between an insulator, a semi-conductor, and a conductor material. In this figure, the ordinate represents the total energy (potential plus kinetic) of the electron, and the abscissa represents distance in one direction in the crystal.

As shown in Fig. 2a, the forbidden region of the insulator is so large that valence electrons cannot move to the conduction band except in the presence of extremely strong external energy sources; hence, the valence band remains filled and the conduction band is empty.

The semiconductor has a small enough gap so that thermal motion results in an appreciable number of electrons in the conduction band and holes in the valence band, as shown by Figure 2b. In most semiconductor materials, the energy gap E_g ranges from a few hundredths of an electron volt to about three electron volts. For example, the energy gap for germanium is 0.7 ev, 1.1 ev for silicon, and 1.4 ev for gallium arsenide. In conductors, there is no energy gap, and the conduction and valence bands overlap, as shown in Fig. 2c. As a result, significant electron flow occurs with only a small amount of applied energy.

The discussion above concerns only pure, or intrinsic, semiconductors. In such semiconductors, every electron in the conduction band is accompanied by a corresponding hole in the valence band. However, in the case of transistors and other semiconductor devices, a large number of **free carriers** (either electrons or holes) is produced by the controlled addition of small amounts of certain impurities.

For example, if an impurity such as arsenic which contains five valence electrons is substituted for a germanium atom, only four of these electrons are used to form the covalent bond. The remaining electron is free and is readily excited into the conduction band. Instead of leaving a hole behind in the valence band (as occurs when an electron is thermally excited into the conduction band), the loss of this free electron to the conduction band ionizes the arsenic atom, i.e., the arsenic atom gives up its extra electron and becomes positively charged. Because of the small activation energy needed to ionize arsenic, practically all such **donor atoms** are ionized at room temperature. Such a material is referred to as an extrinsic **n-type** semiconductor; the energy-band diagram for such a material is shown in Fig. 3a. In the diagram, the plus signs in the valence band represent the few holes created by thermal excitation of electrons into the conduction band. As shown, the total number of electrons in the conduction band equals the sum of the donor atoms plus the holes in the valence band.

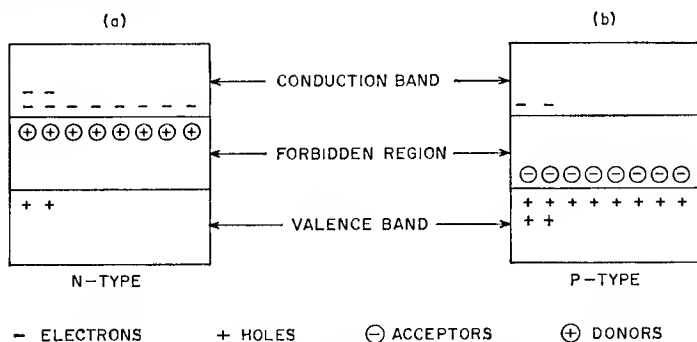As a result, the entire semiconductor crystal remains electrically neutral.

Fig. 3.   Energy-band diagrams for extrinsic n-type
and p-type semiconductors.

Fig. 3b shows the energy-band diagram for an extrinsic **p-type** semiconductor material, e.g., germanium doped with gallium. In this case, each impurity atom substituted for a germanium atom has one less valence electron than the germanium. The missing electron needed to complete the covalent bond is then taken from a neighboring germanium atom. As a result, the gallium atoms acquire an extra electron, and thus become negatively ionized **(acceptor atoms)**. The electrons which were used to complete the bonding leave positively charged holes behind them. The small number of electrons in the conduction band represent those electrons that acquired enough energy through thermal agitation to leave the valence band. The total number of holes in the valence band equals the sum of the acceptor atoms plus the electrons in the conduction band. As a result, the semiconductor again remains electrically neutral.

CONVENTIONAL JUNCTIONS

Semiconductor p-n or n-p junctions are frequently formed by alloying or diffusing a dopant material into an oppositely doped semiconductor. For example, indium, an acceptor, can be alloyed to germanium which is doped with arsenic, a donor. Alternately, arsenic may be diffused into germanium which is doped with gallium, an acceptor. In either case, a junction is formed between the n-type and p-type regions of the semiconductor.

The current-flow mechanism across this junction is shown in Fig. 4a. This representation shows an n-type semiconductor containing a large number of donors, and a p-type containing a large number of acceptors.

Fig. 4.   Two-dimensional representation of charges
           in n-p semiconductor (a) at zero-bias volt-
           age and (b) corresponding energy-band dia-
           gram.

The transition region from n- to p-type semiconductors
consists of a dipole layer formed by immobile negatively
charged acceptor atoms (not compensated by holes) and posi-
tively charged donor atoms (not neutralized by electrons). The
electric field associated with this dipole layer is very high
(in the order of 10000 volts per centimeter). Because of this
high field intensity, any free carriers (i.e. mobile) cannot re-
main in this region, but must either recombine or be swept
across the junction and away from the transition region. This
transition region is frequently referred to as the **depletion
layer** or **space-charge region**.

Fig. 4b shows the corresponding energy-band diagram for
the junction under zero-bias voltage. The energy gap E_g is
the same on both sides of the junction, but the potential en-
ergy for electrons on the p-type side is increased with respect
to the n-type side. The resulting **potential barrier** (E_B) results
from the presence of the dipole layer of the transition region.

As a result of their random motion, some electrons ap-
proach the junction from either side. Because of the much
larger number of mobile electrons on the n-type side, propor-
tionally more electrons approach the junction from that side.
If there were no potential barrier, these electrons would cross
into the p-type side, until ultimately a uniform distribution of
electrons would exist throughout the semiconductor. How-
ever, because of the potential barrier, only those few electrons
having thermal energy greater than E_B can actually cross the
junction. Thus, a small but finite current exists due to the
diffusion of electrons from the n-type to the p-type material.

On the p-type side, some of the thermally generated electrons in the conduction band diffuse towards the junction. The direction of the electric field accelerates these electrons across the junction and into the n-type side. This current exactly counterbalances the diffusion current from the n-type to the p-type side; thus the net electron current is zero. The same conditions apply to the flow of holes in both directions across the junction. As a result, the net current is zero, as expected with zero applied voltage.

When a negative-bias voltage is applied to a conventional n-p junction, the energy level of electrons in the p-type material is further increased by the negative potential supplied by the voltage source. As shown in Fig. 5a, the position of the p-type energy bands is then considerably higher than that of the n-type bands. This change in energy level effectively increases the height of the junction barrier, and reduces the diffusion of electrons from the n-side across the junction to a negligible amount. Because electrons always seek the lowest energy level, the small number of electrons in the conduction band of the p-type material continue to cross the junction as before. The higher potential barrier serves to accelerate these electrons even more than for the zero-bias case. Similarly, the diffusion of holes from the p-type to the n-type side is reduced to practically zero, while the hole current from the n-type to the p-type side of the junction is not affected. The net result is a small amount of **reverse current,** as shown by point A on the current-voltage curve of Fig. 5.
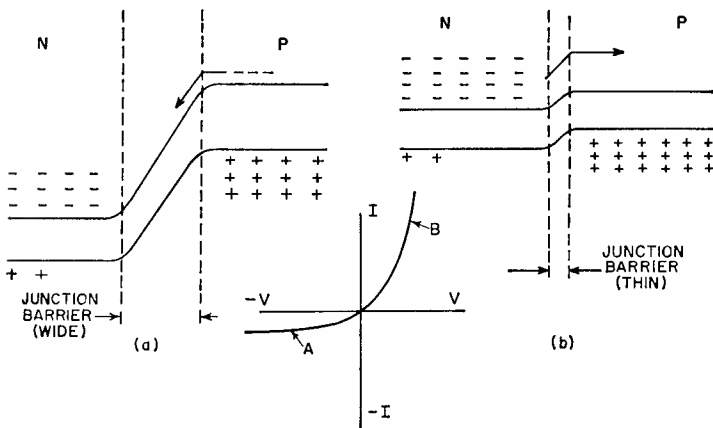
Fig. 5.   Energy-band diagrams for conventional diode under (a) reverse-bias conditions and (b) forward-bias conditions.

Under positive-bias conditions, the height of the potential barrier is reduced, as shown in Fig. 5b. The flow of electrons from the p-type to the n-type side, and of holes from the n-type to the p-type side, remains unchanged. However, the lower potential barrier permits a larger diffusion current to flow (i.e., electrons from the n-side cross to the p-type side and holes from the p-side cross to the n-type side). Because this diffusion current is an exponential function of barrier height, even small applied voltages result in a very large **forward current,** as shown by point B on the current-voltage curve of Fig. 5.

TUNNEL-DIODE JUNCTIONS

As mentioned previously, tunnel diodes use much higher doping levels than conventional diode or transistor devices, and, as a result, the transition region is much narrower. Typically, the transition region in tunnel diodes is less than 100 angstroms (0.000001 centimeter), as compared with approximately 10,000 angstroms (0.0001 centimeter) for a conventional junction. This difference in width accounts for the major difference in current-flow mechanism between tunnel diodes and conventional semiconductor devices.

According to the laws of classical physics, an electron can not penetrate a potential barrier. It can only "climb over" the barrier if its energy is greater than that of the barrier. This concept governs the flow of current across a conventional junction. However, the theory of quantum mechanics has shown that there is a small but finite probability that an electron having insufficient energy to climb the potential barrier can, nevertheless, penetrate it if the barrier is sufficiently narrow. Moreover, the electron has the same energy after passing through the barrier as it did before. This phenomenon, which is called "**tunneling**", is the basic mechanism governing the flow of current for most of the voltage range of interest in circuit applications of tunnel diodes.

Fig. 6a shows the energy-band diagram for a tunnel-diode junction under zero-bias conditions. The cross-hatched regions represent those energy states in the conduction and valence bands which are occupied by electrons. The horizontal dashed line indicates the level to which the energy states on both sides of the junction are occupied by electrons. At zero applied voltage, this horizontal line is continuous, as shown. Conduction-band electrons from the n-type side can then tunnel into the p-type valence band, and the valence-band electrons from the p-type side can tunnel into the conduction band. The magnitude of these two current components is indicated in Fig. 6a

by the dashed arrows across the junction. Because these components exactly balance each other at zero bias, the net current is zero.

When a reverse bias is applied, all energy levels on the p-type side are increased in relation to those of the n-type side, as shown in Fig. 6b. Because there are then many available states on the n-side facing the electrons in the p-type valence band, a large current of electrons can easily flow from the
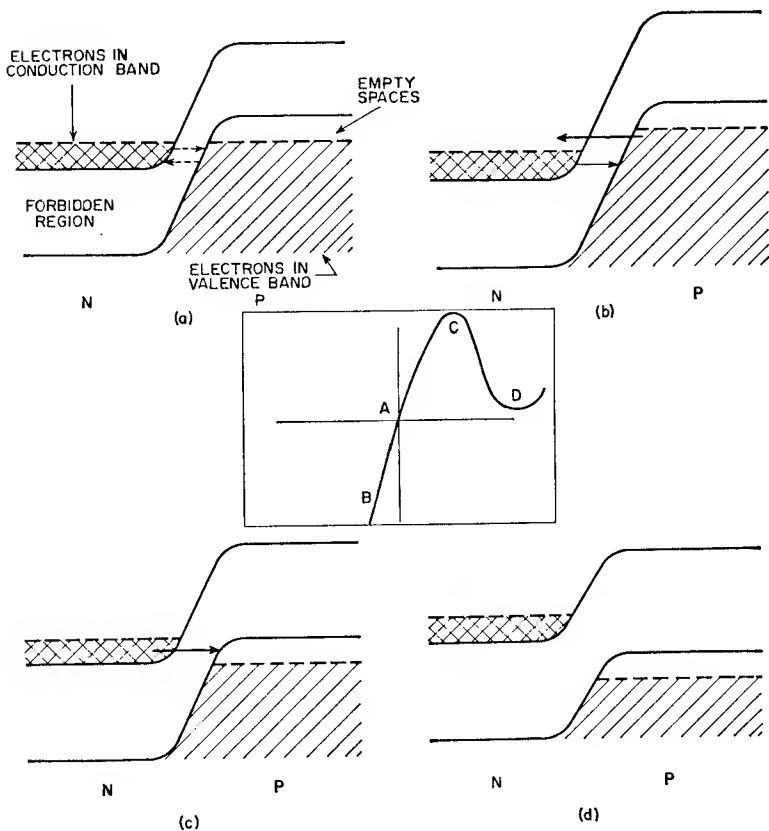
Fig. 6.   Energy-band diagrams for n-p tunnel-diode junction at (a) zero-bias voltage, (b) reverse-bias voltage, (c) peak voltage, and (d) valley voltage.

p-type to the n-type side. This heavy reverse flow is indicated by the large arrow in the diagram. The current flowing from the n-type to the p-type side remains the same as in Fig. 6a.

The tunneling phenomenon depends exponentially on the electric field across the barrier (approximately the total barrier height divided by the transition region width divided by the electronic charge). As a result, the reverse current increases very rapidly for even small voltages. In addition, because the supply of electrons in the p-type valence band is so large, and because of the large supply of available empty states in the n-type conduction band facing the electrons, the tunnel diode is highly conductive for all values of reverse bias (see Fig. 1).

For small forward-bias voltages, the energy level of the p-type side is decreased in relation to the n-side as shown in Fig. 6c. In this case the n-type conduction-band electrons are opposite unoccupied states in the p-type valence band, while the p-type valence-band electrons are shown opposite the forbidden energy gap of the n-type side. The conduction-to-valence band current thus remains the same as in Fig. 6a whereas the current flowing in the opposite direction is reduced to zero; thus, current flows in the forward direction.

When the forward voltage is increased further, some conduction band electrons on the n-type side are opposite the forbidden-energy gap of the p-type side, and the conduction-to-valence-band current is reduced. The forward current then decreases as the forward voltage increases. This current-voltage relationship accounts for the negative-resistance region of the tunnel diode. Finally, for a forward-bias voltage equal to the valley voltage, tunneling completely ceases. The energy-band diagram for this condition is shown in Fig. 6d.

Forward current flow in a tunnel diode, however, does not cease completely at the valley-voltage point, as shown in the current-voltage curve of Fig. 6. The small amount of current in this region, called **excess current,** is actually a combination of several phenomena. Some tunneling may still occur as a result of localized impurity states (not the controlled dopant impurities) in the forbidden region. In addition, the edges of the energy-band diagram may be somewhat distorted as a result of the very high doping levels, so that the valence and conduction bands extend into the forbidden region at some points. Furthermore, tunneling and recombination in the depletion layer produce a current component which, unlike the conventional diode current, exhibits a non-exponential dependence on temperature. At voltages greater than the valley voltage, the height of the barrier is reduced to a level which permits conventional current to flow over the barrier.

TUNNEL RECTIFIERS

In addition to its negative-resistance properties, the tunnel diode has an efficient rectification characteristic which can be used readily in many rectifier applications. When a tunnel diode is used in a circuit in such a way that this rectification property is emphasized, rather than its negative-resistance characteristic, it is called a tunnel rectifier. In general, the peak current for a tunnel rectifier is less than one milliampere.

The major differences in the current-voltage characteristics of tunnel rectifiers and conventional rectifiers are shown in Fig. 7. In conventional rectifiers, current flow is substantial in the forward direction, but extremely small in the reverse direction (for signal voltages less than the breakdown voltage
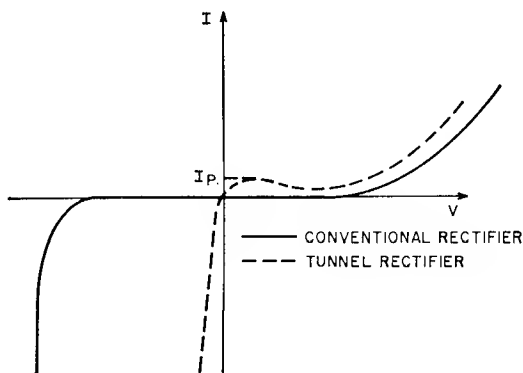
Fig. 7.   Characteristics curves for tunnel rectifier
and conventional rectifier.

for the device). In tunnel rectifiers, however, substantial reverse current flows at very low voltages, while forward current is relatively small. Consequently, tunnel rectifiers can provide rectification at smaller signal voltages than conventional rectifiers, although their polarity requirements are opposite. (For this reason, tunnel rectifiers are sometimes called "back diodes".)

Because of their high-speed capability and superior rectification characteristics, tunnel rectifiers can be used to provide coupling in one direction and isolation in the opposite direction. More information on their applications is given in the section on Switching.

CONSTRUCTION AND MATERIALS

The structure of the tunnel diode is extremely simple, as shown in Fig. 8. A small dot (approximately two mils in di-

ameter) of highly conductive n-type (or p-type) material is
alloyed to a pellet of highly conductive p-type (or n-type)
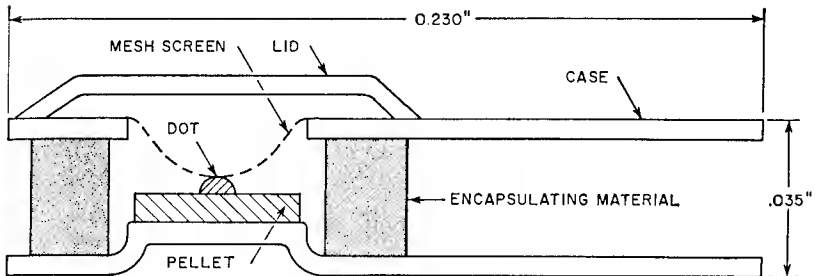
Fig. 8.   Structure of typical RCA tunnel diode.

material to form the semiconductor junction. The pellet (ap-
proximately 0.025 inch square) is then soldered into a low-
inductance, low-capacitance case. A very fine mesh screen is
added to make the connection to the dot, and the junction area
is reduced by etching to produce the desired peak currents.
The device is then encapsulated, and a lid is welded over the
cavity.

Tunnel-diode packages must be designed to provide both
low inductance and low capacitance. This requirement im-
mediately eliminates a large number of possible mounting and
packaging approaches, including all the methods commonly
used for transistors and conventional diodes. The package
shown in Fig. 8 was chosen as a good compromise for both re-
quirements; its junction area is very small, and its inductance
is approximately 4×10^{-10} henry. This induction range is suit-
able for most high-frequency applications. Special packages
have been developed for some microwave applications in which
even lower inductances are required.

Tunnel diodes can be constructed from a variety of semi-
conductor materials, including germanium, silicon, gallium
arsenide, indium phosphide, indium arsenide, and indium anti-
monide. The choice of material is a significant factor in de-
termining the principal parameters of the device. In general,
materials having small forbidden energy gaps, low effective
masses, and low dielectric constants provide large tunneling
probabilities. These materials permit the use of small junc-
tions and low capacitance for given peak currents, and thus
provide extremely fast switching speeds.

At the present time, most commercially available tunnel

diodes are fabricated from either germanium or gallium ar-
senide. The current-voltage characteristics of germanium and
gallium arsenide tunnel diodes are compared in Fig. 9. Ger-
manium devices offer high speed, low noise, and low rise times
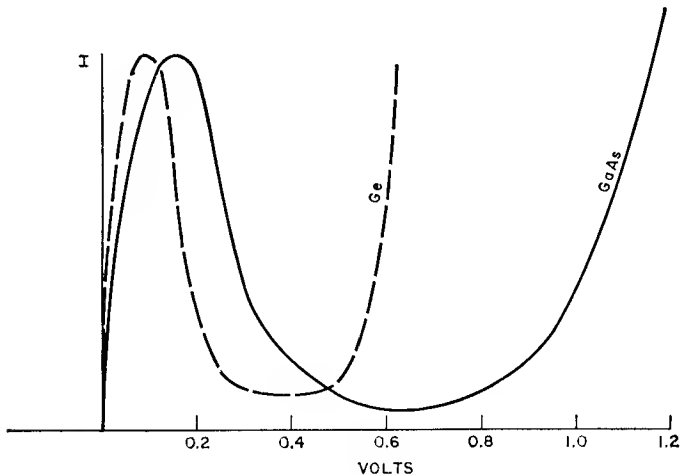
Fig. 9.   Static characteristics for germanium and
             gallium arsenide tunnel diodes.

(as low as 40 picoseconds). Gallium arsenide diodes, which
have a larger voltage swing than germanium diodes, are being
used in an increasing number of applications.

Indium antimonide cannot be used at normal room tempera-
tures because of its small bandgap. Indium arsenide presents
fabrication problems which make it difficult to control the de-
sired peak-current-to-valley-current ratio. Silicon presents the
same problems as indium arsenide, and also produces lower-
speed devices than germanium or gallium arsenide.
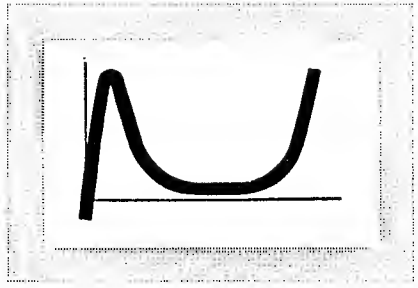
CHARACTERISTICS

Because of the inherent simplicity of tunnel diodes, the number of electrical characteristics of interest to circuit designers is relatively small in comparison to those for electron tubes or transistors. The essential **static characteristics** are indicated in Fig. 10, which shows the current-voltage characteristic curve for a tunnel diode. The **peak-point forward current** I_P is the value of current at which the slope of the current-voltage characteristic changes from positive to negative as the forward voltage is increased. For a given semiconductor, I_P depends primarily on the resistivity of the crystal
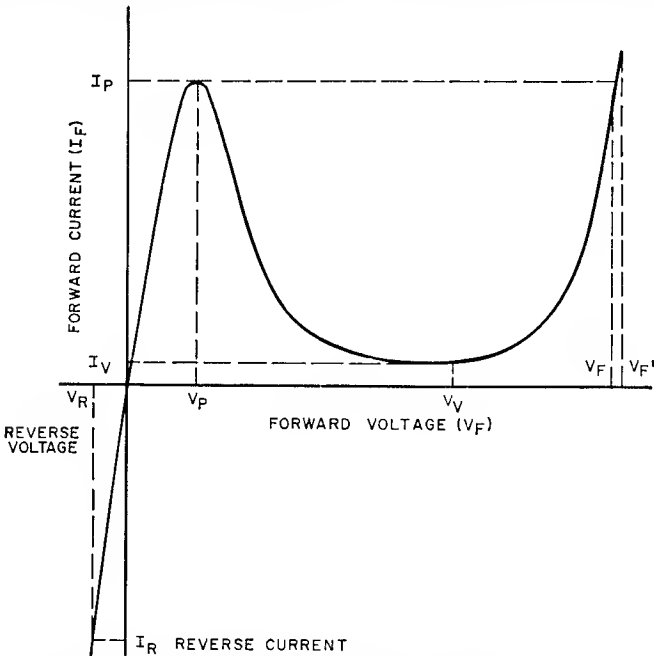
Fig. 10.   Static current-voltage characteristic of tunnel diode.

17

and the junction area of the device, and can be closely controlled during fabrication to within a few per cent of the desired value. Tunnel diodes have been made with peak currents ranging from several microamperes to several hundred amperes. The actual value used is determined primarily by the application, as shown in Table I.

TABLE I

Application	Peak Current Range
Tunnel Rectifier	0.1 to 1 ma
Amplifier	0.5 to 2 ma
Computer Switching Element	2 to 50 ma
Oscillator	5 ma to 1 ampere
DC-to-AC Inverter	above 1 ampere
High-Current Switch	above 1 ampere

The **valley-point current** I_V is the current at which the slope of the current-voltage characteristic changes from negative to positive as the forward voltage is further increased. An important relationship between peak current and valley current is the **peak-to-valley current** ratio $I_P:I_V$. This parameter determines the current swing of the device, and is particularly critical for computer-switching applications. This ratio is typically ten to one for germanium tunnel diodes, and twenty to one for gallium arsenide tunnel diodes.

The **peak voltage** V_P and the **valley voltage** V_V are the voltages at which the peak current and the valley current, respectively, occur. These voltage parameters are determined primarily by the type of semiconductor material used in the tunnel diode. (For high-current diodes, the peak voltage can also be substantially affected by the voltage drop across the series resistance of the diode.)

Voltages in the forward region greater than the valley voltage are designated by the symbol V_F. The forward voltage for which the current is equal to the peak current value is called the **projected peak voltage** V_{PP}. The symbol V_F' designates the forward voltage at which the current is equal to the maximum specified peak current, i.e., the upper tolerance limit on the rated peak current value.

The **dynamic** (or small signal) **characteristics** of tunnel diodes are defined with respect to the tunnel-diode equivalent circuit shown in Fig. 11. The most important of the dynamic
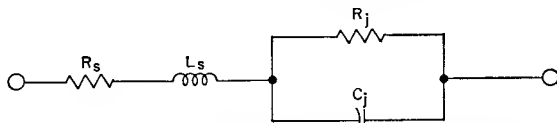
Fig. 11.   Small-signal tunnel-diode equivalent circuit.

characteristics is the **junction resistance** R_j of the tunnel-diode, which is determined from two measured parameters, as follows:

$$R_j = \frac{dV}{dI} - R_s \qquad (1)$$

where dV/dI equals the inverse slope of the current-voltage curve and R_s equals the series resistance of the diode.

The current-voltage characteristic has an inflection point in the negative-resistance region. At that point, the magnitude of the negative resistance is a minimum and is inversely proportional to the diode peak current, as shown by

$$R_{min} = \left| R_j \right|_{min} \cong \frac{V_k}{I_p} \qquad (2)$$

where V_k is a voltage which is characteristic of the semiconductor material. The peak current is the product of tunnel-current density at the peak point J_p and the junction area A_j. The tunnel-current density is a very sensitive function of material properties (e.g., impurity concentration or crystal resistivity) and fabrication techniques (e.g., alloying time and temperature). As a result, J_p is very difficult to control during fabrication. The value of I_P (or R_{min}) must be adjusted by individual etching of each diode to its final junction area. The junction capacitance is not nearly so sensitive to material properties or fabrication techniques, but it is directly proportional to junction area. As a result, the etching process can be used to provide very tight tolerances on peak current, but the junction capacitance is not controlled so closely.

The series resistance can be considered as the resistance of the semiconductor wafer. In a well fabricated diode, the value of the ratio $R_s:R_{min}$ is often less than 0.05; however, it is difficult to maintain this ratio in the fabrication of high-frequency diodes.

The **series inductance** L_s is a property of the diode case (particularly the lead connecting the upper electrode of the diode to the case), and is influenced by the circuit in which the diode is used. The diode **junction capacitance** C_j is the small-signal capacitance associated with the p-n junction alone at a specified bias and frequency. Usually C_j is specified at the valley voltage; at this voltage, C_j is relatively insensitive to voltage and frequency. Also, the high dynamic resistance R_j in the valley region simplifies the problems of measuring C_j. (This measurement is discussed further in the section on Measuring Circuits.)

A small-signal analysis of the tunnel-diode equivalent circuit determines several parameters which are useful in the

selection of tunnel diodes for different applications. The frequency limitations of the tunnel-diode junction alone are determined by the diode capacitance and R_{min}. This frequency capability can be described in terms of a **figure of merit** f_c which is given by

$$f_c = \frac{1}{2\pi R_{min}C_j} \qquad (3)$$

The figure of merit has two very useful interpretations for negligible series resistance; it is the maximum value of the diode **gain-bandwidth** product for linear circuits, and its reciprocal determines the minimum diode **switching time** when the unit is used as a logic element.

The combination of Eqs. (2) and (3) results in the relationship:

$$f_c = \left(\frac{1}{2\pi V_k}\right) \qquad \left(\frac{I_P}{C_j}\right) \qquad (4)$$

where the first term is a constant for a given semiconductor material. The second term (I_P/C_j) is, therefore, a direct measure of the diode speed capability. This parameter is frequently referred to as the diode **speed factor** or **speed index,** and is usually expressed in units of milliamperes per picofarad.

The frequency f_c should not be confused with the **resistive cutoff frequency** f_{ro} which represents the frequency at which the diode no longer exhibits negative resistance for a specified bias. When the bias is adjusted so that f_{ro} is a maximum, its value is given by

$$f_{ro} \text{ max} = \frac{1}{2\pi R_{min}C_j} \sqrt{\frac{R_{min}}{R_s} - 1} \qquad (5)$$

provided that R_{min} is greater than or equal to 2 R_s. If R_{min} is less than 2 R_s, then the bias must be adjusted so that the absolute value of R_j is equal to 2 R_s to obtain the maximum oscillating frequency.

Another quantity of interest in some applications (particularly amplifiers and oscillators) is the **self-resonant frequency** f_{xo} which is given by

$$f_{xo} = \frac{1}{2\pi R_j C_j} \sqrt{\frac{R_j^2 C_j}{L_s} - 1} \qquad (6)$$

This frequency is a maximum when R_j equals R_{min}. The self-resonant frequency is significant because at operating frequencies below f_{xo}, the reactance of the diode is capacitive; above self-resonance, it is inductive.

CIRCUIT BEHAVIOR

Further analysis of the small-signal equivalent circuit of Fig. 11 also provides useful application information. The operation of a tunnel diode as a stable amplifier, sinusoidal oscillator, relaxation oscillator, or switch is determined by the values of R_s, R, C_j, L_s, and R_L, where R is the magnitude of the negative resistance (usually its minimum value, R_{min}) and R_L is the external resistance. The conditions which must be satisfied for the different operating modes are shown in Fig. 12. This chart is plotted in terms of the following parameters:

$$\propto \equiv \frac{R_s + R_L}{R} \tag{7}$$

$$\beta \equiv \frac{(R_s + R_L) \, RC_j}{L_s} \tag{8}$$
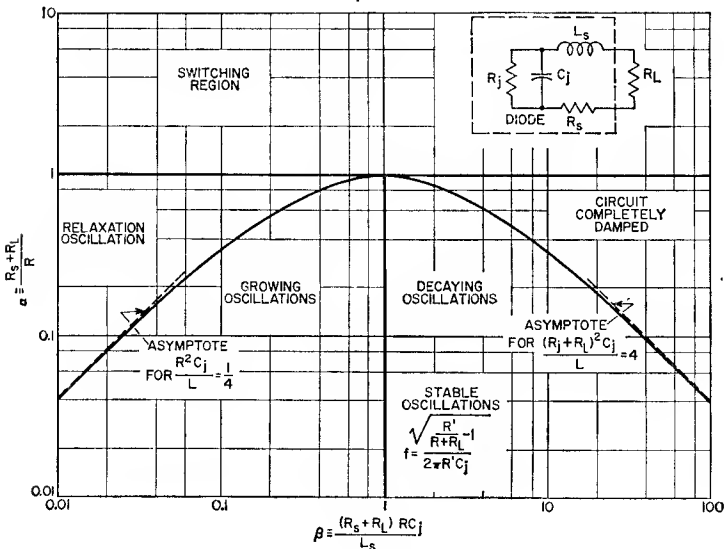
Fig. 12.   Tunnel-diode performance chart.

The value of α determines whether or not the diode operates as a switch. When α is greater than 1, the load line can intersect the current-voltage characteristic at two stable points, as shown in Fig. 13. The diode then acts as a bistable switch.
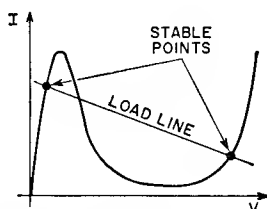
Fig. 13.   Tunnel-diode load-line chart.

When α is less than 1, the diode can be used as an oscillator or amplifier, depending on the values of both α and β. Because this chart is based on a small-signal analysis, the relationships between R_s, R, L_s and C do not apply for the steady-state case of an oscillator. Under steady-state conditions, however, the negative resistance has an effective value, R', such that $\beta = 1$. For this condition, the actual frequency f of a sinusoidal oscillator becomes

$$f = \frac{1}{2\pi R'C_j} \sqrt{\frac{1}{(R_s + R_L)} - \frac{1}{(R'C_j)^2}} \qquad (9)$$

and because $\beta = 1$, this equation may be simplified as follows:

$$f = \frac{1}{2\pi} \sqrt{\frac{1}{L_s C_j} - \frac{R_s^2}{L_s^2}} \qquad (10)$$

TEMPERATURE VARIATION OF PARAMETERS

To some extent, all electrical parameters of the tunnel diode are affected by temperature variations. In general, the tunneling region of the current-voltage characteristic curve is least affected; the greatest temperature variations occur in the injection region.

The temperature dependence of the peak current of tunnel diodes is a function of the carrier concentration of the crystal used.[1] Fig. 14 shows peak current of a germanium tunnel diode as a function of temperature for different values of p-region carrier concentration. As the doping density is increased, the temperature coefficient changes from negative to slightly positive. Thus, tunnel diodes having excellent peak current-vs.-temperature characteristics can be produced by proper choice of carrier concentration.

Because the diode speed index (I_P/C_j) is a sensitive function of carrier concentration, it is not always possible to achieve a desired temperature response consistent with a speed
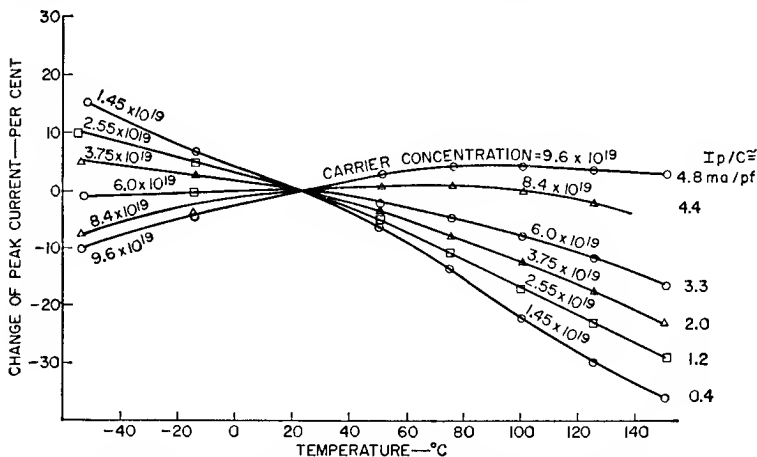
Fig. 14.   Per-cent change of peak current as a function of temperature for different values of carrier concentration and speed index.

index required for a given application. Fortunately, the temperature coefficient of high-speed germanium tunnel diodes is small near room temperature. Fig. 14 also shows the diode speed index corresponding to each value of carrier concentration. Fig. 15 shows typical variations in peak current with temperature for germanium type RCA IN3855.
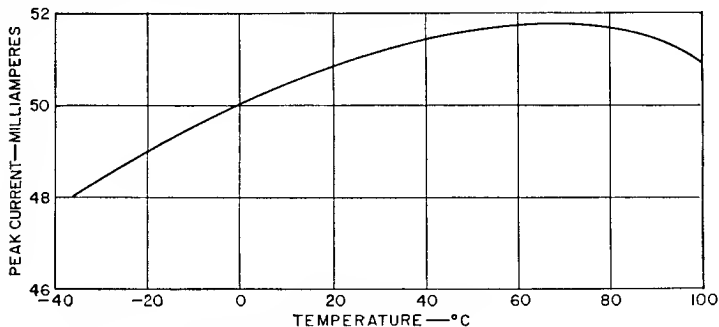
Fig. 15.   Temperature coefficient of tunnel-diode peak current.

Peak voltage is not greatly affected by temperature variations. This parameter has a small negative coefficient, and is slightly dependent on the peak current of the diode. For example, the peak voltage of a 50-milliampere germanium diode having a carrier concentration of about 7.0×10^{19} per cubic centimeter changes by approximately 2 millivolts from 0 to

100 degrees centigrade, or about 20 microvolts per degree. For a five-milliampere diode having an average carrier concentration of 3.5 x 10^{19} per cubic centimeter, the peak voltage changes approximately 4 millivolts from 0 to 100 degrees centigrade, or about 40 microvolts per degree. The slight dependence on peak current may result from the fact that the measured peak voltage V_P is composed of two components, as follows:

$$V_P = V_{Po} + I_P R_s \qquad (11)$$

where V_{Po} is the inherent peak voltage of the diode and $I_P R_s$ is the voltage drop across the series resistance. Because peak current is temperature-dependent, as discussed previously, temperature variations of the peak current also affect the peak voltage. Fig. 16 shows typical variations of peak voltage as a function of temperature.
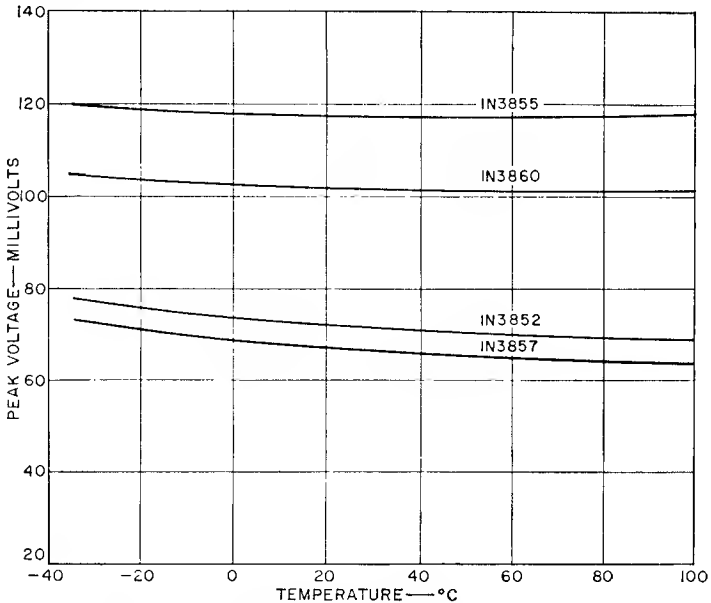
Fig. 16.   Temperature   coefficient   of   tunnel-diode peak voltage.

Valley current has a higher temperature coefficient than other tunnel-diode parameters, and the coefficient itself increases with temperature. For example, the valley current of several five-milliampere germanium tunnel diodes doubles in value from −35 to 100 degrees centigrade, as shown in Fig. 17. This parameter is only slightly dependent on carrier concentration.
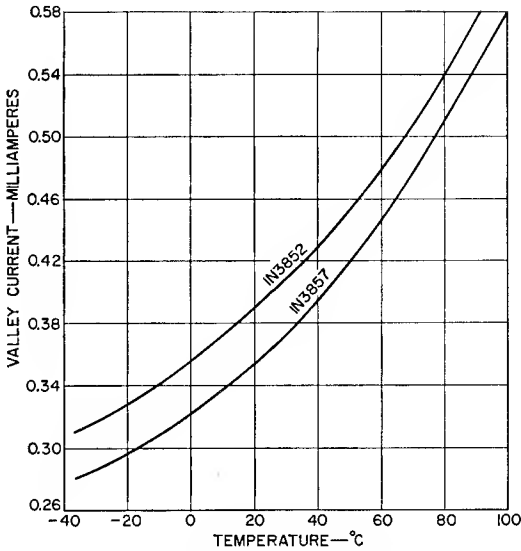
Fig. 17.   Temperature coefficient of valley current.

As shown in Fig. 18, the valley voltage has an approximately linear negative temperature coefficient which ranges from −0.8 to −0.9 millivolts per degree centigrade.
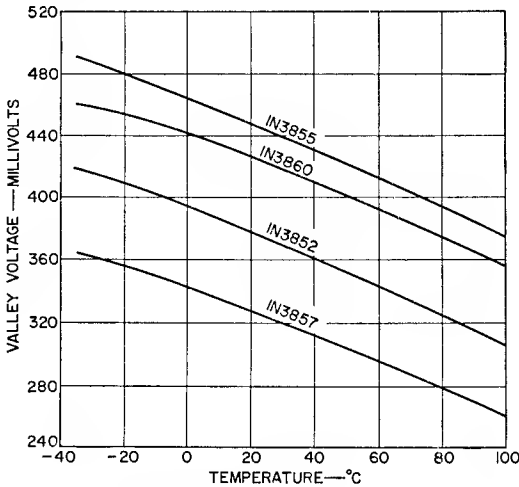
Fig. 18.   Temperature coefficient of tunnel-diode valley voltage.

The forward voltage region also exhibits a negative temperature coefficient. The projected peak voltage V_{PP} has a linear negative temperature coefficient of approximately 1.0

millivolt per degree centigrade, as shown in Fig. 19. This parameter is slightly dependent on peak current and doping density. For example, typical 50-milliampere germanium diodes
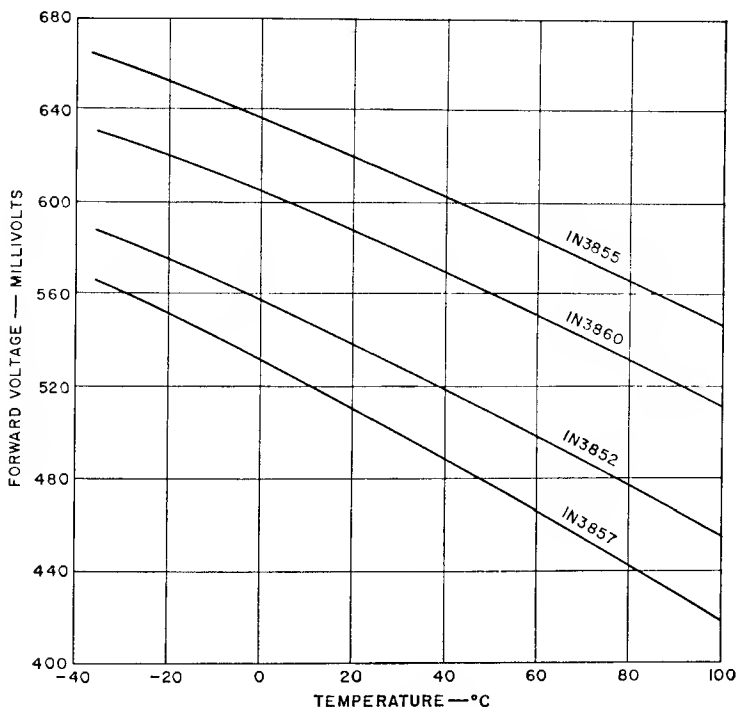
Fig. 19.   Temperature   coefficient   of   tunnel-diode
projected peak voltage.

may have a temperature coefficient for forward voltages as low as −0.9 millivolt per degree centigrade; a five-milliampere unit may have a typical coefficient of −1.1 millivolts per degree centigrade. This variation results partly from the method by which the forward-voltage point is defined and measured. Because V_{PP} is measured at a current equal to the peak current, it is measured at correspondingly lower current levels when the peak current decreases with increasing temperature. (For purposes of comparison, the temperature coefficient of conventional germanium diodes is in the area of 2.5 millivolts per degree centigrade; this rating is much poorer than that of tunnel diodes.)

Because such devices as tunnel rectifiers are operated in the reverse-bias region, it is also important to consider the temperature coefficient of the reverse characteristic. Fig. 20

shows the per cent change in reverse voltage with a constant reverse-current bias. As shown, the total change over the entire temperature range is less than one per cent.
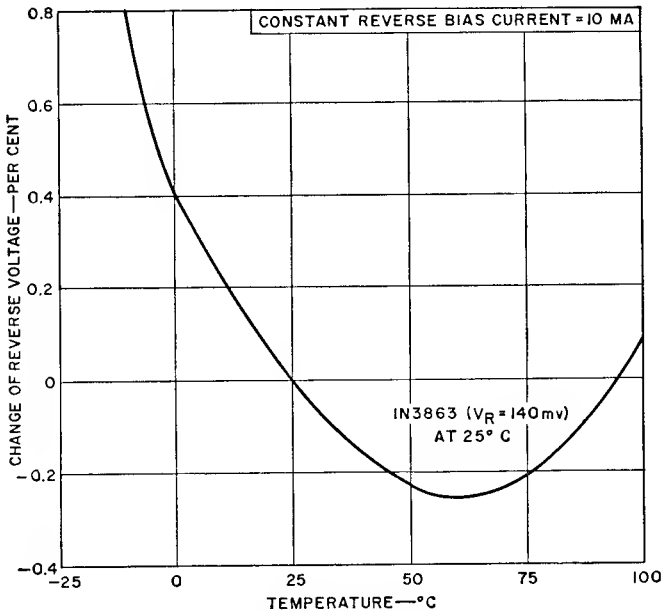
Fig. 20.   Temperature   coefficient   of   tunnel-diode reverse voltage.

LIFE STABILITY OF GERMANIUM TUNNEL DIODES

Accelerated life tests at RCA have shown no inherent failure mechanisms for germanium tunnel diodes. Figs. 21 and 22 show results of long-range tests on type IN3129 diodes. The only deviations in characteristics were slight increases in valley current and slight decreases in valley voltage. In general, the results of shelf-life tests at 100 degree centigrade were also very favorable, as were operating life tests within reasonable dissipation limits.

An accelerated life test was conducted to determine the long-term stability of the peak current of germanium tunnel diodes. In this test, three types of diodes were operated at 25 degrees centigrade, and at average currents several times the specified peak currents of 50, 25 and 5 milliamperes, respectively. Equipment having an accuracy better than 0.25 per cent was used for measuring peak and valley currents. Voltage measurements were accurate to within one per cent.

After 5000 hours of testing, no open or short circuits occurred in any of the units. All five-milliampere diodes, as well as 80 per cent of the 25- and 50-milliampere units, had a peak-current stability of ± 1 per cent or better. None of the units changed more than ± 1.5 per cent in peak current. Average peak-current changes for the five-, 25-, and 50-milliampere types were 0.13 per cent, 0.56 per cent, and 0.70 per cent, respectively. Changes in peak voltage averaged less than one millivolt.
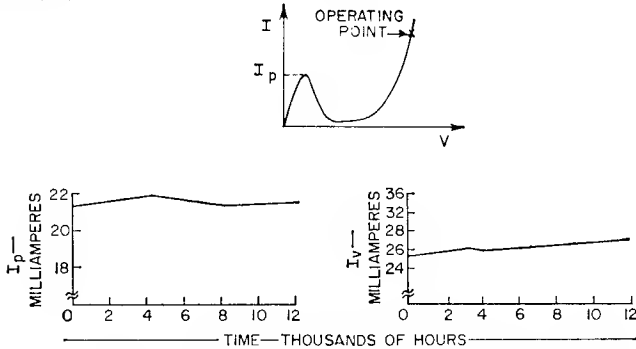
Fig. 21.   High-stress life test results for I_P and I_v of pre-aged RCA 1N3129.
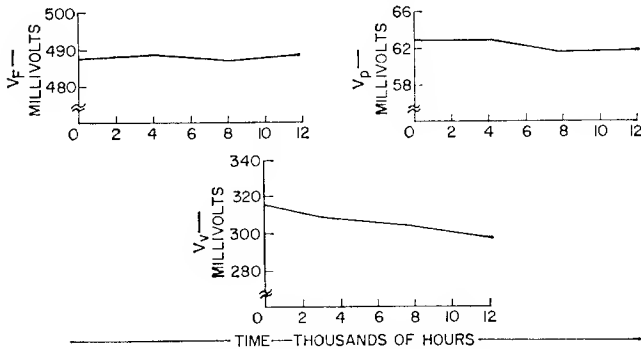
Fig. 22.   High-stress life test results for V_F, V_P, and V_v of pre-aged RCA 1N3129.

All units that had an initial peak-to-valley current ratio greater than 10:1 remained at that ratio after 5000 hours of testing. However, the valley current for a few of the 25-milliampere diodes having an initial ratio of less than 10:1 changed significantly. The average decrease in current ratio for the 50-milliampere and 25-milliampere diodes was 0.9 (for example, from 9.8:1 to 8.9:1). The average ratio for the five-milliampere diodes decreased by approximately 0.5.

Valley-voltage and forward-voltage changes were found

to be inversely proportional to the valley-current changes; however, the percentage change in valley and forward voltage was not as great as that of the valley current.

In another precision life test, high-speed units (50 milliamperes, seven picofarads) operated at accelerated dc conditions (average current several times the peak current) showed somewhat greater changes in peak and valley currents. After 4000 hours, some units exhibited peak-current degradations up to three per cent. In this life test, the power level used was about five times that normally encountered in typical logic circuits such as monostable amplifiers or gates.

LIFE STABILITY OF GALLIUM ARSENIDE TUNNEL DIODES

As previously mentioned, gallium arsenide tunnel diodes offer several advantages over germanium devices. For example, they provide a voltage swing twice the size of that available with germanium. In addition, because the power output at a fixed impedance level varies as the square of the voltage swing, the power output of gallium arsenide devices is about four times that of germanium tunnel diodes having the same negative resistance. When gallium arsenide diodes are operated at high current levels in the forward-injection region, however, serious degradation of the peak current can occur if certain operating limitations are not considered. This degradation, which is believed to be the result of the energy associated with the recombination of injected minority carriers,[2-4] is characterized by decreases in peak current, decreases (or increases) in valley current, and small changes in capacitance and voltage.

No degradation has been observed during operation of gallium arsenide diodes in the reverse region or in the tunneling region. For example, 5-milliampere units have been operated at a reverse current of 50 milliamperes with no noticeable degradation after 2000 hours. Operation in the negative-resistance region (as an oscillator) produces no degradation even at temperatures up to 150 degrees centigrade. When the diode is operated as a relaxation oscillator and the signal swing is quite large, however, the resultant excursions into the forward region may result in degradation unless the precautions described below are observed.

The degradation rate depends on the peak-current-to-capacitance ratio (I_P/C_j) and the forward voltage, as well as on the forward current. For example, 50-milliampere units

were operated at three different current levels (10, 25, and 50 milliamperes) in the forward region. After 800 hours, the units operated at ten milliamperes showed no degradation; the units operated at 25 milliamperes showed degradation of one to five per cent, and the units operated at 50 milliamperes showed degradation of 5 to 25 per cent. In addition, units having the highest speed ratio showed the greatest degradation.

On the basis of extensive life data[5], a limiting condition for safe dc operation of diffused gallium arsenide tunnel diodes at room temperature has been empirically established. This condition is given by

$$\frac{I}{C_j} \leqq 0.5 \ \mathrm{ma/pf} \qquad (12)$$

where I is the average current in milliamperes and C_j is the junction capacitance in picofarads. When the above condition is satisfied, degradation is negligible for any given operating conditions beyond the valley voltage. Fig. 23 shows the results of testing of two tunnel diodes under these conditions.
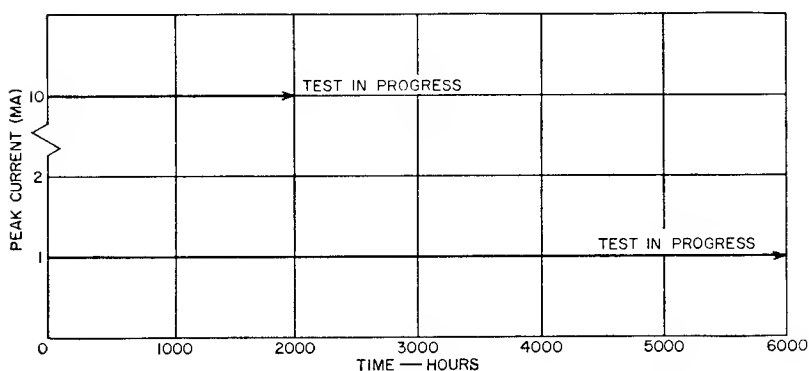
Fig. 23.   Typical life stability of RCA gallium arsenide
             tunnel diodes.

These tests were still in progress during the publication of this manual.

The limiting condition is applicable for both tunnel rectifiers and tunnel diodes. In addition, it applies to high-current diodes which are operated at less than the peak current in the forward region, as well as to low-current units operated at currents greater than the peak current.

RADIATION EFFECTS

Recent tests have shown that tunnel diodes are several orders of magnitude more resistant to nuclear radiation than bipolar transistors. The principal reason for this high resistance to radiation damage is that the tunnel diode is a majority-carrier device. As a result, its electrical characteristics are virtually independent of minority-carrier life times. The operation of the bipolar transistor, on the other hand, depends on minority-carrier life time. The high-energy particles introduced by radiation can seriously reduce life times of minority carriers and thus degrade transistor performance.

In a series of tests, ten tunnel diodes (six germanium and four gallium arsenide) were subjected to heavy doses of radiation. The data from these tests show that the parameter most affected by radiation is the valley current, which increased significantly at dosage levels of 10^{17} nvt (neutrons per square centimeter). This rise in valley current is believed to be a result of the additional energy states within the bandgap of the device which are formed by the neutron bombardment. The current increase is linearly dependent on the total integrated flux. As shown in Table II, the increased valley current reduces the peak-to-valley current ratio as radiation is increased. The tests also indicated that peak current is relatively unaffected by radiation, as shown in Table III.

TABLE II
RADIATION EFFECTS ON PEAK-TO-VALLEY RATIO

	Sample No.	Initial I_P/I_V	Dose necessary to reduce I_P/I_V (nvt x 10^{15})		
			0.9 I_P/I_V	0.75 I_P/I_V	0.5 I_P/I_V
	1	6.4	6.05	22.2	80
	2	6.6	7.0	34.0	150
	3	7.8	4.1	22.0	57
	4	6.8	4.1	23.0	100
	5	6.1	4.1	35.0	126
Ge	6	3.6	8.5	34.0	165
GaAs	7	6.8	5.4	18.0	17
	8	6.0	5.4	18.0	65
	9	23.9	2.7	13.0	37
	10	19.6	1.1	9.0	38

TABLE III
RADIATION EFFECTS ON PEAK CURRENT

	Sample No.	Critical I_P (ma)	Dose necesary to change I_P by 5% (nvt x 10^{17})
	1	87.0	1.63
	2	79.0	1.35
	3	38.9	1.52
	4	36.6	1.20
	5	26.2	1.52
	6	16.4	2.89
GaAs	7	4.0	2.75
	8	4.3	2.75
	9	55.0	1.41
	10	53.0	0.76

REFERENCES

1. A. Blicher, R. Glicksman, R. M. Minton, "Temperature Dependence of the Peak Current of Germanium Tunnel Diodes", *Proc. IRE, 49*, 9, p. 1428, Sept. 1961.
2. R. D. Gold and L. R. Weisberg, "The Degradation of GaAs Tunnel Diodes", *IRE Tran. on Elect. Devices, ED-8*, August 1961.
3. R. L. Longini, "Rapid Zinc Diffusion in Gallium Arsenide", *Solid State Electronics*, 5, p. 127, May-June, 1962.
4. H. J. Henkel, "Aging Phenomena in Gallium Arsenide Tunnel Diodes", *Z fur Naturf., 17a*, p. 358 (1962)
5. A. Pikor, G. Elie, R. Glicksman, "Some Factors Affecting the Degradation of GaAs Tunnel Diodes", *Journal of Electrochemical Society.*
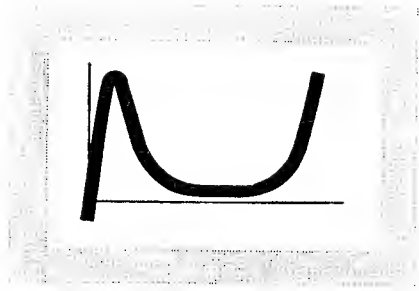
SWITCHING

BECAUSE of its high frequency capabilities and small power requirements, the tunnel diode exhibits excellent switching characteristics. At the present time, tunnel diodes are being widely used as ultra-fast rise-time pulse generators and in ultra-fast counter circuits. They are also especially promising for digital-computer applications in which they offer speeds up to several hundred times faster than those available with transistor circuits. If speeds equivalent to those of transistors are satisfactory, tunnel-diode circuits can be designed which require only a small fraction of the power consumption of the best transistor micro-power circuit.

SWITCHING THEORY

Fig. 24 shows a simple tunnel-diode switching circuit which has a high-impedance input and a constant load resistance. The load line for this circuit and its intersections (points 1 and 3) with the typical tunnel-diode characteristic curve are shown in Fig. 25. When the power is first turned on, point 1
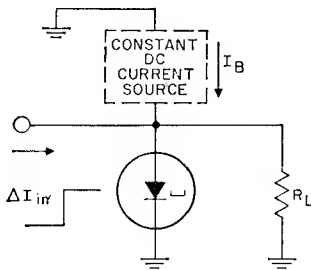
Fig. 24. Tunnel-diode switching circuit loaded with linear resistance.

is the circuit operating point. When a step input of current $\triangle I_{in}$ is applied, the load line shifts, as shown by the dashed
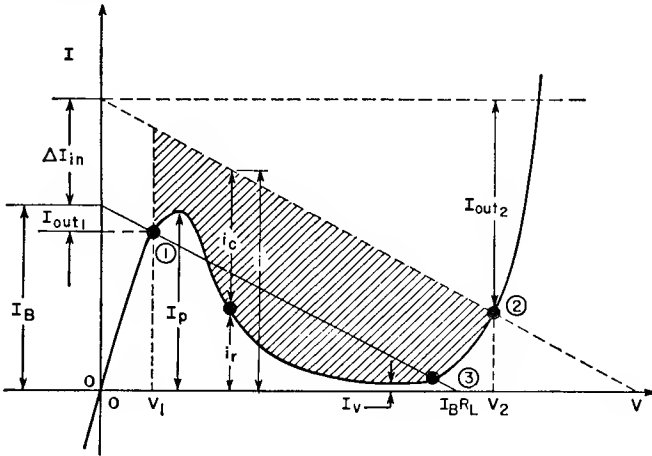
Fig. 25.   Tunnel-diode characteristic with switching
load line.

line in Fig. 25, and the operating point switches from point 1 to point 2. The **forward-current gain** G for the circuit is the ratio between the increase in current to the load ($I_{out2} - I_{out1}$) and the increase in the input current ($\triangle I_{in}$), as follows:

$$G = \frac{I_{out2} - I_{out1}}{\triangle I_{in}} \tag{13}$$

Because the value of $I_{out2} - I_{out1}$ can never be greater than the value of $\triangle I_{in} + I_P - I_V$, the maximum current gain G_{max} is given by

$$G_{max} = 1 + \frac{I_P - I_V}{\triangle I_{in}} \tag{14}$$

Eq. (14) indicates the importance of a large peak-to-valley-current ratio in the determination of the ultimate gain of tunnel diodes.

The **switching speed** of a tunnel diode is determined primarily by its junction capacitance and negative resistance. In the equivalent circuit shown in Fig. 11, the series resistance R_s and the junction resistance R_j determine the static characteristic of the tunnel diode. The series inductance L_s and the junction capacitance C_j together with R_s and R_j, limit the transient or switching response. The series resistance is generally negligible in switching; if spurious oscillations and recovery time are not considered, the series inductance may also be neglected

in the determination of rise time or switching speed. Fig. 26 shows the simplified equivalent circuit for tunnel-diode switching.
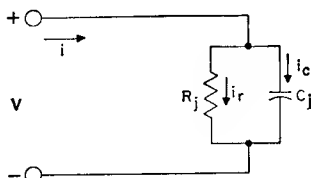
Fig. 26.   Simplified tunnel-diode equivalent circuit.

The junction capacitance C_j may be considered to be constant during switching. Therefore, the switching speed or rise time of the tunnel diode in switching from point 1 to point 2 of Fig. 25 depends solely on the amount of charging current i_c passing through the junction capacitance. This current is the difference between the input current i to the tunnel diode and the current i_r flowing through R_j. The currents i, i_c, and i_r for a particular point during switching are shown in Fig. 25. The **rise time** t_r of the device during switching from point 1 to point 2 is given by

$$t_r = C_j \int_{V_1}^{V_2} \frac{dV}{i_c} \tag{15}$$

where $i_c = i - i_r = (I_B + \triangle I_{in}) - \dfrac{V}{R_L} - i_r$

The fastest switching is accomplished when a constant-current lead line is used (i.e., when R_L is very large). Under these conditions, and if the overdrive is small relative to I_P, then $I_B + \triangle I_{in}$ is approximately equal to I_P, and Eq. 15 can be written as follows:

$$t_r \cong C_j \int_{V_P}^{V_F} \frac{dV}{I_P - i_r} \tag{16}$$

Because under these conditions i_r is generally small in comparison to I_P for most of the switching cycle, it can be approximated as a constant I_V. The equation for rise time can then be simplified as follows:

$$t_r \cong C_j \int_{V_P}^{V_F} \frac{dV}{I_P - I_V} = C_j \frac{V_F - V_P}{I_P - I_V} \tag{17}$$

The value of $V_F - V_P$ is approximately 0.5 volt for germanium and one volt for gallium arsenide. If the small constant current I_v is eliminated from Eq. (17), the following useful relationships can be obtained:

$$\text{for germanium } t_r \cong \frac{C}{2\ I_P} \qquad (18)$$

$$\text{for gallium arsenide } t_r \cong \frac{C}{I_P} \qquad (19)$$

In both these relationships, constant-current load-line switching is assumed.

Tunnel-diode **fall time**, i.e., switching time from a high to a low state, is calculated in a manner similar to that described above for rise time.

The series inductance L_s has very little effect on rise and fall times, especially if constant-current switching is used. However, the series inductance does affect **recovery time** and, therefore, limits the maximum repetition rate of switching. For example, when a tunnel diode is switched from the peak point to the high-voltage region, the current must then be reduced to the valley point before the diode can be switched to the low-voltage region. The time required to reduce the current to the valley point is limited by the time constant L_S/R_D, where R_D is the average value of the diode resistance in the high-voltage region. The recovery time in the low-voltage region is affected in the same manner.

MULTIVIBRATOR CIRCUITS

When suitable biasing is used, tunnel diodes may be utilized in astable, monostable, or bistable modes of operation. The dc load lines required for these three modes are shown in Fig. 27, and a circuit for obtaining the required biasing is shown in Fig. 28. The dc load line I, which intersects the tunnel-diode characteristic at point A in the unstable negative-resistance region, provides biasing for the **astable** mode. Load line II, which intersects the tunnel-diode characteristics at the stable point B, provides biasing for the **monostable** mode. Load line III, which intersects the tunnel-diode characteristics at the two stable operating points C and E, provides biasing for **bistable** operation (point D is unstable and is not used).
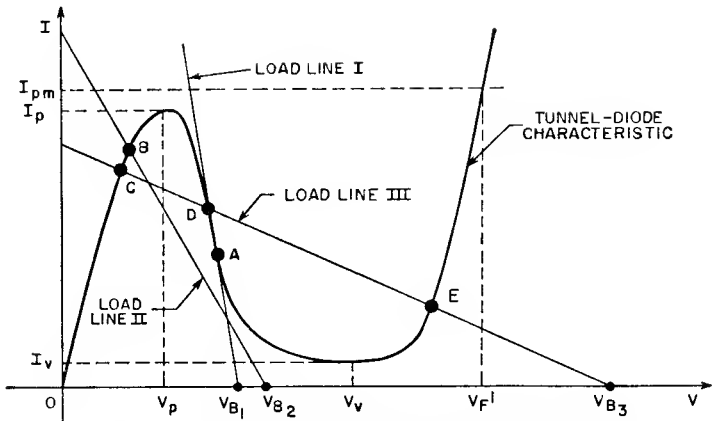
Fig. 27.   Tunnel-diode characteristic showing three
basic types of biasing modes.
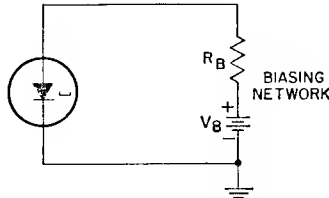
Fig. 28.   Tunnel-diode biasing circuit.

Astable Multivibrator

The design of tunnel-diode astable multivibrators or **relaxa-
tion oscillators** uses the astable biasing mode shown by the
dc load line I in Fig. 27. A circuit of this type is shown in Fig.
29a; V_{B_1} and R_{B_1} provide the necessary load line, and induc-
tance L_1 controls the frequency of operation. Three criteria
must be met for this circuit to perform properly: (1) the dc
load resistance R_{B_1} must be less than the minimum negative
resistance of the tunnel diode, i.e., $R_{B_1} < R_{min}$; (2) the load
line must intersect the tunnel-diode characteristic in the nega-
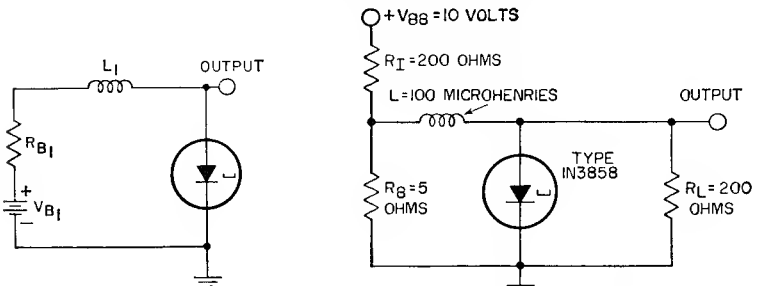
Fig. 29.   (a) Basic tunnel-diode astable multivibrator
and (b) practical circuit.

tive-resistance region, i.e., $V_P < (V_{B_1} - I_D R_{B_1}) < V_V$, where I_D is the static tunnel-diode current; (3) the total inductance must be large enough so that the biasing point is unstable under ac conditions, i.e., $(L_1 + L_s) > (R_{B_1} + R_s) R_{min} C_j$. The highest frequency of operation for this type of circuit, therefore, is limited by tunnel-diode inductance, capacitance, and negative resistance.

Fig. 29b shows a practical example of a tunnel-diode astable multivibrator circuit. The frequency of oscillation for this circuit is 100 megacycles. The equivalent dc-load resistance R_{B_1} is equal to $(R_B) \times (R_I)$ divided by $(R_B + R_I)$, or 4.875 ohms. The equivalent supply voltage V_{B_1} is equal to $(V_{BB}) \times (R_B)$ divided by $(R_B + R_I)$, or 244 millivolts.

The linearized tunnel-diode characteristic shown in Fig. 30 illustrates the switching trajectory and allows an approximate determination of the **repetition rate**. When L_1 is assumed to be large enough to permit negligible current change during switching, the switching trajectory given by path ABCD in the
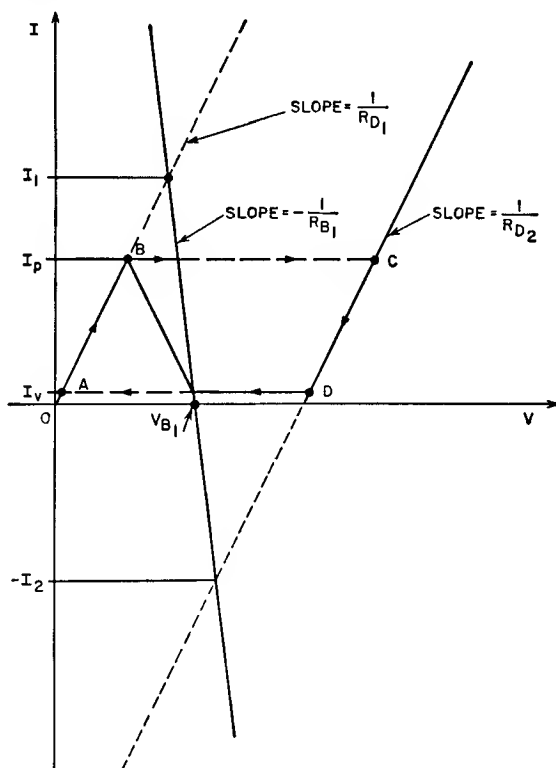
Fig. 30.   Astable circuit operation shown on linearized tunnel-diode characteristic.

diagram is obtained. The time during which the tunnel diode is in the low-voltage state AB is determined by the charging of L_1 through R_{D_1} and R_{B_1}, as follows:

$$t_{AB} = \frac{L}{R_{B_1} + R_{D_1}} \ln \frac{I_1 - I_V}{I_1 - I_P} \tag{20}$$

where R_{D_1} is the diode resistance in the low-voltage state and I_1 is as defined in Fig. 30. The time during which the tunnel diode is in the high-voltage state CD is determined by the discharging time of L_1, as follows:

$$t_{CD} = \frac{L}{R_{B_1} + R_{D_2}} \ln \frac{I_2 + I_P}{I_2 + I_V} \tag{21}$$

where R_{D_2} is the diode resistance in the high-voltage state and I_2 is as defined in Fig. 30. Because these times are much longer than the time spent in the negative-resistance region, the repetition rate, or frequency f, of the astable circuit is given by

$$f = \frac{1}{t_{AB} + t_{CD}} \tag{22}$$

Fig. 31a shows the output waveform calculated for the linearized tunnel-diode astable multivibrator. An actual tunnel-diode output appears as shown in Fig. 31b. As shown, the time spent in the negative-resistance region is very short.
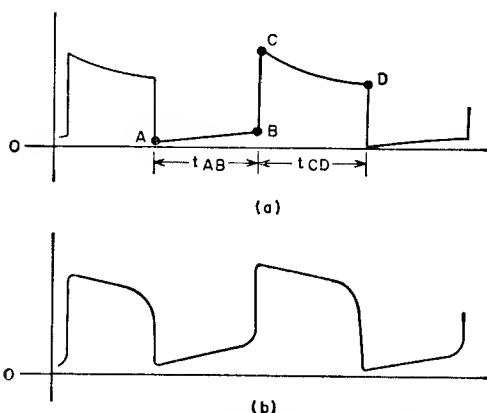
Fig. 31.   Astable multivibrator waveforms for (a) linearized tunnel diode and (b) actual tunnel diode.

Monostable Multivibrator

Tunnel-diode monostable multivibrators may be designed in a manner similar to that described for the astable multivibrator. Monostable operation is obtained when the biasing

characteristic or dc load line intersects the tunnel-diode volt-
age-current curve at only one stable point, either below the
peak point or above the valley point, as shown in Fig. 32a. A
typical monostable multivibrator circuit is shown in Fig. 32b;
waveforms for the two modes of biasing are shown in Fig. 33.
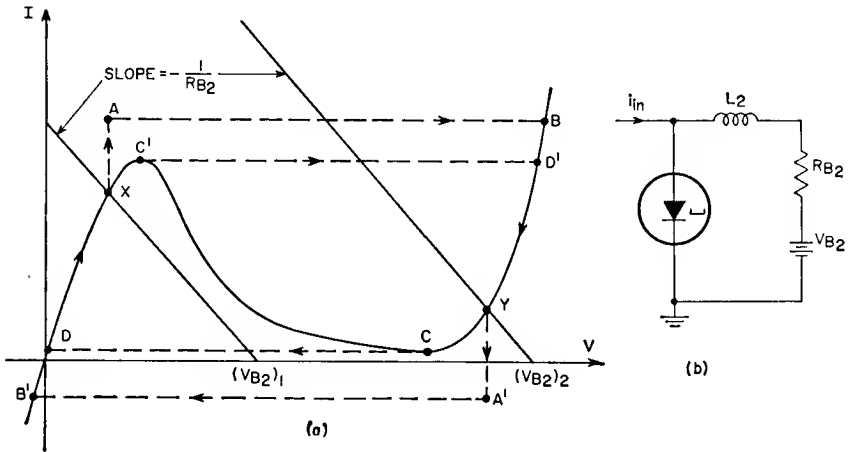
Fig. 32.   (a) Biasing characteristic and (b) mono-
stable multivibrator circuit.
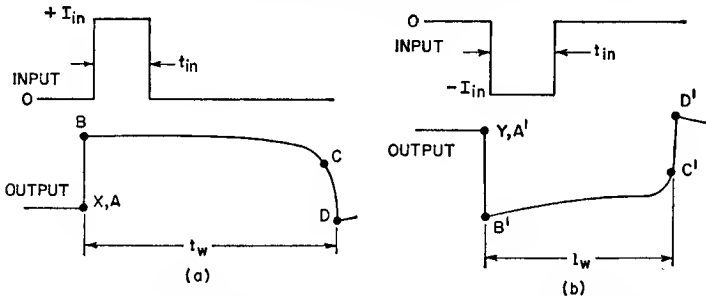
Fig. 33.   Waveforms for tunnel-diode monostable
circuit at (a) biasing below the peak point
and (b) biasing above the valley point.

For proper "one-shot" operation, the input pulse width t_{in} must
satisfy the following relationship:

$$t_r < t_{in} < t_w \qquad (23)$$

where t_w is the **delay time,** or pulse width of the output wave-
form, and t_r is the tunnel-diode rise time or switching time.

The pulse width is controlled by the size of the inductance
L_2, the resistance R_{B2}, and the resistance presented by the tun-
nel diode. When the idealized tunnel-diode characteristic shown
in Fig. 34a is used, the approximate pulse width may be cal-
culated for a condition of biasing below the peak-point, as
follows:

$$t_w = \frac{L_2}{R_{B_2} + R_{D_2}} \ \ln \ \frac{I_2 + I_D + I_{in}}{I_2 + I_V} \qquad (24)$$

where the currents I_2, I_D, I_{in}, and I_V are as given in Fig. 34a.
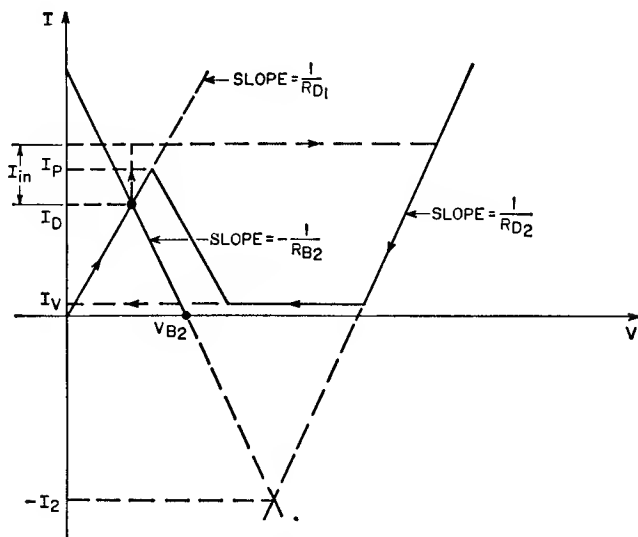
Fig. 34a.   Monostable operation.

Fig. 34b shows a practical example of a monostable multivibrator circuit which uses biasing below the peak point. This circuit has a pulse width, or delay time, of five nanoseconds and a maximum repetition rate of 70 megacycles per second. The equivalent dc load resistance R_{B_2} is 9.75 ohms, and the equivalent supply voltage V_{B_2} is 250 millivolts.
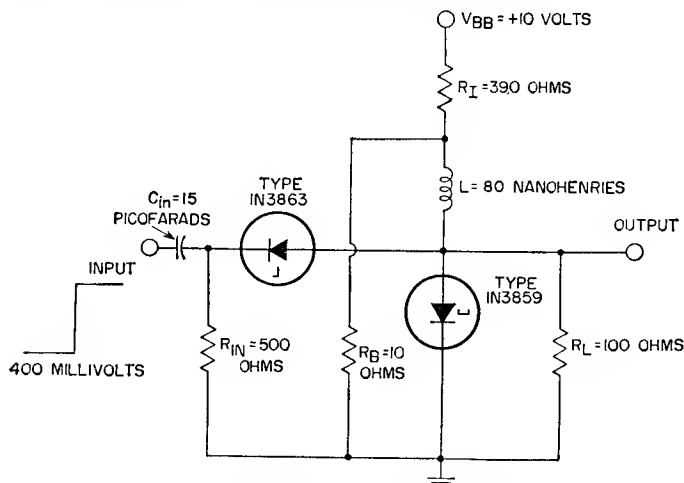
Fig. 34b.   Practical monostable multivibrator.

Bistable Multivibrators

Because of their inherent memory capabilities, tunnel diodes can be readily used in the design of bistable multivibrator circuits. Fig. 35a shows a simple tunnel-diode bistable
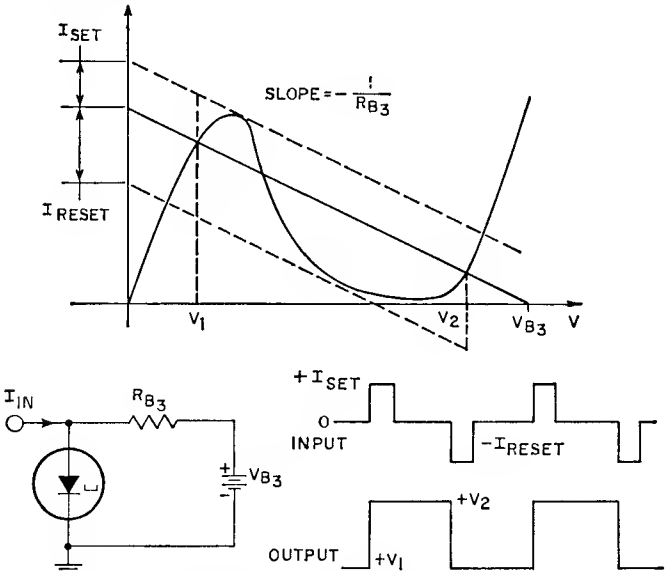
Fig. 35a.   Simple bistable characteristic, circuit, and waveforms.

(flip-flop) circuit and its biasing and waveform characteristics. This circuit requires a positive pulse to set the flip-flop and a negative pulse to reset. A practical example of a set-reset bistable multivibrator circuit is shown in Fig. 35b. This circuit has a maximum repetition rate of 200 megacycles per
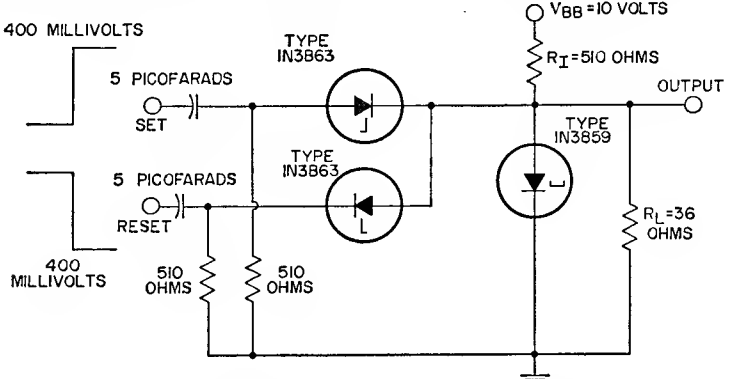
Fig. 35b.   Practical set-reset bistable multivibrator circuit.

second, an R_B resistance of 29.2 ohms, an equivalent load-line resistance R_{B3} of 27.5 ohms, and an equivalent supply voltage V_{B3} of 542 millivolts.

Fig. 36a shows a flip-flop circuit which can be set and reset with pulses of the same polarity. In this circuit, the size of L_3 is determined by a compromise between ease of reset and recovery time of the circuit. Fig. 36b shows a practical
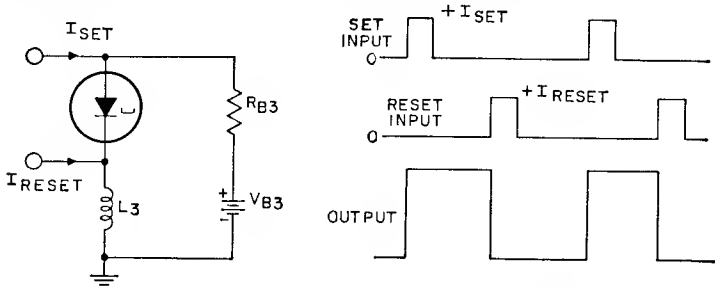
Fig. 36a.   Set-reset flip-flop circuit and waveforms.

example of a set-reset circuit which uses positive triggering. This circuit has a maximum repetition rate of 100 megacycles per second, a load-line resistance of 28.5 ohms, and a load-line voltage of 510 millivolts.
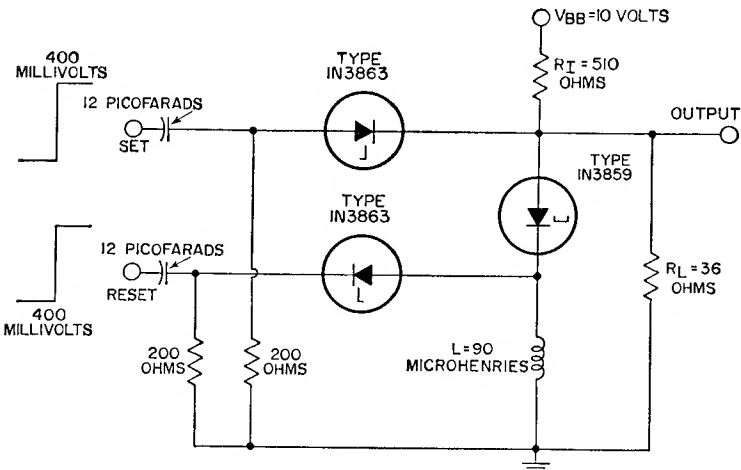
Fig. 36b.   Practical set-reset flip-flop circuit having positive triggering.

The design of a triggered flip-flop circuit[6] using tunnel diodes is somewhat more complicated, as shown in Fig. 37a. Again, the value of the inductance L_3 is determined by a compromise between good triggering and fast recovery time. A practical example of such a circuit is shown in Fig. 37b. This

circuit, which has a maximum repetition rate of 100 mega-
cycles per second, may be cascaded with identical stages to
form a binary-counter circuit.
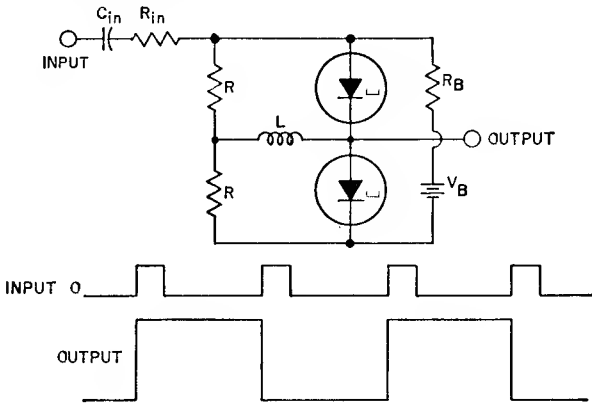
Fig. 37a.   Triggerable flip-flop circuit and waveforms.
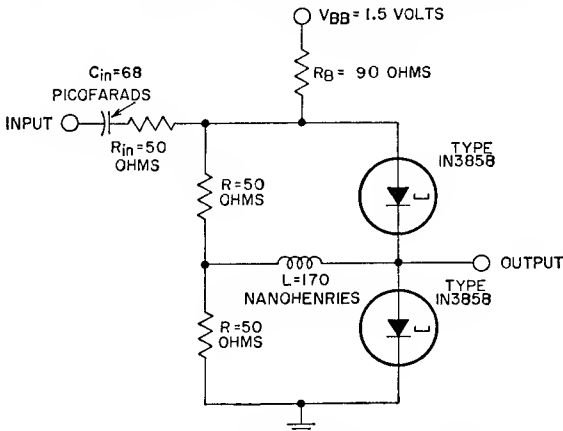
Fig. 37b.   Practical triggerable flip-flop circuit.

LOGIC CIRCUITS

Tunnel-diode switching is accomplished when a given
"threshold" or turning point is exceeded, either the peak point
or the valley point of the device. Thus, the word threshold is
associated with tunnel-diode logic circuits, or **gates**.

Fig. 38a shows a tunnel-diode bistable **OR gate** with re-
set; the operation of such a circuit is shown in Fig. 38b.
Normal biasing for the tunnel diode is at point A. When
any one of the inputs supplies a current I_{in}, the tunnel diode
switches to point B. Upon relaxation of the input, the operat-
ing point moves to C, a stable point. As a result, the tunnel

diode must be reset back to point A before any more logic can be performed. This resetting is accomplished by means of the reset pulse source shown by the dashed load line II.
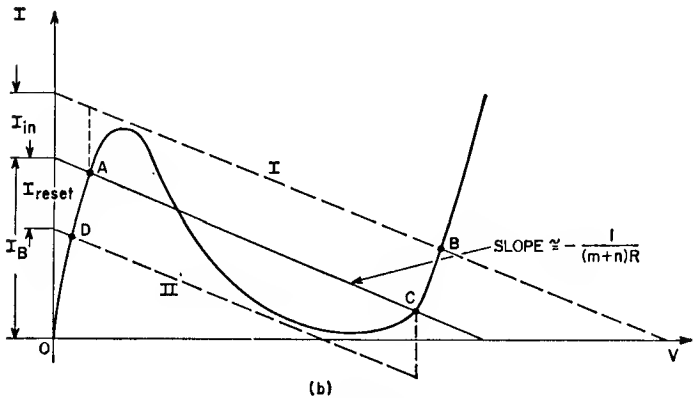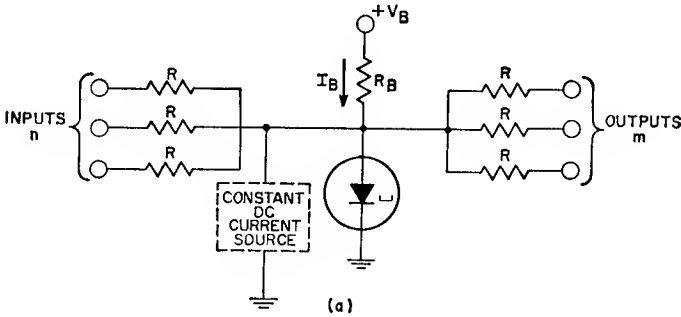
Fig. 38.   (a) Tunnel-diode bistable OR gate with reset and (b) Operating characteristics.

A bistable **AND gate** is designed in a manner similar to that described for the OR gate, except that all inputs must supply current before the tunnel diode switches to the high state.

The logic circuit shown in Fig. 38a has two disadvantages. First, because of the relatively low current gain of the tunnel diode, worst-case design produces a circuit having impractical fan-in and fan-out when realistic tolerances are used. (**Fan-in** is the maximum number of inputs to a logic gate; **fan-out** is the maximum number of outputs that can be driven from a logic gate.) Secondly, because the tunnel-diode input and output terminals are the same, the signal may propagate in either direction; as a result, phased power supplies for V_B are required for unidirectional flow of information. This requirement makes the system much more complex and costly.

Both these disadvantages are overcome by the circuit shown in Fig. 39. This circuit uses a cascaded-amplifier arrangement which produces considerably larger current gain per stage; consequently, reasonable fan-in and fan-out are possible when practical tolerances are used. In this circuit, tunnel diode TD_2 may have a peak current from two to five times that of TD_1, depending upon the tolerances. This higher peak current accounts for the larger amplification.
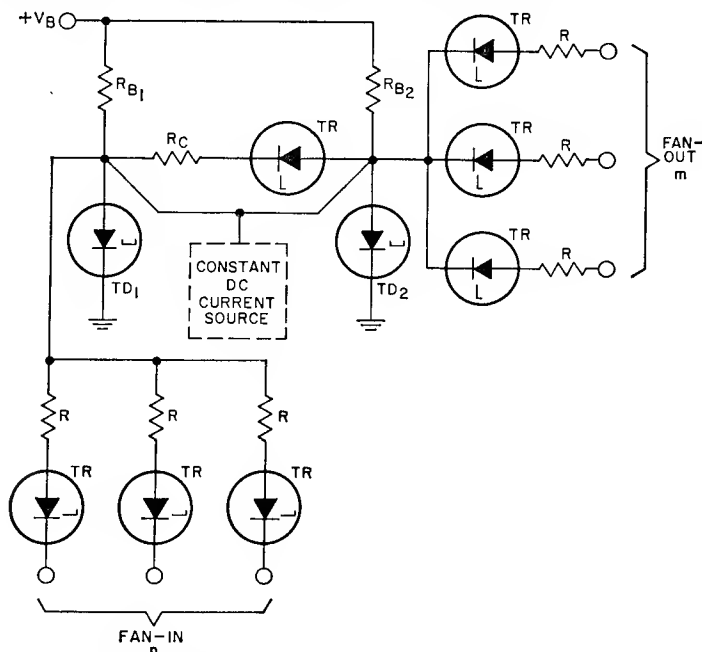
Fig. 39. Cascaded-amplifier bistable OR and AND gate using tunnel rectifiers.

In addition, the circuit of Fig. 39 does not require phased power supplies because the tunnel rectifiers used in the inputs conduct current in only one direction. Although the reset pulse is still required with this circuit, a low-current pulse can generally be used. This pulse may be considered a **clock source** for synchronous logic circuits. The use of tunnel rectifiers also provides better gain by unloading inputs. In cases where extra-large fan-in and fan-out are needed, cascading may be extended to include three tunnel diodes in tandem. If cascading is extended beyond three diodes, the circuit becomes very costly and, at the same time, the stage propagation delay becomes proportionately longer.

A tunnel-diode logic circuit may be made self-resetting if it is monostable rather than bistable, as shown in Fig. 40a. This circuit also offers faster switching speeds than bistable

gates. This advantage is demonstrated in Fig. 40b, which shows that the switching trajectory (dashed line) is constant current during transition from the low to the high state, or vice versa.
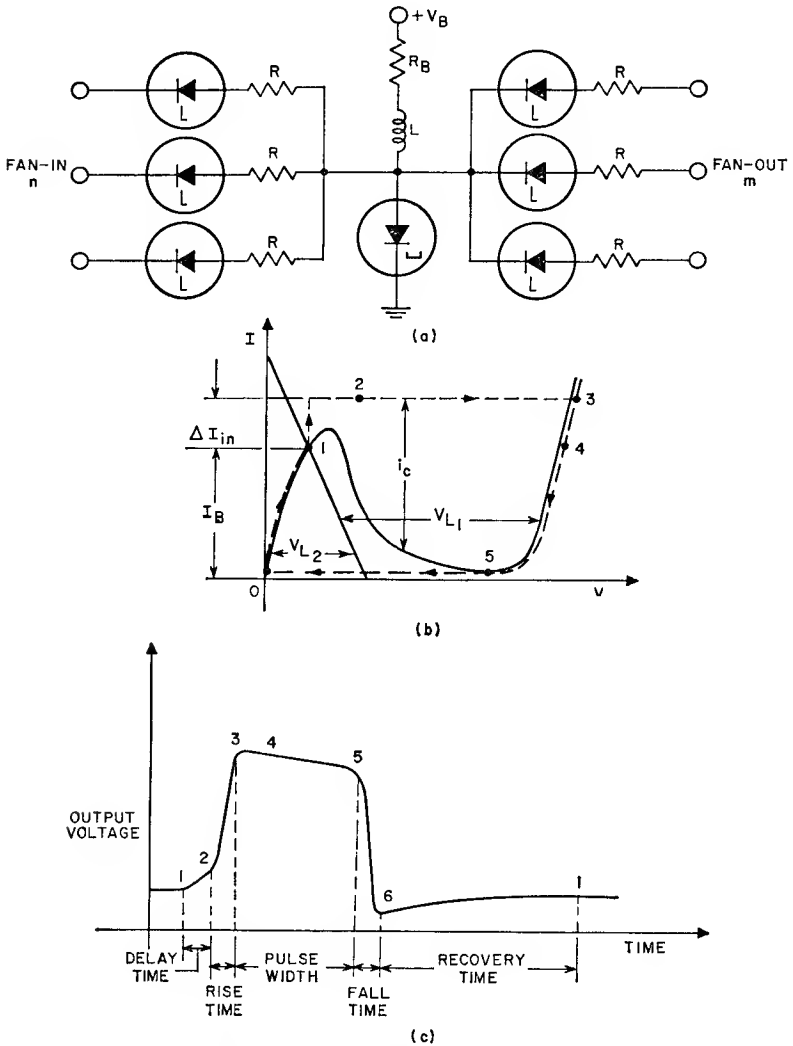
Fig. 40. (a) Monostable logic circuit, (b) operating characteristic, and (c) output waveform.

As indicated by the output waveform in Fig. 40c, both the pulse width and recovery time are determined by the size of inductance L. The rate of change of current through L is given by

$$\frac{diL}{dt} = \frac{V_L}{L} \qquad (25)$$

As a result, the pulse width is inversely proportional to V_{L_1}, and the recovery time is inversely proportional to V_{L_2}, as defined in Fig. 40b.

The pulse width and recovery time determine the maximum repetition rate of the monostable circuit. The minimum pulse width is determined by the driving requirements on the inputs to the gate. Therefore, maximum speed is obtained by making the recovery time as small as possible or by making V_{L_2} as large as possible. This latter requirement can be readily achieved by the use of **nonlinear** biasing.

Nonlinear biasing or load lines are obtained by the use of a **tunnel rectifier,** as shown in Fig. 41a. In this circuit, the
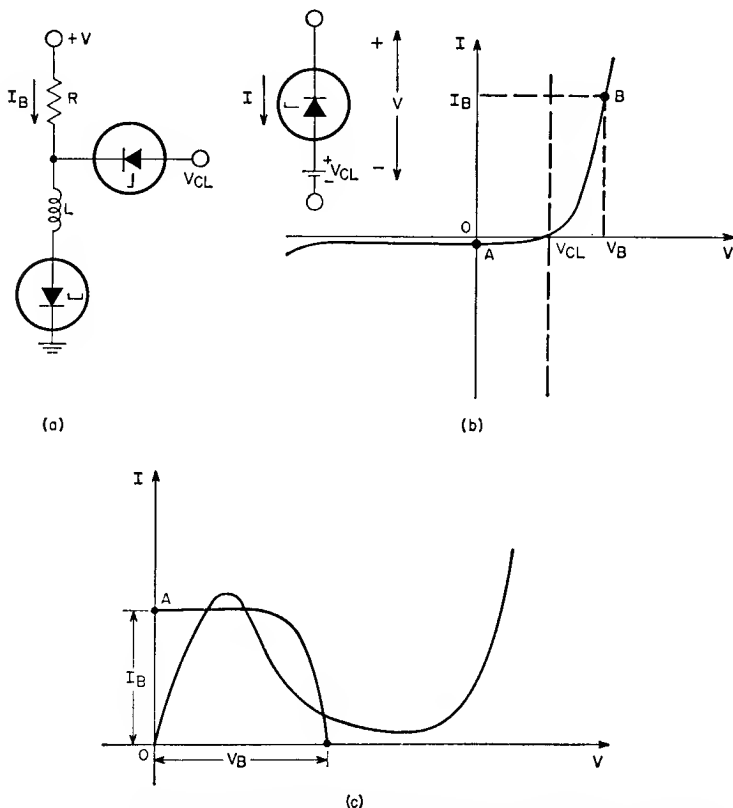
Fig. 41. (a) Tunnel-diode and tunnel-rectifier circuit, (b) composite characteristic of tunnel rectifier and voltage V_{CL} in series, and (c) nonlinear load line on tunnel-diode characteristic.

tunnel rectifier in series with the voltage V_{CL} results in the composite static characteristic shown in Fig. 41b. This non-linear characteristic may be plotted as a load line on the tunnel-diode characteristic in the same manner as a linear load line,[7, 8] as shown in Fig. 41c.

Fig. 42 compares nonlinear and linear biasing, and shows the major advantages of the former. First, nonlinear biasing results in a considerably larger V_{L_2} and, consequently, a much faster recovery time than linear biasing. Secondly, nonlinear biasing significantly improves current-gain capabilities, as shown by the much smaller I_{in} required to switch the tunnel diode over the peak at the same percentage of overdrive.
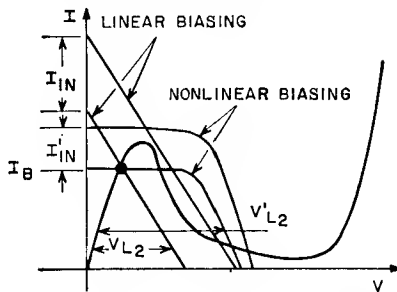
Fig. 42.   Comparison of linear and nonlinear biasing.

A monostable OR-gate circuit and an AND-gate circuit employing nonlinear biasing are shown in Figs. 43 and 44, respectively. These circuits feature tunnel-rectifier coupling for directionality, as well as cascaded monostable amplifiers for sufficient high-speed gain to obtain reasonable fan-in and fan-out.
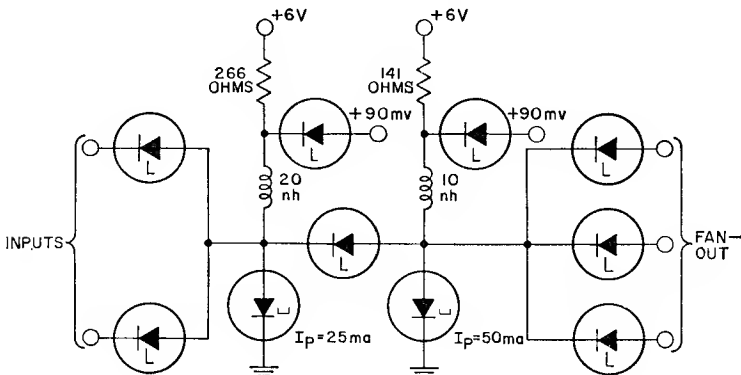
Fig. 43.   Complete monostable OR gate using germanium tunnel diodes and rectifiers.
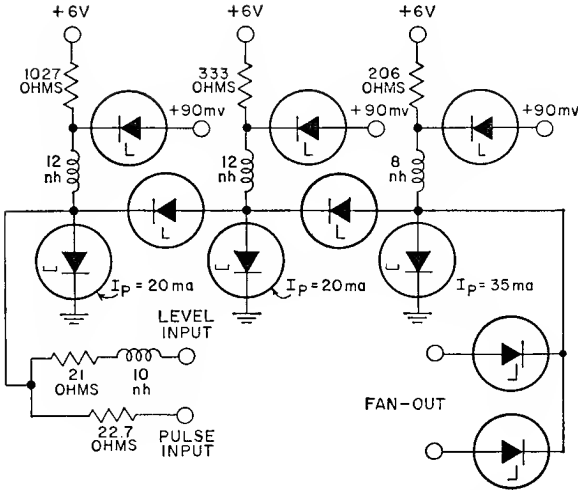
Fig. 44.   Complete monostable AND gate using ger-
manium tunnel diodes and rectifiers.

Fig. 45 shows a compatible level-producing bistable circuit
which can be used with monostable OR and AND circuits. This
bistable circuit is used to obtain storage registers, counters,
and inversion (through the reset input), as well as to eliminate
timing problems in AND gates by gating levels against pulses
wherever necessary.

The three circuits shown in Figs. 43, 44, and 45 form a
complete set of logic blocks (having one-nanosecond logic de-
lays and 200-megacycle per second repetition rates) for use in
a large-scale computer.[9-11] (These circuits as well as that
shown in Fig. 49 use tunnel diodes which are presently in the
development stages. These devices, however, are available from
RCA upon request.) These circuits have all been designed for
worst-case operation. Logical interconnection of these circuits
is accomplished by use of coaxial cable which prevents cross-
talk, effect of common-ground paths, and other transient noise
problems at high speeds (200 megacycle per second and up).

These three logic circuits may be used to build an ultra-
high-speed shift register, as shown in Fig. 46. The shift regis-
ter uses two AND gates and two bistable units in each stage.
A counter may also be constructed by use of a modified form
of the circuit shown in Fig. 46. The circuit is connected in a
ring so that the A_i output is connected to the $\bar{A}_0$ input; the
counter then has a scale of 2i where i is the number of stages in
the ring. This counter functions properly when all stages are
initially set to zero.
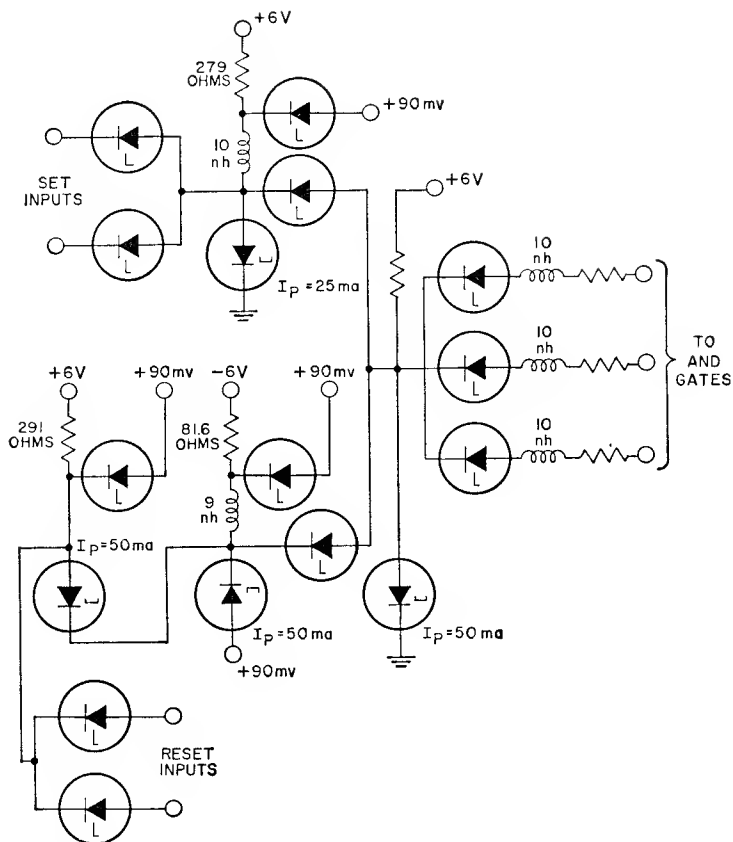
Fig. 45.   High-speed bistable circuit having two set
and reset inputs.
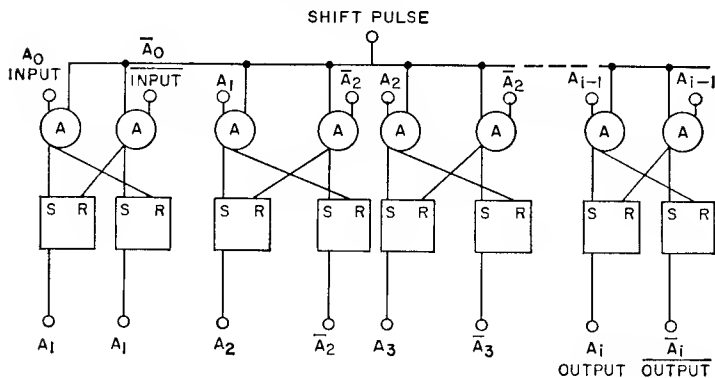
Fig. 46.   Block diagram of shift register.

When low-peak-current tunnel diodes and tunnel rectifiers are used in the circuits of Fig. 43, 44, and 45, a micro-power computer can be designed which requires several hundred times less power than low-power transistor circuits at no sacrifice in operating speed.

COMPUTER MEMORIES

Because of its voltage-controlled negative-resistance characteristic, the tunnel diode is an ideal element for computer memories. Its ultra-high-speed capabilities make the tunnel-diode memory many times faster than other presently used memory systems.

Fig. 47 shows a 25-nanosecond-cycle-time memory cell which uses a germanium tunnel diode and a gallium arsenide tunnel rectifier.[11, 12] The memory cell is read by applying a pulse to the word line which causes a sensed output to appear on the digit line. The write operation is achieved by applying pulses having the indicated polarities to both the word line and the digit line.
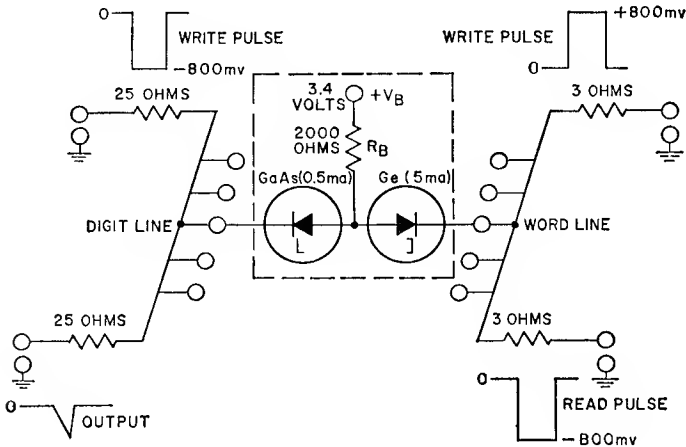
Fig. 47.   Basic memory cell.

The basic operation of the memory cell is demonstrated in Fig. 48. The voltage supply V_B and resistor R_B produce a current which allows the germanium tunnel diode to be either in a low-voltage state (storing a "1") or high-voltage state (storing a "0"), as shown by points A and B, respectively, in Fig. 48a. Reading from the cell is attained by applying a negative word-line voltage to the tunnel diode, as shown in Fig. 48b. If the tunnel diode is in the low state, it is switched to the high

state. Because the current which switches the tunnel diode
must pass through the tunnel rectifier, a negative output pulse
is obtained on the digit line only when the tunnel diode is
caused to switch. Writing into the memory is achieved when
a negative voltage appears on the digit line in coincidence with
a positive voltage on the word line, as shown in Fig. 48c. This
condition switches the tunnel diode to the low state, and a "1"
is set into the cell.
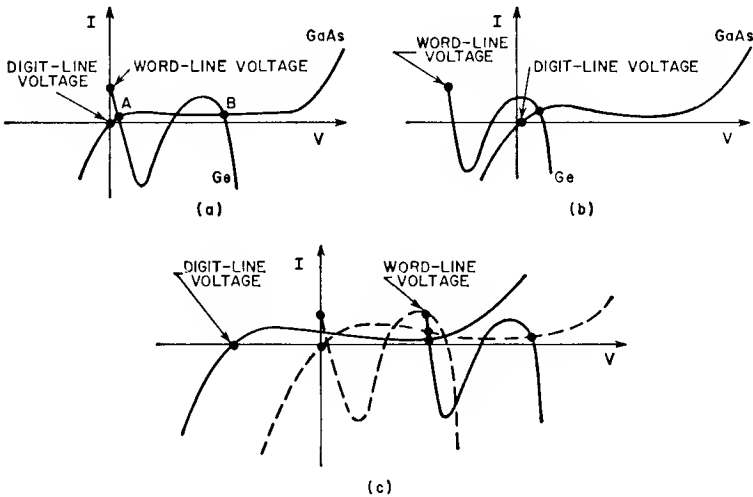
Fig. 48.   Operation of memory cell.

The peripheral circuits (selection, sensing, and driver cir-
cuits[11, 12]) are shown in Fig. 49. The word switch having X
and Y inputs selects the word addressed. The word-switch
driver then places a negative-voltage pulse on the word line,
which reads the information from the memory cell. When a "1"
is stored in the cell, an output is obtained on the digit line
which is in turn amplified by the sense amplifier. The sense
amplifier feeds the output back to the digit driver, which then
places a negative-voltage pulse on the digit line. Because the
word-switch driver is monostable, its negative pulse terminates;
this action in turn causes the word driver to be switched posi-
tively. The positive-pulse output of the word driver to the
word line and the negative-pulse output of the digit driver to
the digit line are made coincident; consequently, the tunnel
diode in the memory cell is reset to the low state and the in-
formation is regenerated. Obviously, if the memory cell origi-
nally contained a zero, there would be no input to the sense
amplifier and no output from the digit driver. The memory
cell would then not be reset, but would remain in the "0" state.
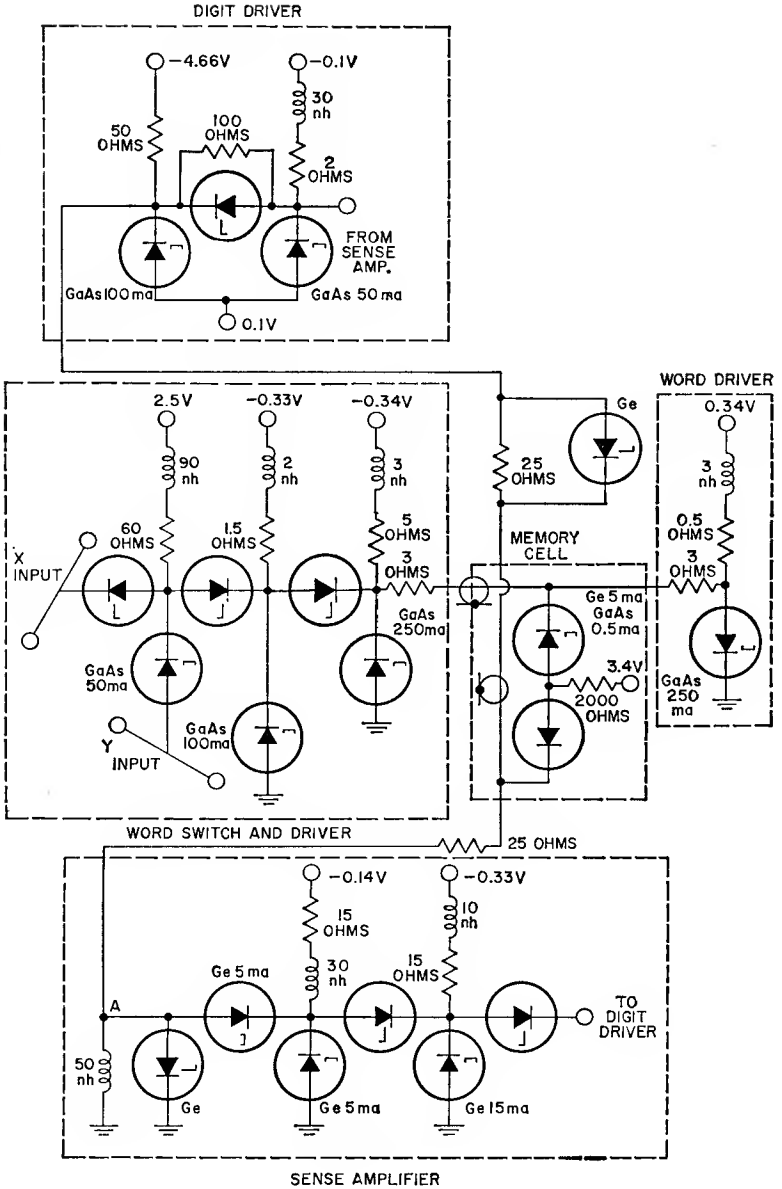
Fig. 49.   Peripheral memory circuits.

HYBRID CIRCUITS

The combination of transistors and tunnel diodes in hybrid circuits offers many advantages. For example, the combination of these two devices in switching circuits offers the possibility of speeds many times faster than those of circuits using transistors only. Accordingly, the speed of present-day computer circuits (particularly those in the arithmetic unit) could be generally improved through the use of hybrid circuits. In addition, hybrid circuits eliminate many of the difficulties of circuits using tunnel diodes only, such as lack of isolation between input and output and the tight tolerances required to achieve reasonable circuit gains. In general, tunnel-diode and transistor hybrid circuits provide a good compromise between high speed and circuit complexity.

Basic Combinations

In the basic tunnel-diode and transistor combination, the tunnel diode is placed in parallel with the base-emitter terminals of the transistor, as shown in Fig. 50a; the resulting composite characteristic is shown in Fig. 50b. This combination can be operated in either the common-emitter or common-base configuration. In **common-emitter** operation, the tunnel diode is used primarily to speed up the input to the transistor; it may also provide some current gain in addition to that obtained from the transistor. In **common**-base operation,[13] the tunnel diode provides all the current gain, as well as high speed. In both modes, the transistor provides both isolation between input and output and voltage gain.
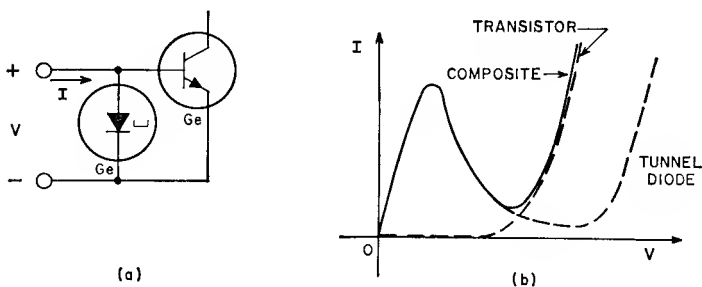
Fig. 50.   (a) Basic tunnel-diode and transistor combination and (b) composite characteristic.

Although Fig. 50a shows the combination of a germanium tunnel diode with a germanium transistor, the use of gallium arsenide tunnel diodes with germanium transistors or the com-

bination of gallium arsenide or germanium tunnel diodes with silicon transistors is also possible. The use of gallium arsenide tunnel diodes with germanium transistors has been found to be the most practical combination because it requires the least control of characteristic-voltage tolerances. The use of silicon transistors requires an offset bias on the emitter even in combination with gallium arsenide tunnel diodes.

Common-Emitter Circuits

The combination of tunnel diodes and transistors in a common-emitter configuration results in a natural bistable circuit, as shown in Fig. 51a. The composite operating characteristic in Fig. 51b shows the two stable points X and Y, and the set and reset currents necessary to accomplish these functions.
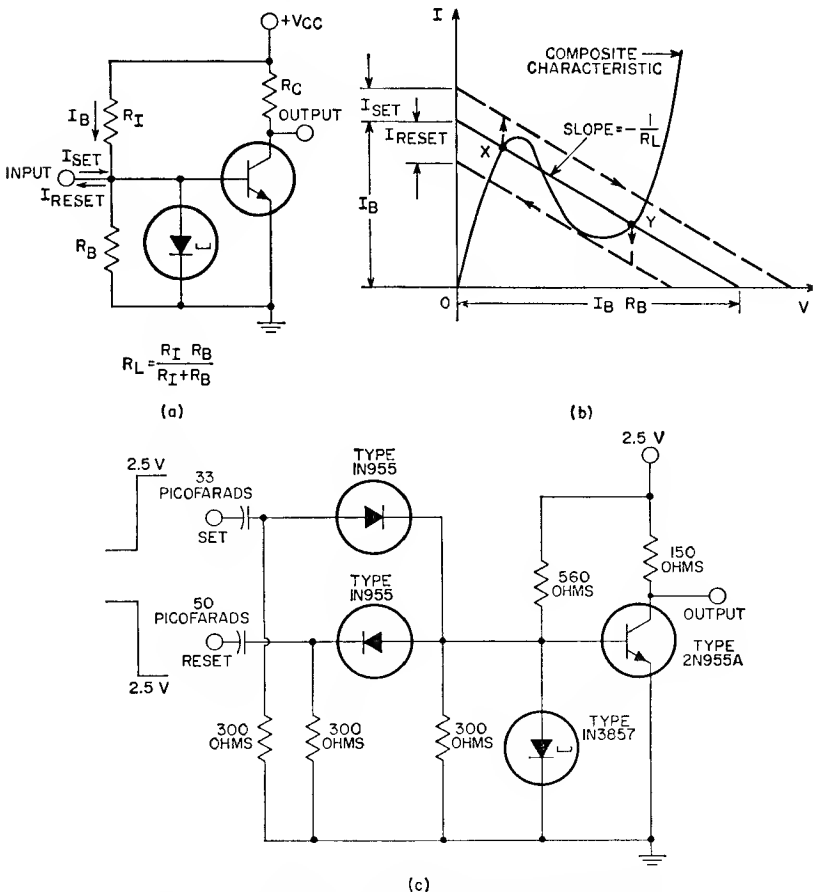
Fig. 51.   (a) Common-emitter bistable circlit, (b) characteristic, and (c) practical circuit.

For proper operation, the current flowing into the base at point B must be sufficient to saturate the transistor. The switching speed of this bistable unit is much faster than that obtained with a transistor alone. Storage and fall time are also fast because the tunnel diode presents such a low impedance during turn-off. In addition, these high speeds are achieved without the use of any reactive or speed-up elements because the tunnel diode provides essentially a perfect step input to the transistor. A practical example of a common-emitter bistable circuit is shown in Fig. 51c. This circuit has a maximum repetition rate of 50 megacycles per second.

Monostable operation of the common-emitter combination is also easily obtained, as shown in 52a. The operation of the circuit is illustrated in Fig. 52b, which shows that the stable

$$R_L = \frac{R_I \, R_B}{R_I + R_B}$$

(a)

(b)

(c)
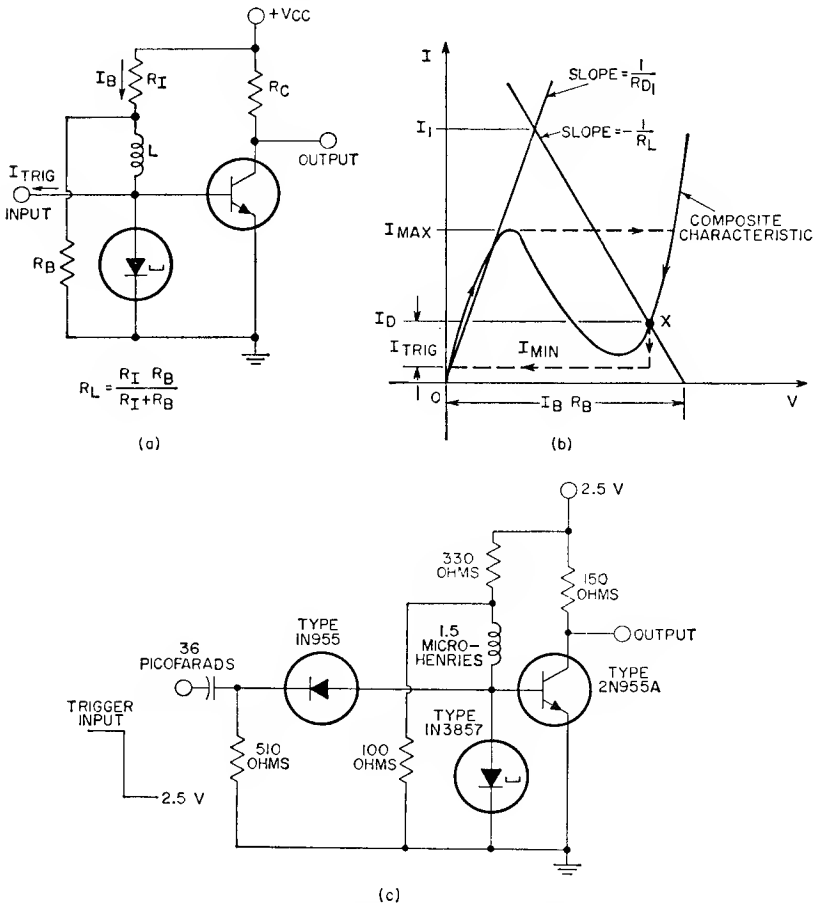
Fig. 52.   (a) Common-emitter monostable circuit, (b) characteristic, and (c) practical circuit.

point on the composite characteristic is established when the transistor is "on" and saturated. A trigger pulse of current momentarily switches the tunnel diode to the low state, and turns the transistor off. The inductance L then allows the current in the tunnel diode to increase towards I_1. When this current, plus the current I_B, exceeds the peak current of the tunnel diode ($I_{max} = I_P$), it switches to the high state, the circuit returns to stable point, and the transistor is turned on and saturated. The pulse width or delay time is the off-time of the transistor and is given by

$$t_{off} = \frac{L}{R_L + R_{D_1}} \ln \frac{I_1 - (I_D - I_{Trig})}{I_1 - I_{max}} \qquad (26)$$

where $R_L = \dfrac{R_I R_B}{R_I + R_B}$ and I_1, I_D, I_{Trig}, and I_{max} are defined in Fig. 52b.

Fig. 52c shows a practical example of a common-emitter hybrid monostable circuit. This circuit has a maximum repetition rate of 25 megacycles per second and a delay time of 20 nanoseconds.

An astable multivibrator circuit is shown in Fig. 53a; the operation of the circuit is described in Fig. 53b. This circuit is astable because the dc load line formed by R_L intersects the composite characteristic in the negative-resistance region. The inductance L causes the circuit to follow the switching trajectory ABCD. As a result, the transistor switches on and off at a rate determined by L and the slope of the composite characteristic in both the on and off regions. When these slopes are
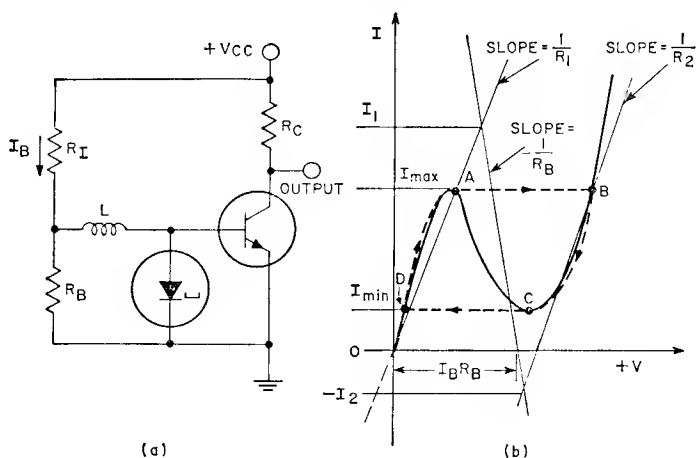
Fig. 53.   (a) Common-emitter astable circuit and
            (b) operating characteristic.

approximated by R_2 and R_1, as shown in Fig. 53b, the on and off times are given by

$$t_{on} \cong \frac{L}{R_L + R_2} \ln \frac{(I_2 + I_{max})}{(I_2 + I_{min})}$$

$$t_{off} \cong \frac{L}{R_L + R_1} \ln \frac{(I_1 - I_{min})}{(I_1 - I_{max})} \qquad (27)$$

where I_1, I_2, I_{max}, and I_{min} are as defined in Fig. 53b.

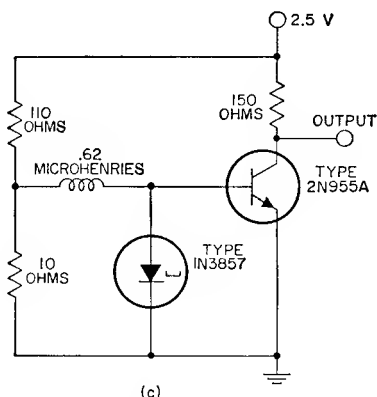Fig. 53c shows a practical example of an astable multivibrator circuit. The frequency of oscillation for this circuit is 20 megacycles.

Fig. 53c.   Practical common-emitter astable circuit.

The bistable, monostable, and astable circuits shown have two major advantages over circuits using only transistors. First, they offer speed and repetition rates considerably faster than those possible without the use of the tunnel diode. Second, they are much simpler in construction and require fewer components.

The common-emitter bistable circuit is a storage element and, therefore, is useful in counters and shift registers. A very simple ring counter[14] using the hybrid bistable circuit is shown in Fig. 54. In this ring-counter circuit, transistors T_1 through T_N are normally cut off; as a result T_1 must be set "on" to start the circuit counting. Thus, T_1 is in the "1" or "on" state and all other transistors are in the "0" state. When a negative-going pulse appears at the input, all the tunnel diodes tend to be switched to the low state, and T_1 is turned off. As
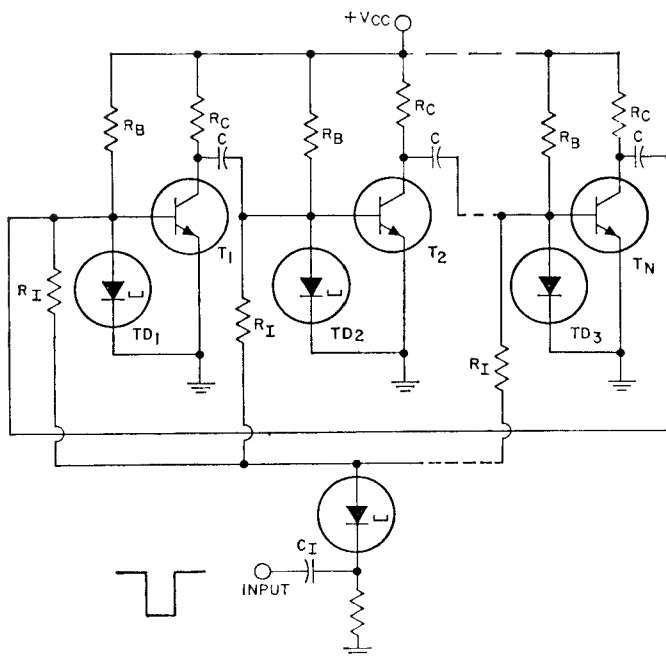
Fig. 54.   Hybrid ring counter.

the collector of T_1 rises toward $+V_{CC}$, current flows through R_C and C into the base circuit of T_2. This instantaneous current is greater than the sum of the input current and the peak current of TD_2. Therefore, TD_2 is switched to the high state, and T_2 is turned on to the "1" state. Because the current through C decays exponentially as it charges toward V_{CC}, the input current must be terminated before the capacitor current becomes small enough to return TD_2 to its low state. Thus, the following two conditions on input-pulse length must be satisfied for effective operation:

INPUT-PULSE LENGTH $>$ TRANSISTOR TURN-OFF TIME

INPUT-PULSE LENGTH $<$ TURN-OFF TIME +
CURRENT DECAY TIME

These conditions are achieved by proper selection of C_1 to provide the necessary differentiated waveform from the input.

A shift register using the common-emitter bistable circuit is shown in Fig. 55. This shift register uses two of the basic bistable units to form one stage. The message is read into T_1 and then shifted by a channel-A clear pulse to T_1' for temporary storage so that T_1 can receive the next bit. The channel-B clear pulse follows the channel-A clear pulse so that the first
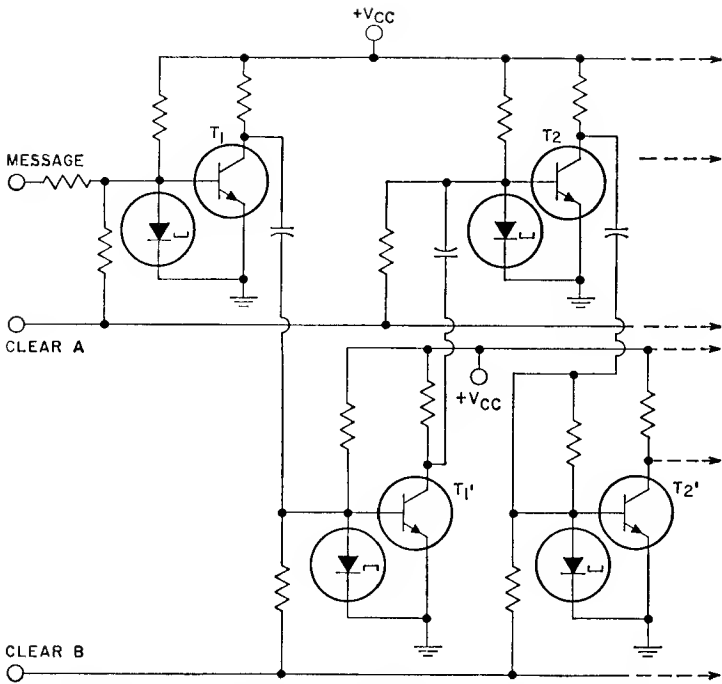
Fig. 55.   Hybrid shift register using two bistable units.

bit is shifted into T_2 before the next clear pulse from A is generated.

Fig. 56 shows a shift register which uses only one basic bistable unit to form a stage. In this circuit, small time delays are necessary to prevent the signal from the previous stage from appearing at the same time as the shift pulse. This shift register therefore uses a dynamic type of temporary storage
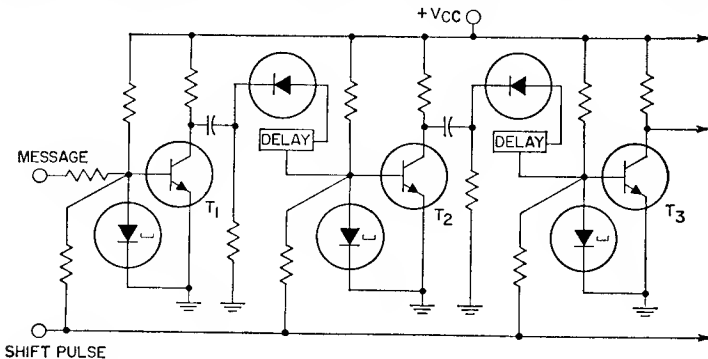
Fig. 56.   Hybrid shift register using one bistable unit.

rather than the static temporary storage used in Fig. 55.

Common-Base Circuits

The common-base configuration is the fastest of the tunnel-diode and transistor combinations, because the tunnel diode provides all the current gain at very high speed. Consequently, common-base operation appears to be the best selection for high-speed logic circuits. However, common-emitter circuits offer much higher current-gain possibilities and, therefore, larger fan-in and fan-out for the same component tolerances. Consequently, if lower speeds are acceptable, common-emitter circuits are the best choice.

The basic common-base hybrid logic gate is shown in Fig. 57a; a practical example of this circuit is shown in Fig. 57b.

"OR" GATE		"AND" GATE	
R = 1100 ohms	Max. m = 2	R = 1050 ohms	Max. m = 2
R_B = 465 ohms	n = 3	R_B = 680 ohms	n = 6
R_C = 865 ohms		R_C = 890 ohms	
$V_{CC} = V_{BB}$ = 15 volts		$V_{CC} = V_{BB}$ = 15 volts	
V_{CL} = 5 volts		V_{CL} = 5 volts	
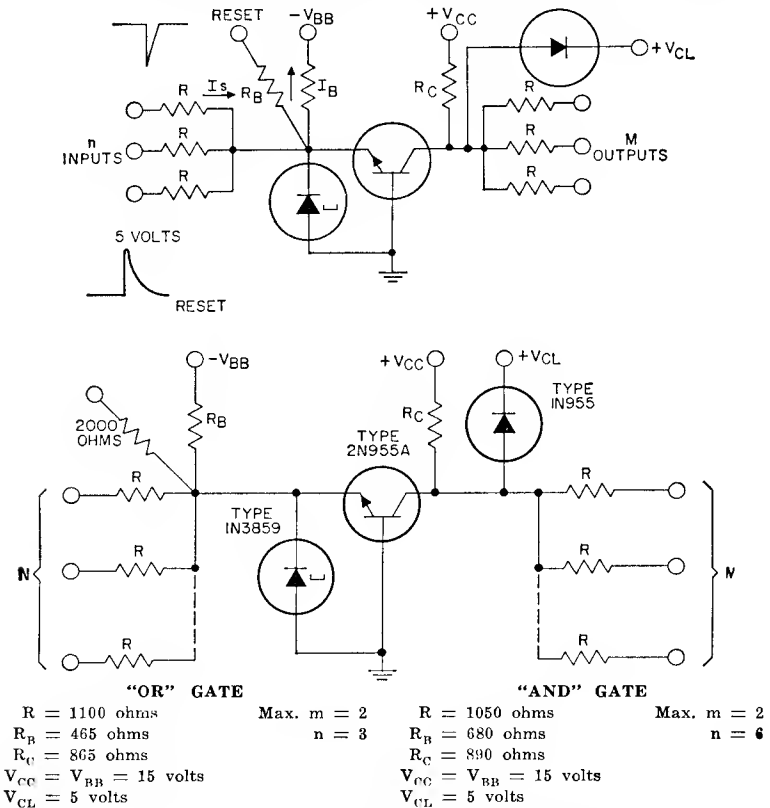
Fig. 57.   (a) Basic common-base logic gate and (b) practical common-base logic gate having propagation delay of five nanoseconds per stage.

The operation of this circuit as an OR or AND gate is dependent upon the bias current I_B and the number of inputs n, as shown in Figs. 58 and 59. In both cases, it is assumed that a current I_S flows into each of the inputs when the gate is not energized. The effect of a pulse at any one of the inputs is that the current out of the tunnel-diode node is increased by the amount I_S.
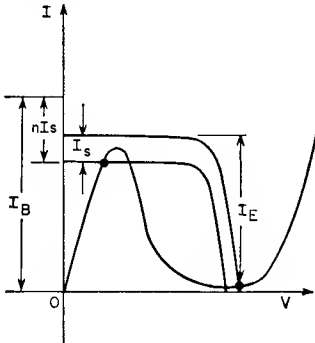
Fig. 58.   OR-gate biasing.   Fig. 59.   AND-gate biasing.
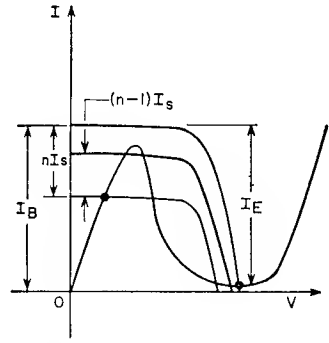
The output rise time of this logic circuit is primarily determined by the current step response of the transistor and the output capacitance from collector to ground. The total signal-propagation delay per stage in this type of circuit is the sum of the tunnel-diode delay, the transistor turn-on delay, and the transistor rise time. This type of circuit offers stage delays as low as a few nanoseconds when fast, low-capacitance transistors are used.

Fig. 60 shows the inversion circuit, or complementary gate, for common-base logic circuits. In this circuit, the state of the
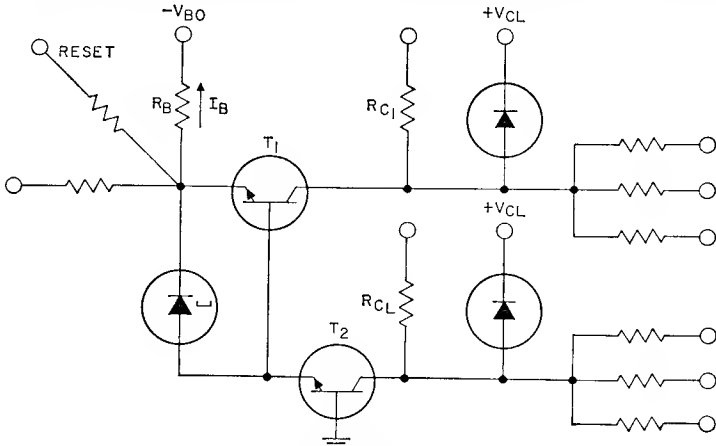
Fig. 60.   Basic complementary gate.

tunnel diode determines which of the transistors becomes energized. When the tunnel diode is in the low state, transistor T_1 is not conducting and T_2 is conducting. When the tunnel diode is switched to the high state by the proper input, T_1 is made to conduct, and T_2 is effectively cut off because it receives only the base current from T_1.

The unique current-routing properties of the complementary-gate circuit permit the design of many simple circuits offering both improvements in speed and savings in components. Among these circuits is the binary adder shown in Fig. 61a. The operation of this circuit assumes that a "0" input corresponds to the current I_S, and, that a "1" drops the input current to zero. Therefore, if all inputs are "0", the net current out of node A is zero, and both transistors are cut off (C_N and S_N equal "0").
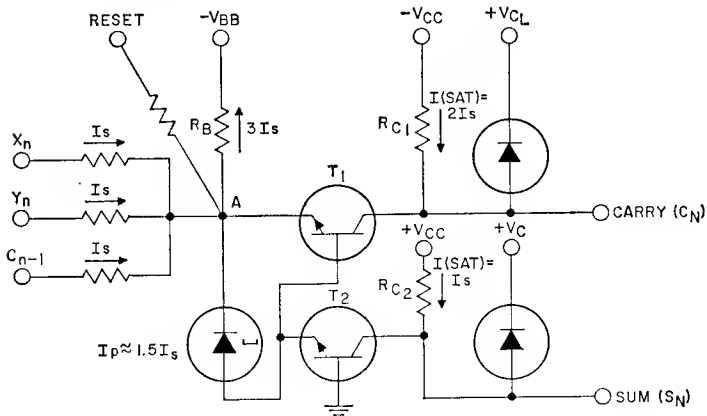
Fig. 61a.   Hybrid full-adder circuit.

If any one of the inputs becomes negative, the net current out of node A is I_S. Because I_S is less than the peak current I_p, it flows entirely through the tunnel diode and in transistor T_2, which is then turned on and saturated while T_1 remains cut off ($C_N = 0$, $S_N = 1$). When any two of the inputs go to "1", the net current out of node A is $2 \times I_S$; because this current is then greater than I_p, the tunnel diode is switched to the high state. Hence, all this current ($2 \times I_S$) flows in T_1, and T_2 is essentially cut off because it receives only the base current of T_1 ($C_N = 1$, $S_N = 0$).

If all three inputs are "1", the current out of node A is $3 \times I_S$; as a result, the tunnel diode is in the high state and transistor T_1 is conducting. However, the collector circuit is designed so that T_1 saturates at a current of $2 \times I_S$. This condition means that the net base-current flow of T_1 must be ap-

proximately I_S (assuming negligible current through the tunnel diode). Therefore, T_2 is receiving a current I_S and is also on and saturated (and the outputs $C_N = 1$, $S_N = 1$ are achieved).

Fig. 61b shows a practical example of the binary adder circuit. The typical propagation delay for this circuit is eight nanoseconds for "carry", and 16 nanoseconds for "sum". In this example, the C_n output can be used to drive the C_n input of the n + 1 state.
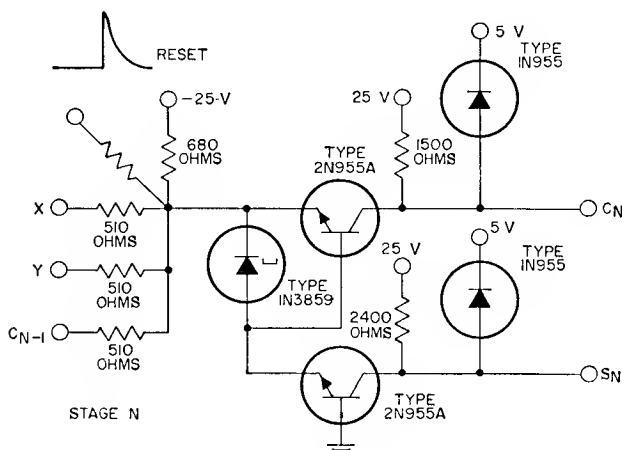

Fig. 61b.   Practical example of binary adder circuit.

REFERENCES

6. H. Ur, "Tunnel-Diode Binary Counter Circuit", *Proc. IRE*, June, 1961.

7. M. H. Lewin, "Negative-Resistance Elements as Digital Computer Components", Ph.D. Thesis, Princeton University, June, 1960.

8. B. Rabinovici and J. Klopper, "Designing Tunnel-Diode Circuits Using Composite Characteristics", *Electronics*, February 16, 1962.

9. R. H. Bergman, "Tunnel-Diode Logic Circuits", *Trans. IRE PGEC*, December, 1960.

10. R. H. Bergman, M. Cooperman, and H. Ur, "High-Speed Logic Using Tunnel Diodes", *RCA Review*, June, 1962.

11. RCA Project Lightning (NOBSR-77523), Report No. 11a, Aug. 31, 1961, (Available from Office of Technical Services, Department of Commerce, Washington, D.C.)

12. M. M. Kaufman, "A Tunnel-Diode—Tunnel-Rectifier 15-Nsec Memory", *Solid State Design*, February, 1962.

13. J. J. Amodei and W. F. Kosnocky, "High-Speed Logic Using Common-Base Transistors and Tunnel Diodes", *RCA Review*, December, 1961.

14. F. P. Heiman, "100-Mc Tunnel-Diode Ring Counter", *Proc. IRE*, July, 1961.
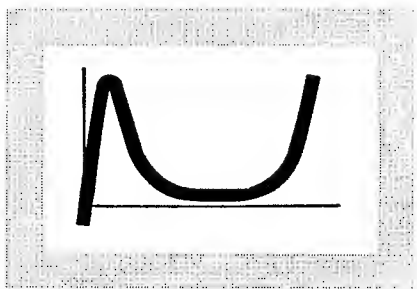
MICROWAVE
OSCILLATORS

TUNNEL diodes hold great promise as microwave oscillators because they are not limited by transit-time effects. Specially constructed experimental units have produced fundamental oscillations at frequencies as high as 100 gigacycles.[15, 16] Commercially available tunnel diodes can be used in oscillators having useful power outputs at frequencies as high as X-band.[17-19]

Compared to vacuum tubes, tunnel diode oscillators are inexpensive, require only a fraction of a volt dc bias, and are rugged and reliable in severe environments. Compared to transistor-driven varactor frequency-multiplier circuits, they are simple and compact, and afford higher dc-to-rf conversion efficiencies.

CIRCUIT ANALYSIS

Practical microwave tunnel-diode oscillators generally use transmission-line or waveguide circuits. For the following analysis, however, the much simpler case of lumped-element circuits is considered. Many properties of distributed oscillator circuits can also be determined from such an analysis. In addition, lumped circuits themselves are of considerable practical interest for many applications.

Fig. 62 shows an equivalent tunnel-diode circuit which is useful for analysis of oscillator circuits at frequencies up to X-band. For rf applications, R_j (v) in Fig. 62 represents the incremental junction resistance at the bias point $(R_j$ (v) = $dv/dI_j)$. For most of the region of interest, this quantity is negative.
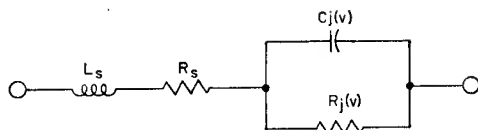
Fig. 62.　Tunnel-diode equivalent circuit for micro-
wave frequencies.

The junction capacitance $C_j(v)$ is given by the following
relation:

$$C_j(v) = K (\phi - v)^{-1/2} \qquad (28)$$

where ϕ is the contact potential (approximately 0.8 volt for
germanium and 1.1 volt for gallium arsenide) and K is a
constant.

From Fig. 62, the impedance of the tunnel diode Z_d at its
terminals is given by

$$Z_d = R_s - \frac{|R_j|}{R_j^2 C_j^2 \omega^2 + 1} + j \left(\omega L_s - \frac{R_j^2 C_j \omega}{R_j^2 C_j^2 \omega^2 + 1} \right) \quad (29)$$

From this expression, two parameters of a tunnel diode
may be derived which are of prime importance in the consid-
eration of rf oscillation. The first of these is the **resistive cut-
off frequency,** i.e., the frequency above which the real part of
the diode impedance is positive. This frequency f_{ro} is given by

$$f_{ro} = \frac{1}{2\pi |R_j| C_j} \sqrt{\frac{|R_j|}{R_s} - 1} \qquad (30)$$

The second important parameter is the **self-resonant fre-
quency,** i.e., the frequency at which the imaginary part of the
diode impedance is zero. This frequency f_{xo} is given by

$$f_{xo} = \frac{1}{2\pi} \sqrt{\frac{1}{L_s C_j} - \frac{1}{R_j^2 C_j^2}} \qquad (31)$$

Below self-resonance, the diode is capacitive; above self-
resonance, it is inductive. It is obvious that a tunnel diode does
not oscillate at frequencies above f_{ro}. (Harmonies, however,
may be produced at frequencies several times f_{ro}.)

OPERATION BELOW SELF-RESONANCE

The circuit shown in Fig. 63a represents the simplest
tunnel-diode oscillator for frequencies below self-resonance.
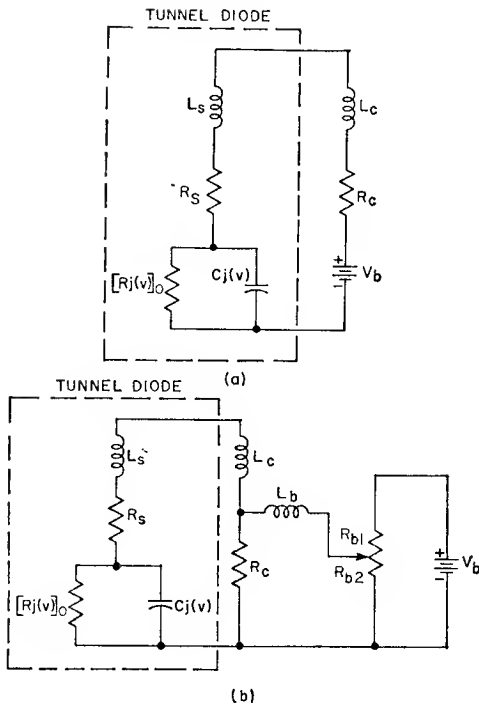
Fig. 63.   Tunnel-diode circuits for operation below
self-resonance.

This arrangement consists of a tunnel diode shunted by a series
inductance L_c, a series resistance R_c and a dc voltage source
V_b, which is usually a battery. If, as in many cases, the lead
inductance associated with V_b is much greater than the desired
value of L_c, the circuit shown in Fig. 63b may be used. In this
circuit, the resistor R_c may be placed very close to the diode.
As a result, the inductance of the bias leads L_b does not affect
the operation of the circuit, provided both R_{b1} and R_{b2} are
much larger than R_c.

The complete solution of the circuit of Fig. 63 may be ob-
tained by use of Kirchhoff's current-and-voltage-law equations.
These expressions are nonlinear differential equations, and
their solutions[20] yield the transient response of the network.
In most practical cases, however, only the **steady-state condi-
tions** are of interest, and they may be found quite simply from
the requirement that the total circuit impedance be zero in the
steady state. This requirement leads to the following equation:

$$Z_T = R - \frac{|R_{je}|}{R_{je}^2 C_{je}^2 \omega_s^2 + 1} + j\left(\omega_s L - \frac{R_{je}^2 C_{je} \omega_s}{R_{je}^2 C_{je}^2 \omega_s^2 + 1}\right) = 0$$

$$(32)$$

where $R = R_s + R_c$, $L = L_s + L_c$, ω_s in the steady-state frequency of oscillation, and R_{je} and C_{je} are the effective steady-state values of R_j and C_j, respectively.

Exact evaluations of R_{je} and C_{je} are difficult, and require lengthy graphical or numerical calculations. However, these terms may be replaced, to a first approximation, by their average values R_j and C_j. As a result, Eq. (32) becomes

$$Z_T \approx R - \frac{|R_j|}{\bar{R}_j^2 \bar{C}_j^2 \omega_s^2 + 1} + j\left(\omega_s L - \frac{\bar{R}_j^2 \bar{C}_j \omega_s}{\bar{R}_j^2 \bar{C}_j^2 \omega_s + 1}\right) = 0 \quad (33)$$

Because both the real and imaginary parts of Eq. (33) must simultaneously be equal to zero, the following equivalent solutions for the **steady-state frequency of oscillation** result:

$$f_s \approx \frac{1}{2\pi |R_j| \bar{C}_j} \sqrt{\frac{|\bar{R}_j|}{R_s + R_c} - 1} \qquad (34)$$

and

$$f_s \approx \frac{1}{2\pi} \sqrt{\frac{1}{(L_s + L_c)\,\bar{C}_j} - \frac{1}{\bar{R}_j^2 \bar{C}_j^2}} \qquad (35)$$

A comparison of Eqs. (30) and (34) shows that the circuit of Fig. 63 cannot oscillate at frequencies above the cutoff frequency f_{ro}. (The resistive cutoff frequency is sometimes called the **maximum frequency of oscillation**. However, the amplitude of oscillation approaches zero as the oscillation frequency approaches f_{ro}.)

A comparison of Eqs. (31) and (35) shows also that the circuit of Fig. 63 cannot oscillate at frequencies above the self-resonant frequency f_{xo}.

From Eqs. (34) and (35), a relationship may be obtained between the various circuit parameters:

$$L = R\ |\bar{R}_j|\ \bar{C}_j \qquad (36)$$

Eq. (36) expresses the equilibrium conditions for steady-state oscillations.

OPERATION ABOVE SELF-RESONANCE

Above self-resonance, the tunnel diode is inductive; there-
fore, oscillation at frequencies above self-resonance can only
be achieved if the circuit presents a capacitive reactance to the
diode at the frequency of oscillation. Such a circuit is shown
in Fig. 64a; again, the circuit shown in Fig. 64b should be used
if bias-lead inductance is appreciable.
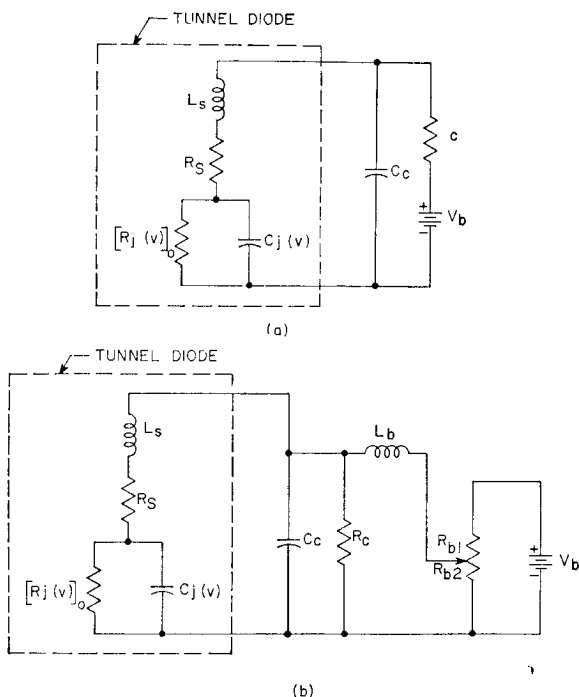
Fig. 64.   Tunnel-diode circuits for operation above
            self-resonance.

By use of the same mathematical analysis as in the pre-
ceding section, the expression for the steady-state frequency
of oscillation ω_s is found to be[19]

$$\omega_s \approx \sqrt{\frac{|\bar{R}_j| - (R_s + R_c)}{L_d |\bar{R}_j| \bar{C}_j + R_c C_c (|\bar{R}_j| \bar{C}_j R_s - L_d)}} \quad (37)$$

A suitable choice of circuit parameters can result in an
oscillation frequency higher than the maximum self-resonant
frequency of the diode. (Of course, the cutoff frequency must
also be higher than the self-resonant frequency.) As shown in

the following section, however, smaller power outputs are obtained above self-resonance; for this reason, the usefulness of such circuits is limited.

POWER OUTPUT

The rf **power output** P delivered by a linear negative resistance is given by

$$P = I_r V_r \tag{38}$$

where I_r and V_r are the rms values of current through and voltage across the negative resistance, respectively. Although an exact formula for the power delivered by a nonlinear resistance is difficult to derive, a good approximation may be obtained by expressing the current as a cubic function of the voltage, as follows:

$$I \approx g_3 V^3 - g_2 V^2 - g_1 \, V \tag{39}$$

Fig. 65 shows that the curve for Eq. (39) follows the actual tunnel-diode characteristic fairly well, provided the voltage excursion is not too great. If Eq. (39) is used, and it is assumed
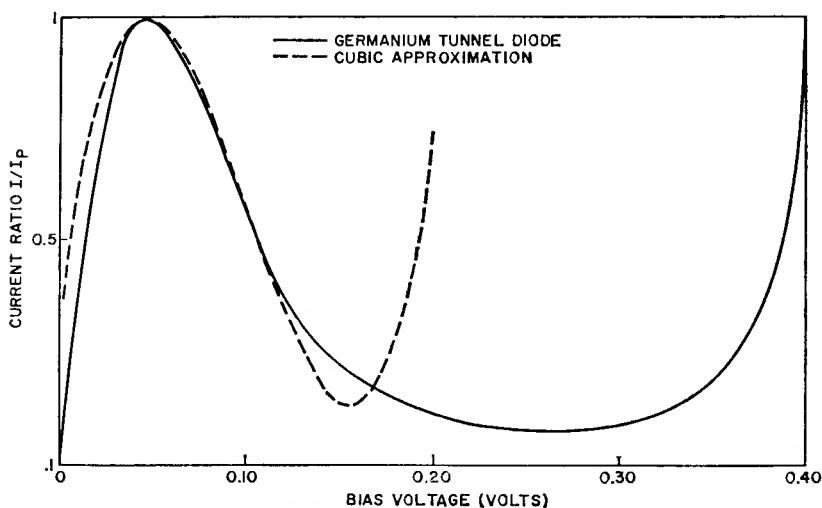
Fig. 65.   Germanium tunnel-diode characteristic and cubic approximation.

that R_s is much less than $|R_j|$, the power output is given by

$$P \approx \tfrac{3}{16} \, (I_p - I_v) \, (V_v - V_p) \tag{40}$$

Experimental results have agreed quite well with Eq. (40) for diode operation at frequencies considerably below cutoff. As mentioned previously, the permissible voltage excursion (or deviation of R_j from its minimum negative value) decreases as the cutoff frequency is approached, and, as a result, the power output is reduced. The value given by Eq. (40) is approached only when the oscillation frequency is not greater than approximately one-third of f_{ro}.

DISTRIBUTED-CIRCUIT OSCILLATORS

At frequencies above a few hundred megacycles, it is usually necessary to use distributed-circuit resonators (transmission lines or waveguides). The mathematical description of oscillators of this type, in which the tunnel diode and its package are considered as distributed elements in the resonator, involves the solution of very difficult nonlinear partial differential equations. The solutions are simplified, however, when it can be assumed that the oscillator consists of lumped elements connected by uniform transmission lines. RCA tunnel diodes are small enough to be treated in this manner up to frequencies above X-band, and stabilizing resistors may be fabricated of approximately the same size.

The steady-state oscillation conditions for distributed-circuit oscillators may be determined in the same way as for lumped-circuit oscillators. It is more convenient, however, to use the admittance rather than the impedance representation of the tunnel diode. The admittance Y_D is given by

$$Y_D = \frac{R_s - \dfrac{|R_j|}{(\omega\ R_j C_j)^2 + 1} - j\left(\omega L_s - \dfrac{\omega\ C_j R_j^2}{(\omega\ R_j C_j)^2 + 1}\right)}{\left(R_s - \dfrac{2R_s\ |R_j|^2}{(\omega R_j C_j)^2 + 1}\right) + \left(\omega L_s - \dfrac{\omega C_j R_j^2}{(\omega R_j C_j)^2 + 1}\right)} \quad (41)$$

(For large oscillations, the effective values R_{je} and C_{je} may differ substantially from their small-signal values; except at frequencies near self-resonance, however, the value of Z_d is not radically altered and the bias-point values may be used as a fair approximation.)

Fig. 66 shows the conductance and susceptance terms of Eq. (41) as functions of frequency for a particular tunnel diode. The oscillator circuit must be designed so that the values of conductance and susceptance presented to the diode are the negatives of the values in Fig. 66 at the frequency of oscillation chosen.
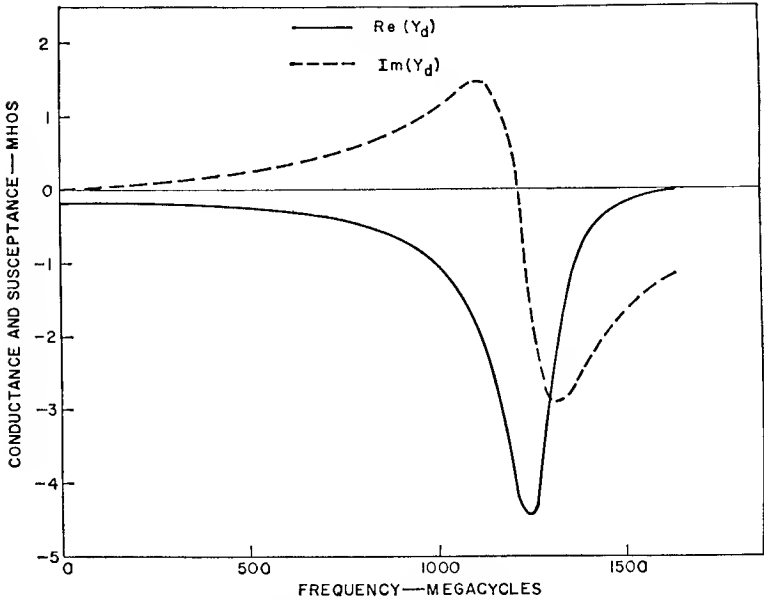
Fig. 66.   Conductance and susceptance as a func-
tion of frequency.

Fig. 67 shows a simple oscillator circuit consisting of a tunnel diode and its stabilizing resistor connected at appropriate points to an open-circuited transmission line. As shown
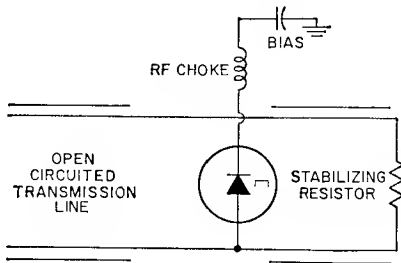

Fig. 67.   Single-transmission-line oscillator.

in Fig. 68, circuits of this type are easily realized in strip-transmission line. The admittance Y_c of this circuit presented to the tunnel diode is given by
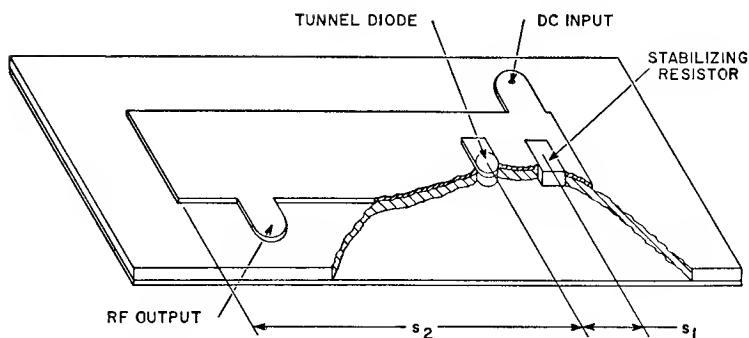
Fig. 68.　Strip-transmission-line cavity oscillator.

$$Y_c = \cfrac{1}{Z_r \left[\left(\dfrac{Z_o}{Z_r} \right)^2 \sin^2 \beta\, s_1 + \cos^2 \beta\, s_1 \right]}$$
$$+ \frac{j}{Z_o} \left[\tan \beta\, s_2 + \frac{1 - (Z_o/Z_r)^2 \sin \beta\, s_1\, \cos \beta\, s_1}{(Z_o/Z_r)^2 \sin^2 \beta\, s_1 + \cos \beta\, s_1} \right] \quad (42)$$

Fig. 69 shows another practical circuit, the re-entrant strip-transmission-line circuit. For this circuit, the admittance is given by

$$Y_c = \frac{1}{Z_r} \left[\frac{B^2}{A^2 + (Z_o/Z_r)^2} \right] + j\, \frac{A}{Z_o} \left[\frac{B^2}{A^2 + (Z_o/Z_r)^2} \right] \quad (43)$$
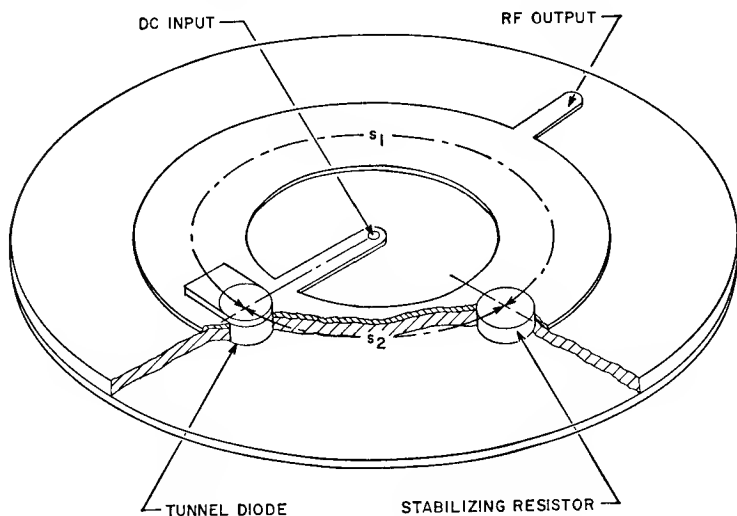
Fig. 69.　Re-entrant-cavity strip-transmission-line oscillator.

The terms used in Eqs. (42) and (43) are defined as follows:

Z_o = characteristic impedance of transmission line

Z_r = impedance of stablizing resistor

β = propagation constant of the transmission line

$A = \cot \beta s_1 + \cot \beta s_2$

$B = \csc \beta s_1 + \csc \beta s_2$

The terms s_1 and s_2 are defined in Figs. 67 and 68. (Eqs. (42) and (43) neglect the effects of rf-output loading.)

Fig. 70 shows curves of Eq. (42) as a function of s/λ, where $s = s_1 + s_2$ for three different values of s_1. This equation is normalized to the characteristic admittance, Y_o ($Y_o = 1/Z_o$), and λ is the transmission-line wavelength at the frequency of oscillation (In this case, $Z_o/Z_r = \frac{1}{3}$.) Fig. 71 shows similar
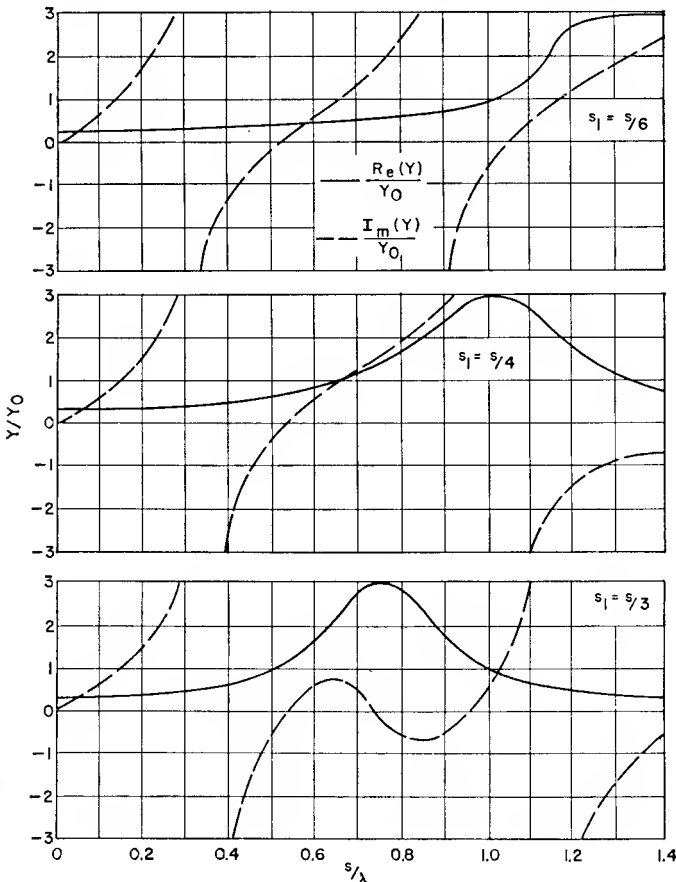
Fig. 70.   Curves for Eq. 42 for three conditions of s_1.

curves for Eq. (43) for three different values of Z_o/Z_r, where $s_1/s = \frac{1}{4}$. These illustrations show that it is possible to vary the conductance and susceptance of tunnel-diode oscillator circuits over a wide range by adjustment of s_1, s_2, and Z_R. In particular, the circuit shown in Fig. 68 can be adapted to a
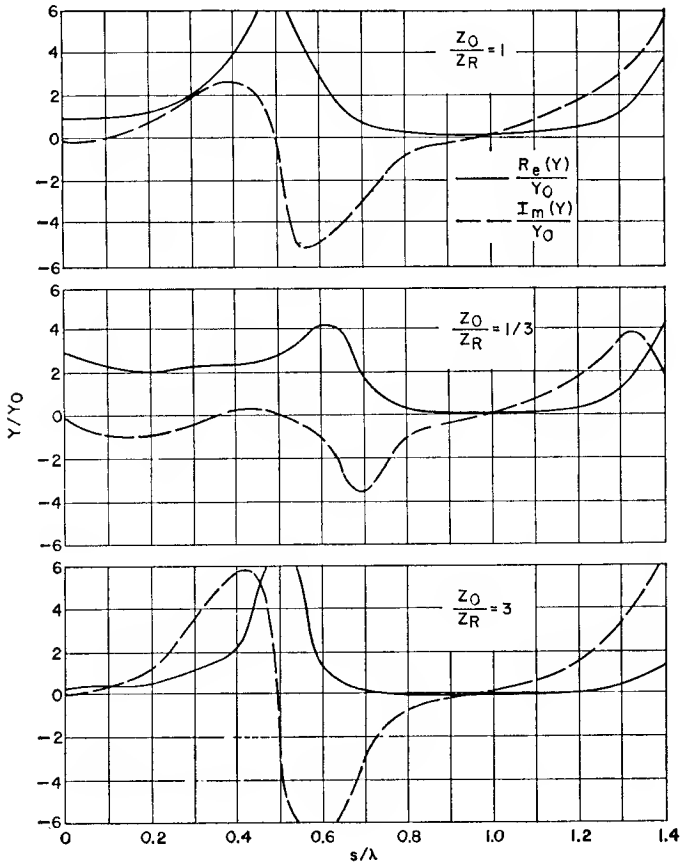
Fig. 71.   Curves for Eq. 43 for three conditions of Z_o/Z_r.

mechanically tuned oscillator if some means is provided for varying the length s_2. Such oscillators are being commercially marketed by RCA with tuning ranges greater than two to one.

The circuits described above can be electrically tuned by the insertion of a varactor diode at a position of high electric field. (A wide range of varactor diodes is available from RCA.)

The frequency of oscillation may also be varied by a change in the bias voltage.[21, 22] Such a change causes variations in both C_j and R_j. Eqs. (36) and (37) show the effects of these variations in lumped circuits. In the case of distributed circuits, the mathematical description is much more difficult and as a result, no expression for the change in frequency with R_j and C_j has been obtained in closed form. However, because the net admittance of the tunnel diode and the circuit must be zero at the frequency of oscillation, the problem may be solved graphically or numerically. The relative change in frequency for a given change in bias voltage depends largely on the Q of the circuit; low-Q strip-transmission-line oscillator circuits have been voltage-tuned over frequency ranges as high as 12 per cent. On the other hand, high-Q ridged-waveguide oscillators have been built for which the frequency of oscillation varied less than 0.6 per cent for a bias-voltage variation over the entire negative-resistance region.

OUTPUT LOADING

Thus far, the effects of the output load on tunnel-diode oscillator performance have been ignored. Variations in load impedance cause frequency pulling or shifting, as in a klystron or magnetron. The degree to which pulling occurs depends upon the Q of the circuit and upon the degree of coupling of the load to the circuit. Decoupling tends to reduce pulling, but severe decoupling reduces the power output.

Frequency stability and power output with load variation also depend upon the particular value of the load impedance chosen. This dependence is best illustrated by reference to a **Rieke diagram.** This type of diagram shows curves of constant power output and frequency deviation in the complex reflection-coefficient plane. From such a diagram, the optimum load impedance for maximum power output may be determined, and oscillator behavior under other load conditions may be studied. A Rieke diagram is usually plotted on a Smith Chart.

Fig. 72 is a Rieke diagram for a 3530-megacycle re-entrant cavity strip-transmission-line oscillator, showing that maximum power output is delivered to a slightly reactive load having a voltage standing-wave ratio of about three. A slight variation in this load impedance causes a relatively large change in frequency of oscillation because the frequency contours converge toward the top of the diagram. Greater frequency stability can be attained by use of a load impedance in the lower region of the diagram at the cost of reduced power

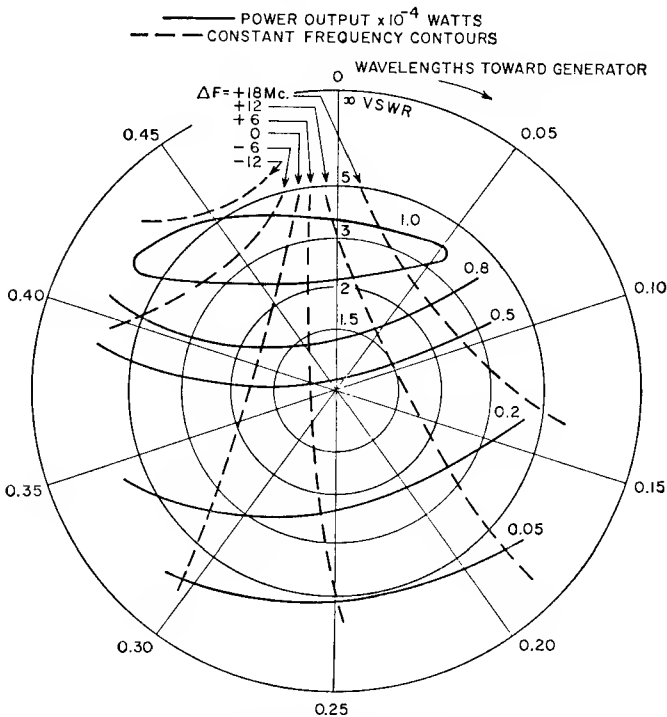output. In general, the choice of load impedance is a compromise between frequency stability and power output.

Fig. 72.   Rieke diagram for 3530-megacycle tunnel-
diode oscillator.

FREQUENCY LOCKING

The frequency of a tunnel-diode oscillator can be locked to that of an external signal several orders of magnitude smaller in amplitude, provided the locking signal is close in frequency to the natural frequency of the oscillator. Locking signals as much as 40 db below the oscillator power output have been successfully employed. Harmonic locking is also possible. Thus, a microwave tunnel-diode oscillator may be locked to a transistor oscillator operating at a fraction of the microwave frequency. The fractional frequency stability of the tunnel-diode oscillator is then the same as that of the locking oscillator. A crystal-controlled transistor oscillator may be employed to provide a very high degree of frequency stability.

An efficient means of injecting the locking signal, without loss of power output, is the use of a **hybrid ring.** Two similar tunnel-diode oscillators may be connected to two arms of the hybrid, while the third arm is connected to the locking signal source. The locked signal is taken out at the fourth arm.

PARALLEL OSCILLATORS

A hybrid may also be used to connect three tunnel-diode oscillators in parallel, and thus obtain power output almost equal to the sum of the individual power outputs. Several such hybrid circuits may, in turn, be connected together to increase the number of paralleled oscillators.

DESIGN EXAMPLE

As a practical example of a microwave tunnel-diode oscillator, the equations derived above may be applied to the strip-transmission-line cavity oscillator of Fig. 68. A typical circuit of this type may be made to produce substantial power output at frequencies in L- and S-bands. The example uses an RCA-40058 gallium arsenide tunnel diode, which has the following characteristics.

$$\text{Peak current } I_p = 50 \text{ milliamperes}$$
$$\text{Incremental resistance } |\overline{R_j}| = 4.4 \text{ ohms}$$
$$\text{Junction capacitance } \overline{C_j} = 6 \text{ picofarads}$$
$$\text{Series inductance } L_s = 0.4 \text{ nanohenries}$$
$$\text{Series resistance } R_s = 2 \text{ ohms}$$
$$\text{Resistive cutoff frequency } f_{ro} = 6.6 \text{ gigacycles}$$

The design objectives for the oscillator are as follows:
Steady-rate frequency of oscillation $f_s = 2$ gigacycles
Power output $P = 3.7$ milliwatts (theoretical)
The design procedure is to find the diode admittance, by means of Eq. (41), and then to select appropriate circuit parameters so that the circuit admittance, as given by Eq. (42), is the negative of the diode admittance at a frequency of two gigacycles.

By means of the above tunnel-diode characteristics, the diode admittance Y_D at two gigacycles is found to be:

$$Y_D = G_D + j \, B_D$$
$$= -0.109 - j \, 0.212 \text{ mhos} \quad (44)$$

The circuit must be designed so that the real and imaginary parts of Y_c are equal to the negatives of the real and imaginary parts of Y_d, respectively. Therefore, from Eq. (42)

$$Z_R \left[\left(\frac{Z_0}{Z_R} \right)^2 \sin^2 \beta\ s_1 + \cos \beta\ s_1 \right] = 1/G_D \qquad (45)$$

and

$$\frac{1}{Z_0} \left[\tan \beta\ s_2 + \frac{1 - \left(\dfrac{Z_0}{Z_R} \right)^2 \sin \beta\ s_1 \cos \beta\ s_1}{\left(\dfrac{Z_0}{Z_R} \right)^2 \sin^2 \beta\ s_1 + \cos^2 \beta\ s_1} \right] = B_d \quad (46)$$

If values for Z_0 (the characteristic impedance of the strip transmission line) and Z_r (the impedance of the stabilizing resistor) are chosen, Eq. (45) may be solved for s_1. The optimum value of the stabilizing resistor must be chosen empirically. However, its value must be approximately equal to $|\overline{R}_j|$ to provide a monostable operating point which is necessary to produce sinusoidal oscillations. For this example, Z_r is arbitrarily chosen to be five ohms.

Next, Z_0 must be chosen sufficiently low so that the line inductance is low enough to prevent oscillation in a spurious low-frequency mode. In general, Z_0 should be substantially lower than $|\overline{R}_j|$; in this case, Z_0 is chosen to be one ohm.

The following trigonometric identities are then used:

$$\cos^2 \alpha = \tfrac{1}{2} (1 + \cos 2\alpha)$$
$$\sin^2 \alpha = \tfrac{1}{2} (1 - \cos 2\alpha) \qquad (47)$$

Eq. (45) may be solved for $\cos 2\beta\ s_1$, as follows:

$$\cos 2 \beta\ s_1 = \frac{\dfrac{2}{G_D Z_R} - \left(\dfrac{Z_0}{Z_R} \right)^2 - 1}{1 - \left(\dfrac{Z_0}{Z_R} \right)^2} \qquad (48)$$

When the values of G_d, Z_0 and Z_r are determined, it is seen from Eq. (48) that

$$\cos 2\beta\ s_1 = 0.82 \qquad (49)$$

The value of $\beta\ s_1$ is then given by

$$\beta\ s_1 = 2\pi\ (0.0486)\ \text{radians} \qquad (50)$$

When this value of $\beta \, s_1$ is substituted in Eq. (46), $\beta \, s_2$ is given by

$$\beta \, s_2 = 2\pi \, (0.268) \text{ radians} \tag{51}$$

Because $\beta = 2\pi/\lambda g$, Eqs. (50) and (51) may then be solved for s_1 and s_2 as follows:

$$s_1 = 0.0486 \, \lambda g$$
$$s_2 = 0.268 \;\; \lambda g \tag{52}$$

If teflon-fiberglas dielectric strip transmission line is used (this type of line has a relative dielectric constant of approximately 2.5), the transmission line wavelength λg at two giga-cycles is 3.68 inches. Copper-clad teflon fiberglas material is commercially available having dielectric thicknesses ranging from a few thousandths of an inch or less, to as much as a quarter of an inch. Information is available in the literature on the design parameters of strip-transmission line.

REFERENCES

15. R. Trambarulo and C.A. Burrus, "Esaki Diode Oscillators from 3 to 40 KMC", *Proc. IRE*, Vol. 48, p. 1776, October 1960.

16. C.A. Burrus, "Millimeter Wave Esaki Diode Oscillators" *Proc. IRE*, Vol. 48, p. 2024, Dec. 1960.

17. H.B. Hauer, "A 4 MW, 6 KMC Tunnel-Diode Oscillator", Digest of Technical Papers, 1962 International Solid State Circuits Conference, Phila. Pa., Feb. 1962.

18. C.S., Kim, "High-Frequency High-Power Operation of Tunnel Diodes", *Trans. IRE*, Vol. PGCT-8, pp. 416-425, Dec. 1961.

19. A. Presser and A. Roswell, "L-Band Gallium Arsenide Tunnel-Diode Oscillators with Power Outputs from 10-100 Milliwatts", *Proc. IEEE*, vol. 51, p. 224-225, January 1963.

20. F. Sterzer and D.E. Nelson, "Tunnel-Diode Microwave Oscillators", *Proc. IRE*, Vol. 49, pp. 744-753, April 1961.

21. F. Sterzer, "Stability of Tunnel-Diode Oscillators", *RCA Review*, Sept. 1962.

22. J.K. Pulfer, "Voltage Tuning in Tunnel-Diode Oscillators", *Proc. IRE*, Vol. 48, p. 1155, June 1960.
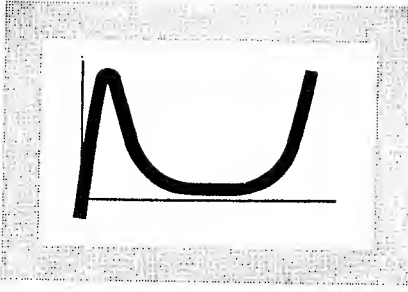
MICROWAVE
AMPLIFIERS

T UNNEL-DIODE amplifiers can be useful as low-noise rf amplifiers in the front end of microwave receivers.[23] Although lower noise figures can be obtained with masers and parametric amplifiers, tunnel-diode amplifiers are dc-activated, i.e., they do not require ac pumping. As a result, tunnel-diode amplifiers are most desirable for low-noise applications in which the primary considerations are low cost, small size and weight, and low power drain.

Tunnel-diode amplifiers are inherently broadband devices because a properly biased tunnel diode has a negative input resistance at all frequencies from dc to the resistive cutoff frequency. When this negative input resistance is combined with a suitable coupling network, a circuit can be designed having an over-all positive input impedance that provides amplification or power gain. Because of this wideband negative-resistance characteristic, bandwidths in excess of an octave can be readily obtained with tunnel-diode amplifiers.[24, 25] Masers and parametric amplifiers require extensive development before bandwidths in excess of ten per cent can be achieved. The wideband negative resistance, however, makes stabilization of tunnel-diode amplifiers an important developmental problem.

Microwave tunnel-diode amplifiers are applicable to various types of communications, radar, and countermeasures systems. In addition, the size and weight of these amplifiers is attractive for tactical electronic equipment. Because of the low power drain of tunnel-diode amplifiers, they should prove quite useful in space applications such as communication satellites. The relatively low cost of tunnel-diode amplifiers also makes them strong contenders in line-of-sight radio-relay systems and phased-array radars.

VARIOUS TYPES OF AMPLIFIER CIRCUITS

All tunnel-diode amplifier circuits employ diodes biased in the negative-resistance region. Direct-coupled tunnel-diode amplifiers are difficult to stabilize and are rarely used at microwave frequencies. However, various types[26] of circuit techniques can be used to achieve a positive input impedance for tunnel-diode amplifiers. The advantages and disadvantages of several methods are discussed below:

Traveling-Wave Tunnel-Diode Amplifiers. In this type of circuit, several tunnel diodes are periodically spaced along a transmission line, as shown in Fig. 73. Traveling-wave tunnel-diode amplifiers were originally developed to achieve octave-bandwidth amplification. However, because very broadband
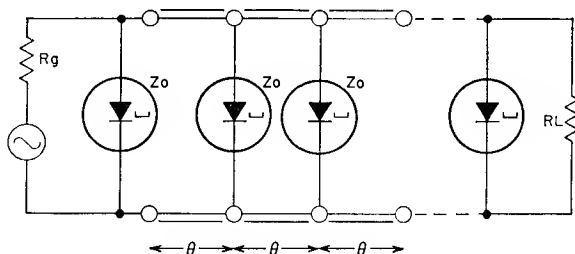
Fig. 73.   Traveling-wave tunnel-diode amplifier.

tunnel-diode amplifiers can be readily realized by other circuit techniques, traveling-wave tunnel-diode amplifiers have not been particularly popular. Nevertheless, some research on this type of circuit is still being done.

Quarter-Wave Coupled Tunnel-Diode Amplifiers. In this method, two tunnel diodes are separated by a length of transmission line that is $\lambda/4$ long at the design-center frequency of the amplifier. An example of this circuit is shown in Fig. 74. This circuit requires a matched pair of tunnel diodes and
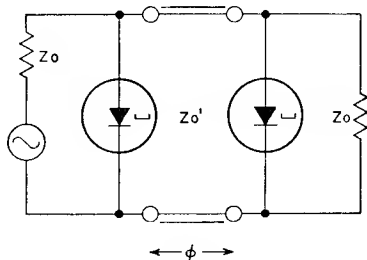
Fig. 74.   Quarter-wave-coupled tunnel-diode amplifier.

has not been used extensively at microwave frequencies.

Hybrid-Coupled Tunnel-Diode Amplifiers. This technique uses a matched pair of tunnel diodes coupled to conjugate ports of a hybrid or 3-db directional coupler, as shown in Fig. 75.
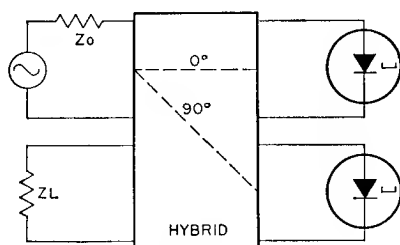
Fig. 75.   Hybrid-coupled tunnel-diode amplifier.

A hybrid coupler is a four-port network that can deliver half the power incident upon port No. 1 to ports Nos. 2 and 3. The fourth port is isolated from the input port by 20 to 40 db. If two signals are delivered to ports Nos. 2 and 3, the hybrid can also combine these signals. In a tunnel-diode amplifier, the hybrid used must provide power division with quadrature phase between outputs. Hybrids such as the "magic-T" or "rat-race" are not applicable unless an external quarter-wave coupling line is used for one of the tunnel diodes. This requirement makes the amplifier more frequency-sensitive and, as a result, is generally not desirable.

Circulator-Coupled Tunnel-Diode Amplifiers. The circulator-coupled amplifier is the preferred approach for most tunnel-diode applications at microwave frequencies. This type of circuit uses a ferrite circulator and only one tunnel diode, as shown in Fig. 76. The ferrite circulator is a non-reciprocal
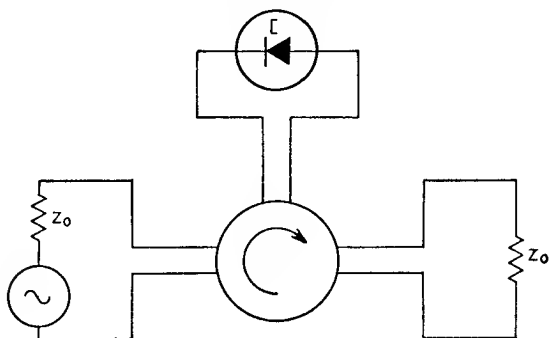
Fig. 76.   Circulator-coupled tunnel-diode amplifier.

device having low insertion loss (in the order of a few tenths of a db) in the forward direction and a high insertion loss (about 20 db) in the reverse direction. Fig. 77 shows another type of circulator-coupled amplifier which uses four ports. This method offers better amplifier stability than the three-port circuit.
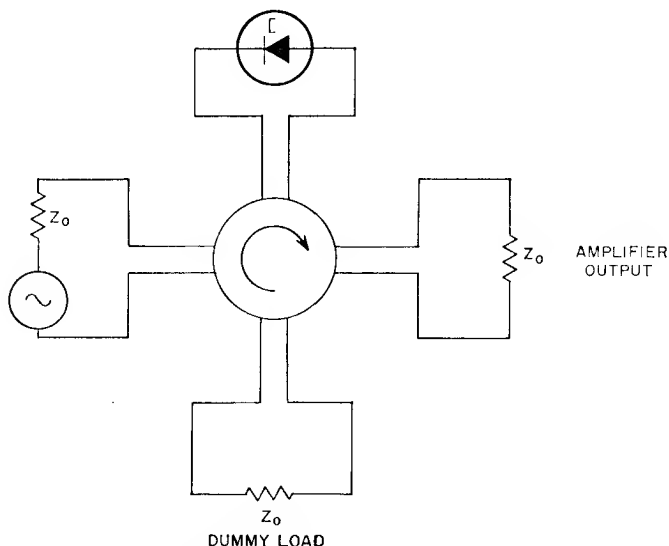
Fig. 77.   Circulator-coupled   tunnel-diode   amplifier having a four-port circulator.

GAIN BANDWIDTH

The circuit parameters of tunnel-diode amplifiers can be combined to form several convenient design values:[25]

$$\omega_o{}^2 = \frac{1}{LC_j} \qquad \eta = \frac{Z_o}{|R_j|} \qquad Z^2 = \frac{L}{C_j}$$

$$\beta^2 = \left(\frac{\omega}{\omega_o}\right)^2 \qquad \gamma = \frac{Z}{|R_j|} \qquad \theta = \frac{R_s}{|R_j|} \qquad (53)$$

where Z_o is the source-load impedance of the quarter-wave-coupled, hybrid-coupled, or circulator-coupled tunnel-diode amplifiers; L is the over-all series inductance, including both tunnel-diode lead inductance and external wiring; and ω is the angular frequency ($2\pi \times$ the signal frequency f_s).

If an ideal hybrid having source-load impedance equal to Z_o is assumed, the gain G for a hybrid-coupled tunnel-diode

amplifier[27] is given by

$$G = 10 \log \ |\Gamma|^2 \qquad (54)$$

where $|\Gamma|$ is the magnitude of the voltage-reflection coefficient of the tunnel-diode network.

By substitution of the parameters of the tunnel-diode network for $|\Gamma|^2$, Eq. (54) can be rewritten as follows:

$$G = 10 \log \left[\frac{(\beta^2 - 1 - \eta + \theta)^2 + \beta^2 (\gamma + \eta/\gamma - \theta/\gamma)^2}{(\beta^2 - 1 - \eta + \theta)^2 + \beta^2 (\gamma - \eta/\gamma - \theta/\gamma)^2} \right] db \qquad (55)$$

If the dissipative resistance of the tunnel diode is neglected (i.e., $\theta = 0$), the expression for gain becomes

$$G = 10 \log \left[\frac{(\beta^2 - 1 - \eta)^2 + \beta^2 (\gamma + \eta/\gamma)^2}{(\beta^2 - 1 - \eta)^2 + \beta^2 (\gamma - \eta/\gamma)^2} \right] db \qquad (56)$$

This expression is for a low-pass prototype circuit in which the lead inductance of the diode acts as a peaking coil. This effect can be seen in Fig. 78, which shows the gain of tunnel-diode amplifiers as a function of the normalized frequency for various degrees of peaking (i.e., different values of the parameter $\gamma = \frac{Z}{|R_j|} = \sqrt{\frac{LC_j}{|R_j|}}$). Larger values of this parameter are used for higher low-frequency values of gain.

If both the lead inductance and junction capacitance of the tunnel diode are neglected, the amplifier gain at dc is given by

$$G = 20 \log \left[\frac{1 + \eta}{1 - \eta} \right] db \qquad (57)$$

Typical values of η for practical tunnel-diode amplifiers range from 0.5 to about 0.8.

If the spreading resistance and the lead inductance are neglected, the gain of the tunnel-diode amplifier is given by

$$G = 10 \log \left[\frac{(1 + \eta)^2 + W^2}{(1 - \eta)^2 + W^2} \right] db \qquad (58)$$

where $W = 2\pi f C_j Z_o$. For a high-gain amplifier (i.e., the value of G approaches ∞), the gain-bandwidth product $BG^{1/2}$ is given by
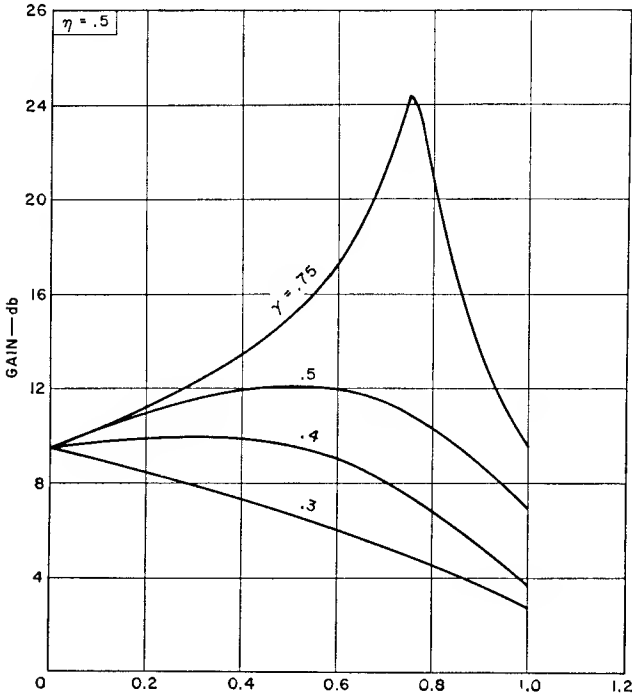
Fig. 78.   Gain as a function of normalized frequency.

$$BG^{1/2} = \frac{1}{\pi \mid R_j \mid C_j} \tag{59}$$

The above gain equations are equally applicable for a circulator-coupled tunnel diode using an ideal ferrite circulator.

NOISE FIGURE

In general, it is convenient to express the noise characteristics of a two-port tunnel-diode amplifier in terms of the noise figure.[28, 29, 30] This term is described quantitively as the signal-to-noise ratio at the amplifier input divided by the signal-to-noise ratio at the amplifier output. The noise figure NF for hybrid-coupled or circulator-coupled tunnel-diode amplifiers using ideal hybrids or circulators is given by

$$NF = 1 + \frac{4}{G}\left[\frac{20\,I_o Z_o}{(1 - \eta - \theta - \beta^2)^2 + \beta^2\,(\gamma - \eta/\gamma - \theta/\gamma)^2}\right] +$$

$$\frac{4}{G}\left\{\frac{\theta/\eta}{\left[1 + \dfrac{\theta}{\eta} - \dfrac{1/\eta}{1 + \beta^2/\gamma^2}\right]^2 + \beta^2\left[\dfrac{\gamma}{\eta} - \dfrac{1/\gamma\eta}{1 + \beta^2/\gamma^2}\right]^2}\right\}$$

$$(60a)$$

where NF is the noise figure as a power ratio and I_o is the static current at the operating point of the tunnel diode. If the inductance is omitted, this equation can be reduced to the following expression:

$$NF = \frac{1}{G} + \left[1 - \frac{1}{G}\right]\left[\frac{1 + 20\,I_o\,|\,R_j\,|}{(1 - R_s/\,|\,R_j\,|\,)\,(1 - f_s/f_{ro})^2}\right] \quad (60b)$$

where f_{ro} is the resistive cutoff frequency.

For a perfect amplifier, the noise figure is equal to unity. For practical amplifiers, the component of the noise figure greater than unity is called the excess noise. The second term in Eq. (60a) is the excess noise caused by shot noise; the third term is excess noise caused by thermal noise in the dissipative resistance of the tunnel diode.

The resistive cutoff frequency of the tunnel diode is given by

$$f_{ro} = \frac{1}{2\pi\,|\,R_j\,|\,C_j}\,\sqrt{\frac{R_j}{R_s} - 1} = \frac{\gamma\omega_o}{2\pi}\,\sqrt{\frac{1}{\theta} - 1} \quad (61)$$

For frequencies less than $\dfrac{f_{ro}}{3}$, the excess noise in the series resistance can usually be neglected. If both β and θ are equal to zero in Eq. (60a) and if the high-gain approximations of $Z_o = |\,R_j\,|$ and G approximately equal to $\dfrac{4}{(1 - \eta)^2}$ are used, the equation for noise figure reduces to

$$NF = 1 + 20\,I_o\,|\,R_j\,| \quad (62)$$

The factor $(20\,I_o\,|\,R_j\,|\,)$ is a function of temperature and is sometimes called the noise constant of the tunnel diode. For germanium tunnel diodes, the noise constant is usually equal to at least 1.1; as a result, the minimum noise figure is about 3.6 db. Lower room-temperature noise figures can be achieved by use of gallium antimonide tunnel diodes; however, these

devices are extremely temperature-sensitive, and the power required to regulate the temperature of a gallium antimonide tunnel-diode amplifier makes such an amplifier much less attractive for many applications.

Maximum gain in a tunnel-diode amplifier occurs when the tunnel diode is biased at the point of inflection on its static current-voltage characteristic curve. Minimum noise figure occurs at a somewhat larger bias-voltage point. As a result, amplifier bias is usually adjusted experimentally to minimize the noise figure.

Eq. (62) can also be used as an approximate estimate of the noise figures of other tunnel-diode amplifiers, such as quarter-wave-coupled amplifiers.

STABILITY

The low-pass prototype tunnel-diode network displays a negative resistance at its external coupling network over a broad range of frequencies outside the useful bandwidth of the amplifier. Consequently, parasitic oscillations (relaxation and/or sinusoidal) may occur if special design precautions are not observed. The first problem that must be investigated is whether or not the tunnel diode being considered can be employed in a stable amplifier.[31] For lossy tunnel diodes, the following practical conditions are sufficient for stability:

$$\frac{R_s}{R_j} = \theta \leqq 0.5$$

$$\frac{L_s}{R_j^2 C_j} = \gamma^2 \leqq 1.0 \qquad (63)$$

Depending upon the circuitry used to inject dc bias into the tunnel diode, spurious relaxation oscillation can occur. Typical tunnel-diode circuits have been analyzed from the standpoint of freedom from these relaxation oscillations.[26, 31] Spurious rf oscillations are avoided if the tunnel-diode network presents a positive input impedance to the external coupling networks (i.e., hybrid or circulator) at all frequencies outside the desired amplifier bandwidth that are less than the resistive cutoff frequency of the diode. Amplifier bandwidths are restricted to the passband of the hybrid or circulator.

The network shown in Fig. 79 is recommended for unconditionally stable microwave tunnel-diode amplifiers, i.e., amplifiers which do not oscillate because of changes in source load

impedance or dc bias. A band-reject filter is used between the tunnel-diode network and the dc-bias source. The resistor R_c is much less than the absolute value of the negative resistance.
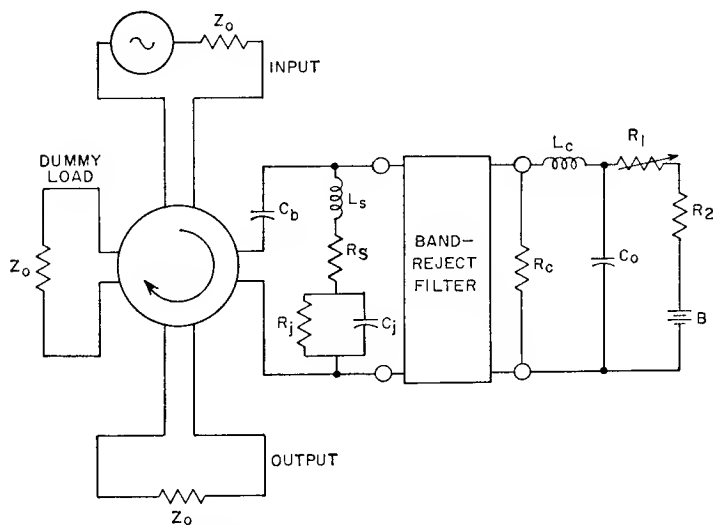
Fig. 79.   Typical circuit of stable microwave tunnel-
diode amplifier.

When the band-reject filter is in its "stopband", the resistor R_c does not act as a load in the tunnel-diode network. At this point, a negative resistance is presented to the circulator and gain is realized. When the band-reject filter is in its passband (i.e., off resonance), R_c acts as a load in the tunnel-diode network. In this case, a positive resistance is presented to the circulator so that no gain and/or spurious oscillations occur.

The bandpass of a narrow-band tunnel-diode amplifier can be shaped by the band-reject filter. The band-reject filter must be free of spurious stopbands, and the resistor R_c must maintain its characteristics at all microwave frequencies below the resistive cutoff frequency of the tunnel diode. For this reason, tunnel-diode cutoff frequencies should be about three to four times the highest value of the amplifier operating frequency. Use of lower cutoff frequencies significantly degrades amplifier noise figure; use of higher cutoff makes stabilization more difficult.

Stable operation within the passband of the amplifier depends upon the type of coupling network used and the voltage-reflection coefficient of the input, output, and dummy loads. For the hybrid-coupled tunnel-diode amplifier having an ideal

hybrid, the stability threshold occurs when the following condition exists:

$$|\Gamma_g| \ |\Gamma_L| \ G = 1.0 \qquad (64)$$

where $|\Gamma_g|$ is the magnitude of the voltage-reflection coefficient of the source and $|\Gamma_L|$ is the magnitude of the voltage-reflection coefficient of the load.

For a tunnel-diode amplifier using a three-port ideal circulator, the stability threshold occurs when the following condition exists:

$$|\Gamma_g| \ |\Gamma_L| \ G^{1/2} = 1.0 \qquad (65)$$

For a tunnel-diode amplifier using a four-port ideal circulator, the stability threshold occurs when the following condition exists:

$$|\Gamma_g| \ |\Gamma_L| \ |\Gamma_o| \ G^{1/2} = 1.0 \qquad (66)$$

where $|\Gamma_o|$ is the magnitude of the voltage-reflection coefficient of the dummy load.

The most favorable conditions of passband stability can usually be achieved by use of a four-port circulator because the value of $|\Gamma_o|$ which is equal to or less than 0.048 (i.e., when the VSWR is equal to or less than 1.10) can usually be obtained readily.

(In the case of mismatched source-load impedances, Eqs. (54) through (60) and (62) must be modified for the calculation of amplifier gain and noise figure.)

DYNAMIC RANGE

The dynamic range of a tunnel-diode amplifier is the range of input signal levels that can be accommodated by the amplifier. The lower limit of the dynamic range of a tunnel-diode amplifier is determined by noise considerations; the upper limit is limited by the large-signal saturation phenomena of the tunnel diode as a device. (The upper limit usually extends to the 3-db gain compression point.) The amplifier gain, the nature of the input signals, and the tunnel diode being used determine what large signals can cause in significant intermodulation, crossmodulation, and harmonic outputs.[32, 33] For typical microwave low-noise tunnel-diode amplifiers, saturation occurs at signal-input levels between -25 and -50 dbm. In general, saturation occurs at somewhat lower levels in tunnel-diode amplifiers than in tunnel-diode converters or parametric amplifiers and converters.

MEASURED RESULTS

Fig. 80 shows the frequency response for a typical broadband hybrid-coupled tunnel-diode amplifier. This circuit does not use a band-reject filter for narrow-banding. Germanium
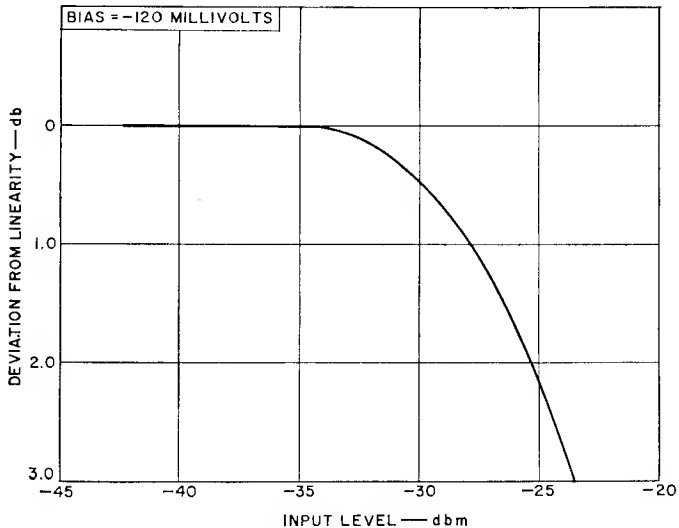
Fig. 80.   Gain as a function of frequency for a hybrid-coupled tunnel-diode amplifier.

tunnel diodes having peak currents of about one milliampere were used with this unit, and noise figures of 4.0 to 4.5 db were obtained. Hybrid-coupled uhf tunnel-diode amplifiers have been developed having useful gain over a five-to-one frequency range. Various circulator-coupled narrow-band amplifiers have also been developed. A typical gain-saturation characteristic for a practical tunnel-diode amplifier is shown in Fig. 81.

REFERENCES

23. H. S. Sommers, "Tunnel Diodes as High-Frequency Devices", *Proc. IRE*, Vol. 47, pp. 1201-1206, July 1959.

24. J. J. Sie, "Absolutely Stable Hybrid-Coupled Tunnel-Diode Amplifier", *Proc. IRE*, Vol. 48, p. 1321, July 1960 plus correction p. 1783, Aug. 1960.

25. H. Boyet, B. Fleri and R. M. Kurzrok, "Broadband Hybrid-Coupled Tunnel-Diode Amplifier in the UHF Re-

gion", *Proc. IRE*, Vol. 50, p. 1527, June 1962.

26. M. E. Hines, "High-Frequency Negative-Resistance Circuit Principles for Esaki-Diode Applications", *BSTJ*, Vol. 39, pp. 477-513, May 1960.

27. R. M. Kurzrok, "Bandwidth of Hybrid-Coupled Tunnel-Diode Amplifier", *Proc. IRE*, Vol. 50, pp. 226-227, Feb. 1962, plus correction p. 466, April 1962.
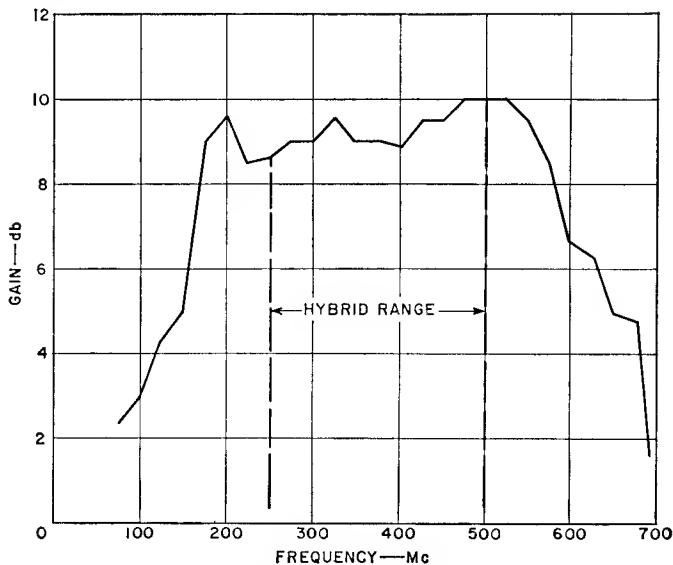
Fig. 81. Typical gain-saturation characteristic of tunnel-diode amplifier.

REFERENCES

28. K. K. N. Chang, "The Optimum Noise Performance of Tunnel-Diode Amplifiers", *Proc. IRE*, Vol. 48, pp. 107-108, Jan. 1960.

29. L. S. Nergaard, Comments on "Shot Noise in Tunnel-Diode Amplifiers", plus reply by J. J. Tiemann, *Proc. IRE*, Vol. 49, pp. 622-623, March 1961.

30. E. O. Nielsen, "Noise Performance of Tunnel Diodes", *Proc. IRE*, Vol. 48, pp. 1903-1904, Nov. 1960.

31. H. Boyet, B. Fleri and C. A. Renton, "Stability Criteria for a Tunnel-Diode Amplifier", *Proc. IRE*, Vol. 49, p. 1937, Dec. 1961.

32. R. M. Kurzrok and A. Newton, "Non-Linear Distortion in Tunnel-Diode Amplifiers", *Proc. IRE*, Vol. 50, p. 1853, August 1962.

33. R. M. Kurzrok, "AM to PM Conversion in Tunnel-Diode Amplifiers", Proc. IEEE, Vol. 51, pp. 377-378, February, 1963.
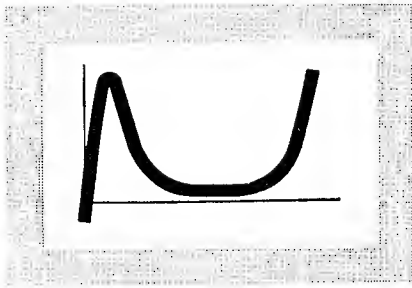
MICROWAVE
CONVERTERS

PRACTICALLY all existing low-noise uhf and microwave receivers make use of the heterodyne principle, i.e., the frequency of the received signal is shifted before high amplification takes place. For frequencies above a few hundred megacycles, crystal diodes have been almost universally used in the frequency converters of such receivers. However, the best uhf crystal converters have conversion losses of 3 to 4 db and noise figures of 4 to 5 db; at microwave frequencies, both conversion losses and noise figures are somewhat higher. Until the recent advent of very-low noise preamplifiers such as masers, parametric amplifiers, and traveling-wave tubes, crystal frequency converters were generally placed directly at the input of the receiver. In more recent designs, a low-noise preamplifier has been placed ahead of the crystal to provide very low receiver noise figures.

There is little likelihood that the noise figure of crystal mixers can be significantly improved by further research. Crystal diodes, which are passive devices, must have some conversion loss, and their noise figure must always equal or exceed this loss. However, microwave diodes with a negative-resistance region (tunnel diodes), exhibit active properties even at millimeter-wave frequencies.[34]

Tunnel-diode frequency converters have lower conversion loss, lower noise figures, larger dynamic range, and greater resistance to burn-out than crystal-diode converters; their use could eliminate the need for preamplifiers in many applications.

EQUIVALENT CIRCUIT

In a tunnel-diode frequency converter, an input signal of frequency f_s and a local-oscillator signal of frequency f_o are impressed across the nonlinear conductance of the diode. In general, a complete set of sideband frequencies is produced, i.e., all frequencies $f_{m, n} = mf_s + nf_o$ (m and n take on all integral values) are present. However, in most practical converters, significant power flow takes place only at the input-signal frequency f_s, the oscillator-frequency f_o, the intermediate frequency $f_i = |f_s - f_o|$, and the image frequency $f_k = |2f_o - f_s|$. In this case, the converter can be represented by the linear three-port frequency-translation network shown in Fig. 82, provided that the amplitude of the sinusoidal local-oscillator voltage across the nonlinear conductance is much greater than the sum of the amplitudes of the voltages at signal, intermediate, and image frequencies.[35]
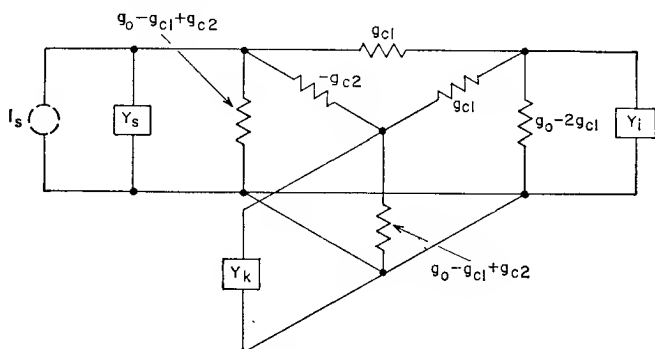
Fig. 82.   Equivalent   linear   three-port   frequency-translation   network   for   tunnel-diode   frequency converter.

In Fig. 82, Y_s is the total admittance at the signal frequency connected across the nonlinear conductance; similarly, Y_k and Y_i are, respectively, the total image- and intermediate-frequency admittances. The quantity g_o is the average value of the nonlinear conductance driven by the sinusoidal local oscillator, g_{c1} is the fundamental conversion conductance, and g_{c2} is the second-harmonic conversion conductance. (The equivalent circuit of Fig. 82 can also be used to calculate the gain of a converter in which the signal mixes with the nth harmonic of the local oscillator ($f_s = 2nf_o - f_k$). In this case, g_{c1} and g_{c2} must be replaced by g_{cn} and g_{c2n}, respectively. The values for g_o, g_c, and g_{c2} are evaluated for germanium tunnel diodes in reference 35.

In practical positive nonlinear-conductance mixers, the following inequalities must always be satisfied:[36]

$$g_o > 0, \; g_o > |g_{c1}|, \; g_o > |g_{o2}| \qquad (67)$$

However, these restrictions do not apply to tunnel-diode converters because tunnel diodes exhibit a negative conductance over part of their current-voltage characteristic.

CONVERSION GAIN

Expressions for the conversion gain (i.e., the ratio of if output power to the available signal power) can also be derived from the equivalent circuit shown in Fig. 82. If, for simplicity, it is assumed that Y_s, Y_k, and Y_l are pure conductances equal to the internal conductance of the generator g_g, the image conductance g_k, and the load conductance g_l, respectively, then the conversion gain K can be expressed as follows:

$$K = \frac{4 g_l g_g M^2}{(g_g + g_{in})^2} \qquad (68)$$

where

$$M = \frac{g_{c1} \; (g_o + g_k - g_{c2})}{(g_o + g_k) \; (g_o + g_i) - g_{c1}{}^2}$$

and where g_{in}, the input conductance, is given by

$$g_{in} = \frac{g_{c1}{}^2 \; (2 g_{c2} - 2 g_o - g_k) - (g_o + g_i) \; (g_{c2}{}^2 - g_o{}^2 - g_o g_k)}{(g_o + g_k) \; (g_o + g_i) - g_{c1}{}^2}$$

Passive converters must have conversion loss, as can be shown by the insertion of Eq. (67) into Eq. (68). Tunnel-diode converters, on the other hand, may have conversion gain when any one of the inequalities in Eq. (67) is reversed. This conversion gain can be made arbitrarily large, and approaches infinity as $-g_{in}$ approaches g_g.

BANDWIDTH

The conversion gain of a nonlinear-conductance frequency converter containing no reactances is independent of frequency. Tunnel diodes, however, contain parasitic capacitances and inductances; as a result, the gain of tunnel-diode frequency converters is frequency-dependent. With available tunnel diodes,

the effect of these reactances is usually negligible at conventional intermediate frequencies (30 megacycles or less), but must be taken into account at uhf and microwave frequencies.

An approximate equivalent ac circuit for an encapsulated tunnel diode consists of three elements connected in series: an inductance L_s, a resistance R_s, and a voltage-dependent resistance R_j (v) (1/g) shunted by a voltage-dependent capacitance C_j (v). L_s results mainly from the inductance of the housing; R_s is the resistance of the ohmic contact, the base, and the internal leads of the package, and is a function of frequency due to skin effect. C_j (v) is the junction capacitance*, and R_j (v) is the total ac resistance of the junction, where v is the voltage across R_j and C_j. The bandwidth of the converter can be calculated in a straightforward fashion if R_s, L_s, and C_j are incorporated into the admittances Y_s, Y_k, and Y_i of the equivalent circuit of Fig. 82, and the equivalent circuit is then used to calculate gain as a function of frequency. This circuit is shown in Fig. 83.
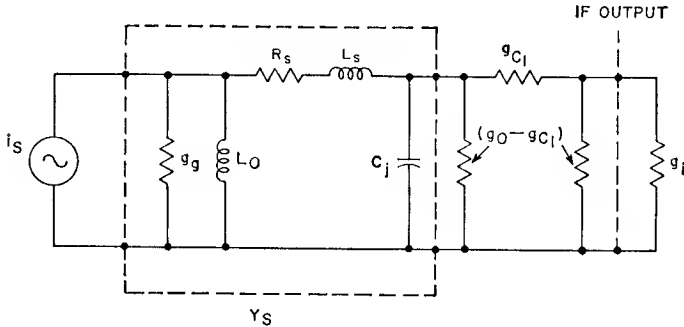
Fig. 83.   Equivalent circuit used for bandwidth calculation.

SPURIOUS OSCILLATIONS

A tunnel diode biased in its negative-resistance region, or driven into this region by an applied local-oscillator voltage, can generate rf oscillations. In autodyne frequency converters, advantage is taken of the self-oscillations of the tunnel diode

---

* The variation of C_j with voltage may be approximated for voltages less than the valley voltage by $C_j(v) \approx K(\Phi-v)^{-1/2}$ where K and Φ are constants. For germanium, Φ is approximately 0.6 volt. For a diode driven by a sinusoidal local oscillator, the average value of C_j is approximately equal to the value of C at the bias point.

to supply the local-oscillator drive. In converters with external local oscillators, however, self-oscillation must be prevented because these oscillations cause spurious responses and instabilities, and usually increase the noise of the converter.

Converter circuits that do not oscillate at any bias voltage without local-oscillator drive are also stable at any bias when driven by the local oscillator. This type of converter circuit must use "stable" diodes, i.e., diodes for which the following inequality exists:[37]

$$L_s < 3R_j{}^2C_j \qquad (69)$$

For stable diodes, the limits on the maximum usable peak current I_p and the minimum time constant R_jC_j are set by Eq. (69); for unstable diodes, these parameters are limited only by semiconductor fabrication techniques. Consequently, unstable tunnel diodes are often useful in high-power or high-frequency converters. (The power-handling capability of a diode is, in general, proportional to I_P. Also, the cutoff frequency, i.e., the frequency above which the real part of the diode impedance becomes positive, is proportional to $(|R_j|C_j)^{-1}$. It has been found experimentally that spurious oscillations in converters using unstable tunnel diodes can be prevented by use of a large local-oscillator drive (V_o is more than 0.1 volt). This procedure is most effective if the local-oscillator frequency is close to the self-oscillation frequency of the converter.

NOISE FIGURE

The noise figure NF of a nonlinear-conductance converter with short-circuited image impedance ($Y_k = \infty$) and with real input admittance can be written as follows:

$$NF = 1 + \frac{T}{T_o} \left(\frac{G_o\ (g_o + g_g)^2}{g_g g_{c1}{}^2} - \frac{2(g_o + g_g)\ G_{c1}}{g_g g_{c1}} + \frac{G_o}{g_g} \right) \quad (70)$$

where T is the ambient temperature and T_o is the standard reference temperature and G_o and G_{c1} are the short-noise conductances of the diode. (G_o and G_{c1} are evaluated for germanium tunnel diodes in reference 35.) In the derivation of Eq. (70), it was assumed that the noise currents at the signal and intermediate frequencies generated by the pumped nonlinear conductance are fully correlated. Also, in accordance with the IRE definition[38], the noise figure is written in terms of available noise output power, and does not take into account any noise contributions from the if load.

The noise figure of a tunnel-diode frequency converter, like the noise figure of a passive converter, must always exceed unity. However, the minimum noise figure that can be achieved with a tunnel-diode converter is lower than the minimum noise figure of a passive converter because the conductances g_o and g_{c1} in a tunnel-diode converter are not restricted by Eq. (67).

EXPERIMENTAL UHF AND MICROWAVE TUNNEL-DIODE CONVERTERS

Fig. 84 shows a simplified equivalent circuit for a converter with image rejection. Except for the dc bias circuit, which is designed to prevent spurious oscillations while the diode swings through the negative-resistance region, the equivalent circuit is similar to conventional passive frequency converters. The sizes of actual converters are generally comparable to those of miniaturized passive frequency converters.
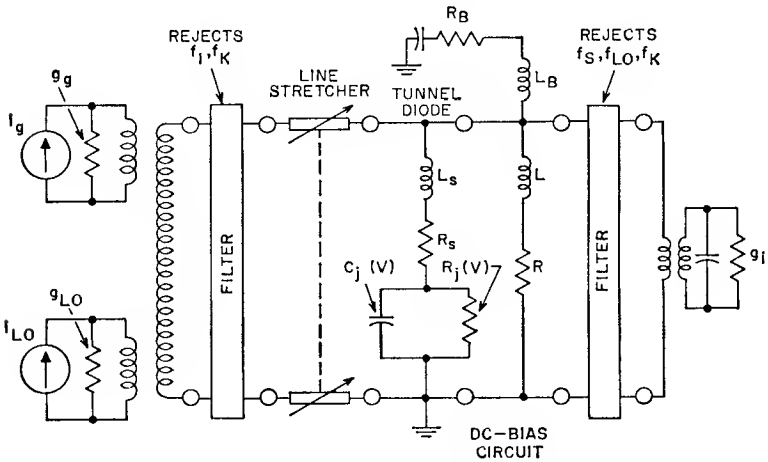
Fig. 84.   Simplified equivalent circuit for tunnel-diode frequency-converter having image rejection.

The conversion gain of a tunnel-diode frequency converter can be adjusted to any convenient value by suitable choice of diode and circuit parameters, bias voltage, and local-oscillator drive. Converters having conversion gain of more than a few db are very sensitive to variations in input impedance. On the other hand, converters having zero conversion gain, or conversion loss, are generally stable with input

VSWR's exceeding 10:1 varied through all phases. Futhermore, the lowest system noise figures (when a 30-megacycle if amplifier having a 1.7 db noise figure is used) are obtained with converters having conversion losses in the neighborhood of zero db.

The system noise figure of a balanced L-band converter is shown in Fig. 85 as a function of local-oscillator power.
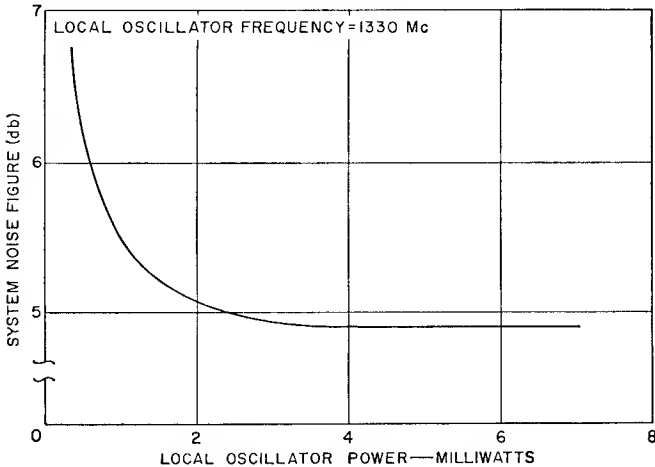
Fig. 85.   System noise figure as a function of local oscillator power for a balanced converter (noise figure of if amplifier equals 1.7 db).

The noise figure varies little for local-oscillator power in the range from about 2 to 7 milliwatts. The use of this relatively high pump power results in a large dynamic range. (Saturation effects occur only when the signal voltage across the diode becomes a significant fraction of the local-oscillator voltage.) Fig. 86 shows the conversion loss of a typical single-ended
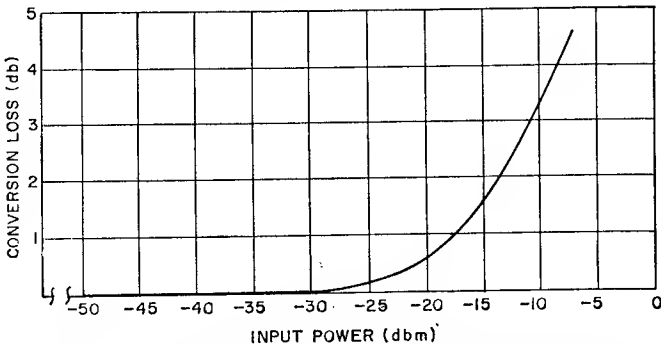
Fig. 86.   Conversion loss as a function of input power for a uhf tunnel-diode frequency converter.

converter as a function of input power. The conversion loss is increased by 3 db at an input of about 0.1 milliwatt. (In some more recent experiments with balanced mixers, 3-db gain compression occurred at a signal level of about one millivolt. The bandwidth of these converters was 250 megacycles centered at a frequency of 1270 megacycles.) The sensitivity of this converter to inputs at unwanted frequencies is comparable to that of crystal-diode converters. For one-per-cent intermodulation distortion, the power in the unwanted signal is about —30 dbm.

Burnout, i.e., detectable deterioration of performance, occurred for cw powers of two watts, and for pulse energies of 170 ergs. These results show that tunnel diodes can handle approximately one order of magnitude more cw power and pulse energy than conventional point-contact mixer diodes.

Table IV lists the lowest system noise figures measured to date. For this test, a 30-megacycle amplifier having a 1.7-db noise figure was used. (The quoted single-sideband noise figures include the losses of the image-rejection filters.)

Table IV
Measured System Noise Figures

Local-Oscillator Frequency (Mc)	Signal Frequency (Mc)	Double-Sideband System Noise Figure (db)	Single-Sideband System Noise Frequency (Image Rejection, 10db)
482	512		5
780		3.9	
1340		4.3	
1340	1370		5.5
2000		5.5	
10400		6.8	

REFERENCES

34. C. A. Burrus, "Millimeter Wave Esaki Diode Oscillator", *Proc. IRE*, Vol. 48, p. 2024, December 1960.

35. E. W. Herold, R. R. Bush, and W. R. Ferris, "Conversion Loss of Diode Mixers Having Image Frequency Impedance", *Proc. IRE*, Vol. 33, p. 603, September 1945.

36. H. C. Torrey and C. A. Whitmer, *Crystal Rectifiers*, McGraw-Hill Book Company, Inc., New York, 1948.

37. L. I. Smilen and D. C. Youla, "Stability Criteria for Tunnel Diodes", *Proc. IRE*, Vol. 49, pp. 1206-1207, July 1961.

38. IRE Standard on Electron Tubes: Definition of Terms, 1957, *Proc. IRE*, Vol. 45, p. 1000, July 1957.
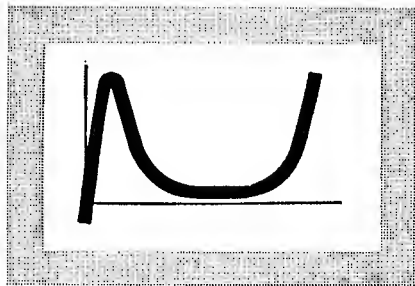
HIGH-CURRENT
DEVICES

H IGH-CURRENT tunnel diodes are best utilized as low-voltage inverters in circuits having low-impedance dc power sources.[39] They can be used for efficient inversion of the output of solar cells, thermoelectric generators, or thermionic converters. Other applications of these devices include overload detectors in dc and ac power supplies, pulse generators, high-speed switches, and oscillators.

High-current tunnel diodes are basically the same as conventional tunnel diodes in theory and construction. However, because of the high current involved, these diodes require a relatively large junction area. As discussed in the section on Characteristics, the peak current of tunnel diodes is directly proportional to junction area for a given crystal carrier concentration. A further difference of high-current tunnel diodes is the type of package used (RCA high-current devices generally use standard rectifier packages such as the DO-4 and the DO-8). In addition, if these diodes are operated at their maximum ratings, it is necessary that they be fastened to external heat sinks.

Conventional tunnel diodes and high-current tunnel diodes differ also in the value of the series resistance R_s. For high-current tunnel diodes, the series resistance should be kept as small as possible, generally in the order of 0.010 ohm, or less. If series resistance is not small, the efficiency of high-current tunnel diodes (especially when operated in inverter circuits) decreases rapidly. Fig. 87 shows the effect of an increase in series resistance on efficiency.

RCA high-current tunnel diodes combine large total junction areas and rugged packages into units of great mechanical strength. In an experiment demonstrating this capability, a 10-
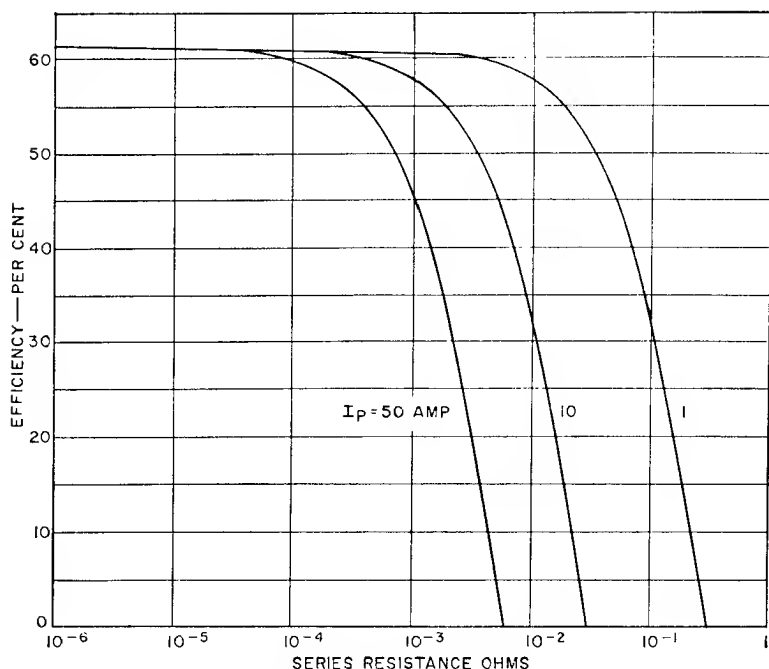
Fig. 87.   Efficiency as a function of series resistance.

ampere germanium unit operating in an inverter circuit was immersed completely into liquid nitrogen. Even at this extreme temperature ($-196°C$), operation was successful. In fact, the inversion efficiency was improved considerably because of increasing peak-to-valley-current ratios at low temperatures.

INVERTER CIRCUITS

The two most common forms of inverter circuits for the conversion of low-voltage dc to higher-voltage ac (or dc) are shown in Figs. 88 and 89. The maximum conversion efficiency[40, 41] η for a diode operating in either circuit (if threshold operation is assumed) is given by

$$\eta \cong \frac{\left(\dfrac{I_P}{I_V} - 1 \right) \left(\dfrac{V_V}{V_P} - 1 \right)}{\left(\dfrac{I_P}{I_V} + 1 \right) \left(\dfrac{V_V}{V_P} + 1 \right)} \tag{71}$$
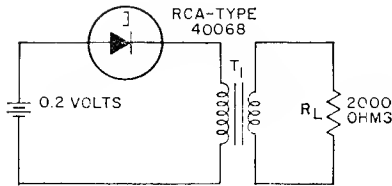
Fig. 88.   Low-voltage dc inversion circuit.
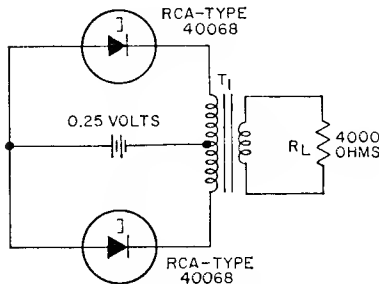
Fig. 89.   Low-voltage dc inversion circuit.

As shown in Fig. 90, it is desirable to have large peak-to-valley current and voltage ratios. For germanium, typical current and voltage ratios are 10 to 1 and 3 or 4 to 1, respectively; these values correspond to efficiencies of 40 to 50 per cent. For GaAs, typical current and voltage ratios are 20 to 1 and 5 or 6 to 1, respectively. The voltage ratio depends primarily on the peak voltage V_P, which in turn depends on the series resistance R_s.

The actual peak and valley voltages, however, consist of two components, as follows:

$$V_P = V_P' + (I_P)\ R_s)$$
$$V_v = V_v' + (I_v)\ (R_s) \tag{72}$$

where V_P' is the voltage across the junction itself. The inherent peak voltage V_P' of germanium diodes may be as low as 45 millivolts; inherent valley voltage V_V' may be in the range of 300 to 400 millivolts. These values correspond to a voltage ratio between 6 to 1 and 9 to 1.

As shown by the above equation, the value of R_s can have a major influence on the measured peak voltage (especially at high peak currents). For example, the typical series resistance
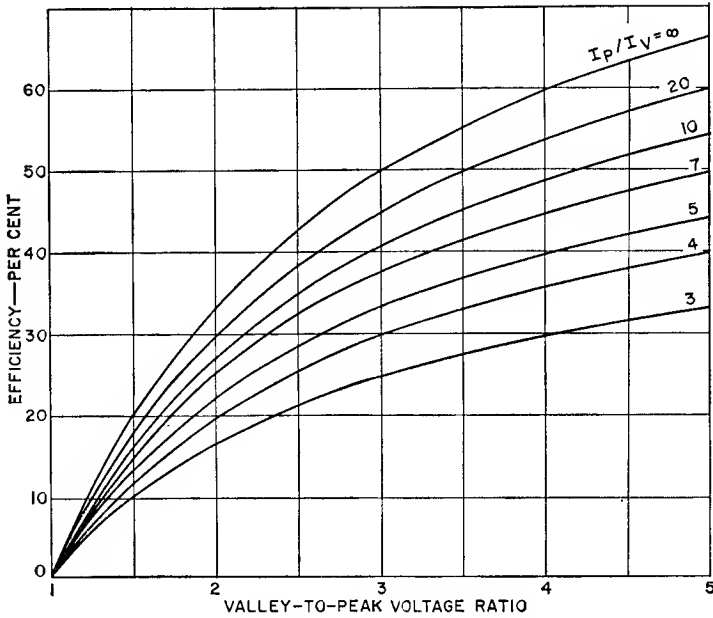
Fig. 90.   Efficiency as a function of valley-to-peak
voltage ratio.

of a one-ampere diode is 0.05 ohm. The value of (I_P) (R_s) is
then 1.0 x 0.05, or 50 millivolts, and the actual peak voltage is
given by

$$V_P = 45 + 50 = 95 \text{ millivolts} \qquad (73)$$

Thus, the series resistance can reduce the voltage ratio ap-
proximately in half. The effect of series resistance on valley
voltage, however, can usually be neglected because the term
$(I_V R_s)$ is only one-tenth of the term $(I_P R_s)$.

If high conversion efficiencies are to be attained, the series
resistance must be reduced as much as possible (see Fig. 87).
Although efficiencies of approximately 50 per cent are presently
realizable, this figure may be raised to 60 to 70 per cent by the
further development of materials such as gallium arsenide.
(Efficiencies greater than 60 per cent have already been ob-
tained with experimental gallium arsenide high-current tunnel
diodes.) Although both germanium and gallium arsenide are
theoretically about equally well suited for high efficiencies, the
greater peak-to-valley-current ratio and high-temperature
capability offered by gallium arsenide may be advantageous
for certain applications.

Although the efficiency of tunnel-diode inverters may seem low compared to the efficiencies of transistorized inverters, it must be remembered that transistors can only operate efficiently at relatively high voltages (one volt or higher). At lower voltage levels, tunnel diodes are considerably more effective, as shown in Fig. 91. At present the high voltages required for effective operation of transistorized inverters are obtained from a series arrangement of low-voltage dc sources (fuel cells, solar cells, thermoelectric generators). This method is not as reliable as the use of parallel supplies because the output of the entire series string is lost if only one cell opens.
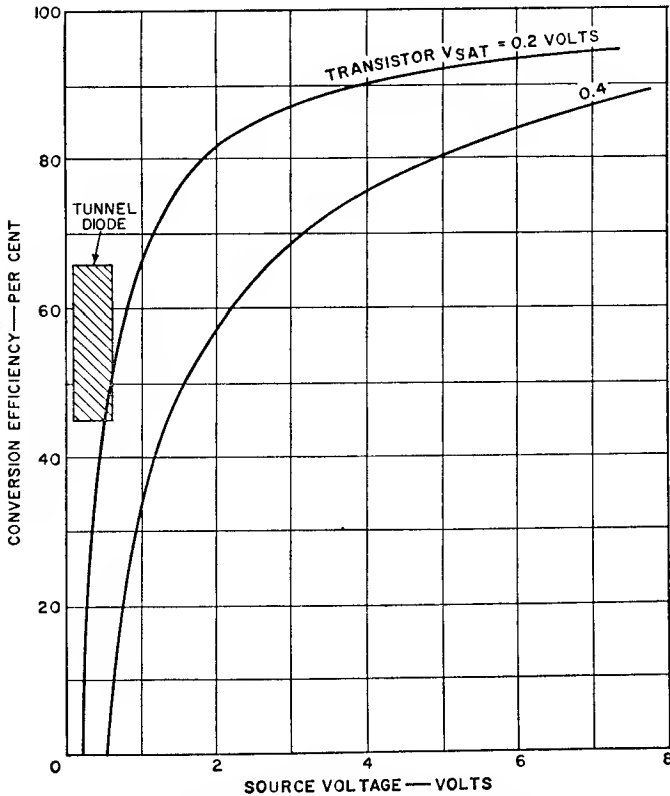
Fig. 91.   Transistor and tunnel-diode efficiency as a function of supply voltage.

The circuit shown in Fig. 88 is basically a relaxation oscillator. If the tunnel diode is biased in the negative region (for germanium diodes approximately 0.11 to 0.33 volts), oscillation having a trapezoidal waveform such as that shown in
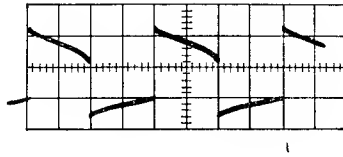
Fig. 92.   Output for a tunnel-diode relaxation oscil-
            lator.

Fig. 92 occurs, provided that the following conditions are met:
First, the total circuit resistance R_T, including diode series re-
sistance, must be less than the absolute value of negative
resistance of the diode at the operating point, as follows:

$$(R_T + R_s) < |R_j| \tag{74}$$

Second, the total circuit series inductance L_T must be greater
than the product of the total circuit resistance, the absolute
value of the negative resistance of the diode, and the junction
capacitance,[42] as follows:

$$L_T > (R_T + R_s) \ (|R_j|) \ (C_j) \tag{75}$$

For high-current units, the second criteria is very easy to meet.
For example, some typical parameters for a 5-ampere diode
are: $(R_j) = 0.02$ ohm, $C = 0.011$ microfarad, $L_{CASE} =$ five
nanohenries. When these values are substituted into Eq. (75),
it is seen that $5 \times 10^{-9} > (0.02) \ (0.02) \ (1.1 \times 10^{-8} =
4.4 \times 10^{-12}$. As a result, the inequality is true, and the second
requirement is met by the inductance of the diode package
alone.

The first requirement is not so easy to meet, however, be-
cause the negative resistance is so small. For a 20-ampere
germanium unit, the minimum negative resistance is about
0.006 ohm. As a result, the sum of the series resistance, the
power-supply resistance, the lead and contact resistances, and
the transformer primary resistance must be less than 6 milli-
ohms. Careful inverter design permits this requirement to be
met.

A theoretical analysis[43] of the single-tunnel-diode inverter
circuit under load and no-load conditions shows that maximum
efficiency is obtained when the diode oscillates with equal posi-
tive and negative periods. An approximate equation for the
frequency of a symmetrically oscillating loaded inverter is
given by

$$f = \frac{1}{4L} \frac{(V_V - V_P)}{(I_P - I_V)} \qquad (76)$$

where L is the inductance of the primary winding of the loaded transformer.

The two-diode inverter circuit shown in Fig. 89 may be described as either parallel or push-pull. This circuit has three possible modes of operation which depend on the bias voltage, load resistance, and transformer-winding polarity and core material. If the transformer primary is wound in opposite directions on each side of the center tap, a parallel mode of operation similar to that of the single-diode inverter mode occurs. Both diodes operate at the same frequency; the output waveform is similar to that shown in Fig. 92.

If the primary is wound in the same direction throughout, a push-pull arrangement results. The push-pull circuit configuration has two possible modes of operation. When the diodes operate in phase (symmetrically), efficiency is very low because the currents are "bucking" each other in the transformer primary. If the diodes operate 180 degrees out of phase (asymmetrically), the currents through the primary add to each other. In this mode of operation, conversion efficiency is high. The output waveform is symmetrical and approximately square, and its frequency is much lower than in the parallel mode of operation. Several excellent analyses and explanations of circuit operation for the push-pull inverter circuit are available in the literature.[44-47]

EXPERIMENTAL CIRCUITS

In the inverter circuit shown in Fig. 88, the primary was constructed of six turns of heavy (No. 14) enameled wire with a center tap. Several hundred turns of fine wire were used for the secondary. The core material used was Carpenter "49", 0.014 inch. A regulated dc power supply was used as the energy source. Figs. 93, 94, 95, and 96 show the variations in tunnel-diode conversion efficiency and frequency as functions of bias or load resistance for two temperature ranges. Input dc power was measured with a dc ammeter and dc voltmeter. The voltmeter was connected directly across the diode. The transformer secondary was connected to a decade resistance box. Output power was measured with a true-rms-reading voltmeter, and computed by use of the following equation:

$$P_o = \frac{V_o{}^2}{R_L} \qquad (77)$$
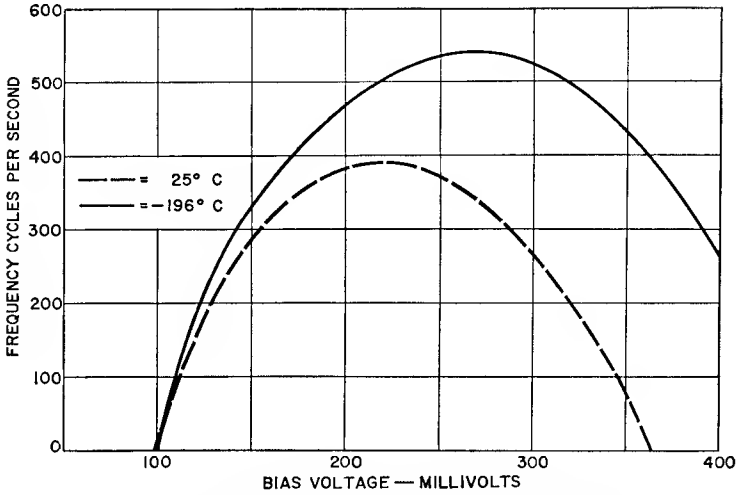
Fig. 93.   Frequency as a function of bias voltage for
RCA-40068 (resistance equals 1000 ohms).
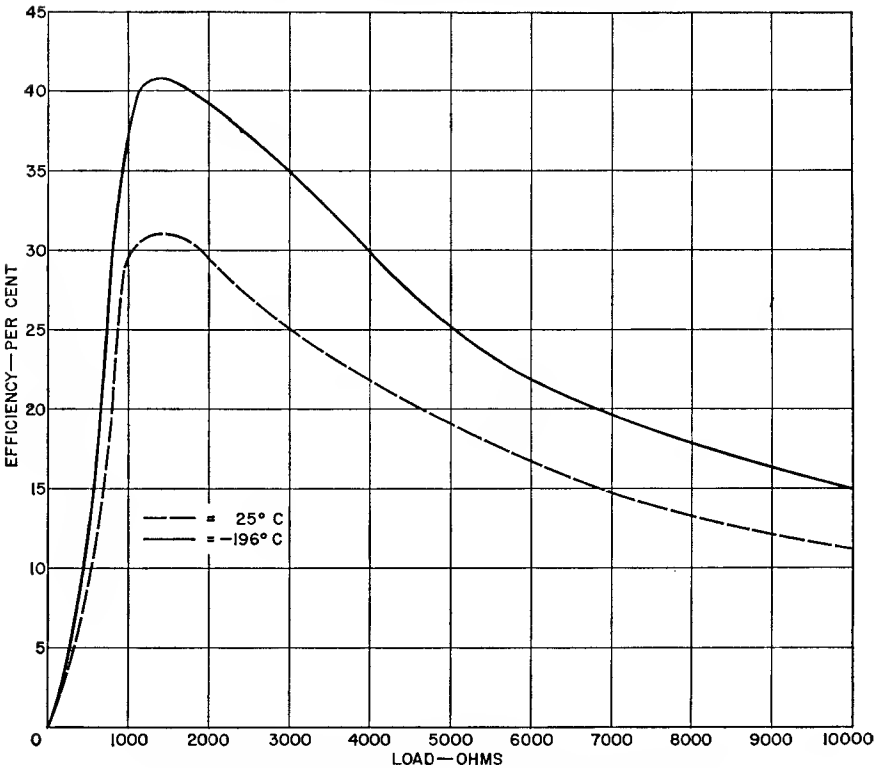
Fig. 94.   Efficiency as a function of resistance for
RCA-40068 (bias voltage is 240 millivolts).
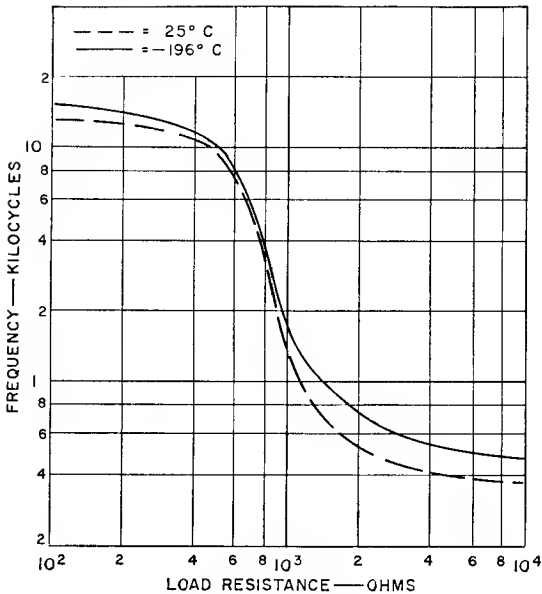
Fig. 95.   Frequency as a function of load resistance
            for RCA-40068 (bias voltage is 240 millivolts).

The curves illustrate the increase of efficiency at −196 degrees centigrade. This improved efficiency results because the peak-to-valley current and voltage ratios increase considerably as the diode is cooled. For example, at room temperature the I_P/I_V ratio was 10 to 1; at liquid-nitrogen temperature it was 26 to 1. The shape of the curves is typical for all types of high-current tunnel diodes operated in a single-diode inverter circuit; however, different values of peak efficiency, frequency, and the like result when different transformers or diodes are used. Figs. 97 and 98 show the actual shape of the waveforms at three different bias levels. The type of diode and transformer used also affect the exact bias voltage or load resistance at which the peak efficiency occurs.

The parallel mode of operation is very similar to single-diode operation. Curves for parameters such as efficiency and frequency have the same general shape as those for the single-diode circuit. The major advantage of the parallel mode over the single-diode circuit is that the output power can be doubled without the use of higher peak-current diodes.
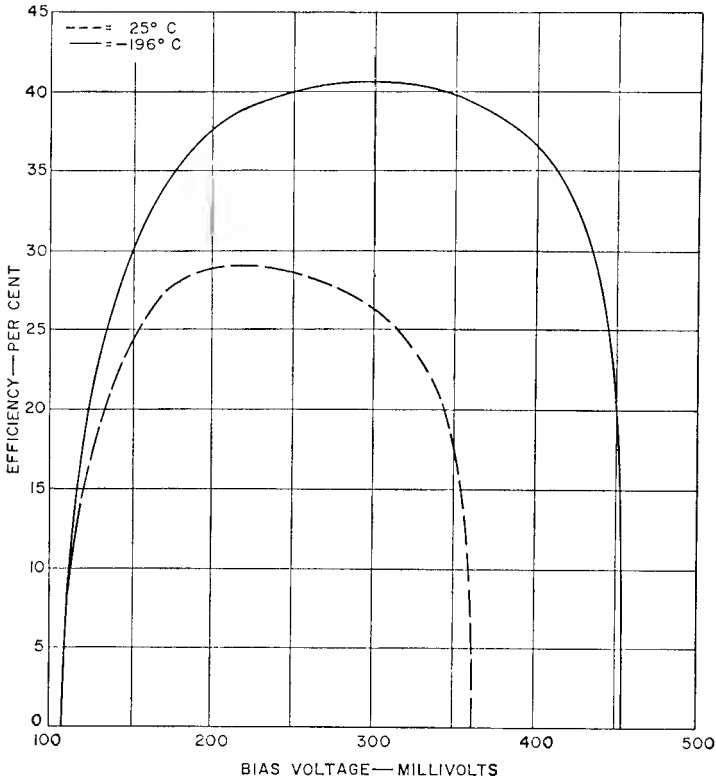
Fig. 96.   Efficiency as a function of bias voltage for
RCA-40068.

Figs. 99 and 100 show the results of operation in the push-pull mode. Fig. 101 shows the general shape of the input and output waveforms. Fig. 102 shows the higher efficiencies obtainable with gallium arsenide. Two striking differences between single-diode and push-pull operation are immediately apparent. First, the output of the push-pull circuit is much squarer and has little "droop" as compared to that of the single-diode circuit. This squareness is continuous over the entire operating-voltage range. Second, the output frequency is much lower and relatively constant. This circuit also allows the power source to deliver a much more constant current than the single-diode circuit. In the single-diode circuit, the diode draws
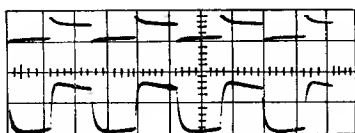
BIAS=236 MILLIVOLTS
HORIZONTAL=200 μSEC/DIV.
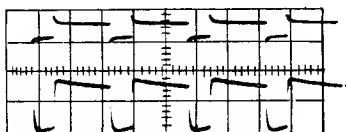
BIAS=300 MILLIVOLTS
HORIZONTAL=500 μSEC/DIV.
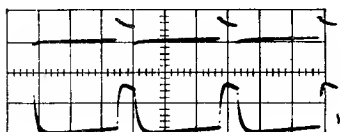
BIAS=150 MILLIVOLTS
HORIZONTAL=200 μSEC/DIV.

Fig. 97.   Waveforms for the single-diode inverter.

heavy current only when it operates near the peak point; as a result, the power supply must furnish a pulsating current.

In addition, the efficiency of the diode itself is materially greater in the push-pull circuit than in single or parallel operation. In single or parallel operation, the diode operates at high forward voltages (greater than valley voltage) for an appreciable part of a cycle, and thus has increased dissipation and loss. In the push-pull mode, the diode spends only a very small fraction of a cycle at voltages beyond the valley point. For the particular transformer used, push-pull operation could be obtained only in the 200- to 280-millivolt region. Beyond these points, the diodes switch to either the low-voltage or high-voltage positive-resistance regions. A wider range of operation would probably result if total external resistance (transformer, connections, and the like) were reduced. Also, if the load is made less than 190 ohms, the symmetrical mode of operation results and, as predicted, the output power is reduced to zero. The critical secondary load resistance is then given by

$$R_L = 2n^2 \left(\frac{[V_V + R_T I_V] - [V_P + R_T I_P]}{I_P - I_V} \right) \qquad (78)$$
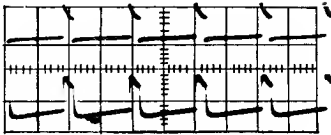
BIAS: 150 MILLIVOLTS
HORIZONTAL: 500 μSEC/DIV.
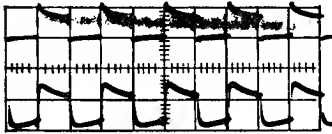
BIAS: 300 MILLIVOLTS
HORIZONTAL: 500 μSEC/DIV.
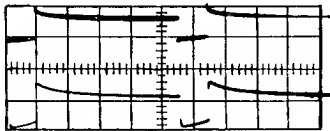
BIAS: 420 MILLIVOLTS
HORIZONTAL: 1 MS/DIV.

VERTICAL SENSITIVITY
UPPER TRACE = 0.5V/DIV.
LOWER TRACE = 50.0V/DIV.

Fig. 98. Waveforms for single-diode inverter.

where R_T is the transformer primary-winding resistance and n is the transformer turns ratio. If a lower load resistance is used, the symmetrical mode of oscillation is destroyed, and no power output results.
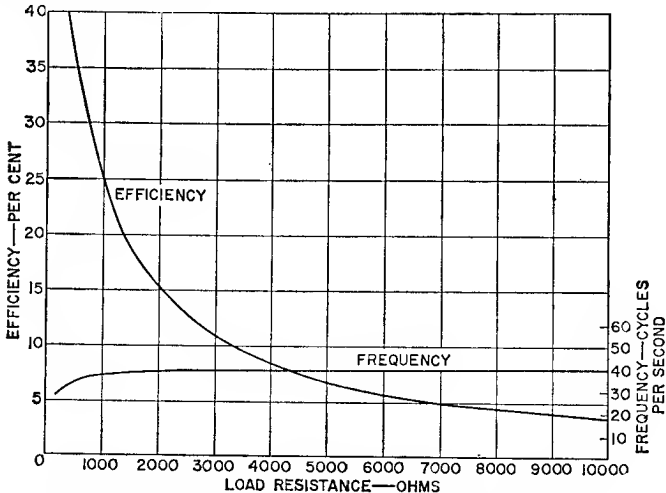
Fig. 99.   Efficiency and frequency as a function of
            load resistance (load resistance is 1000
            ohms).
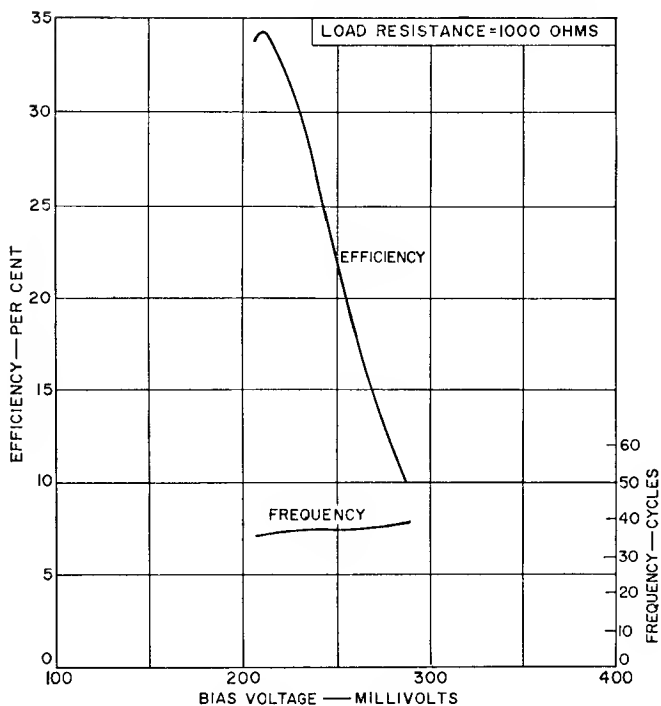
Fig. 100.   Tunnel-diode efficiency and frequency as a
            function of bias voltage.
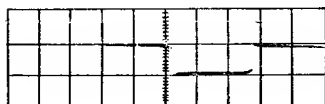
(a)

VERTICAL: 0.5V/DIV.
HORIZONTAL: 5MS/DIV.
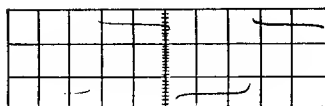
(b)

VERTICAL: 20.0V/DIV.
HORIZONTAL: 5MS/DIV.

Fig. 101.   Inverter waveforms for two RCA-40068's op-
            erated in a push-pull circuit; (a) tunnel-
            diode waveform, and (b) inverter output.
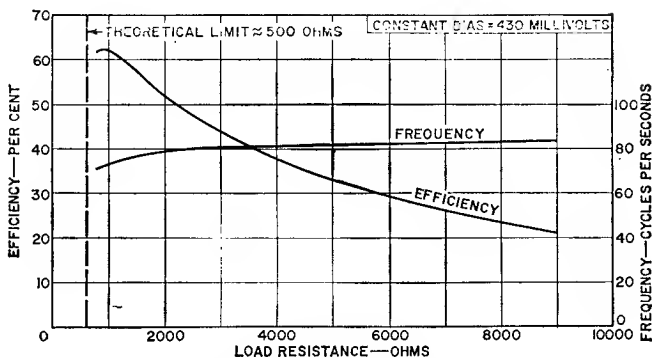
Fig. 102.   Efficiency as a function of load resistance
for six-ampere gallium arsenide tunnel
diodes used in a push-pull inverter circuit.

OTHER CIRCUITS

High-current tunnel diodes may be used to drive high-power transistors in either common-emitter or common-base configurations. For example, Fig. 103 shows the combined use of a germanium tunnel diode and a power transistor in a bistable switching circuit; in such circuits, the low rise time of the diode (as low as one nanosecond) can be used to drive transistors at rates much faster than many other methods presently available.
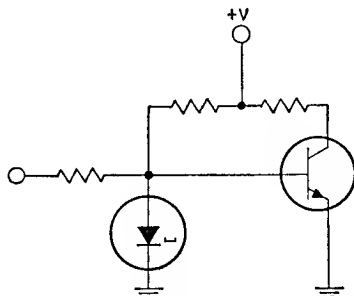
Fig. 103.   Bistable   tunnel-diode-transistor   combination.

If silicon power transistors are used, their higher base-to-emitter voltage makes it necessary either to "bias up" the germanium tunnel diode, as shown in Fig. 104, or to use a gallium arsenide high-current tunnel diode. This application may be a very useful one for gallium arsenide diodes because their higher voltage swing could easily turn on a silicon transistor.

At the same time, the base-to-emitter voltage of the transistor effectively clamps the gallium arsenide diode below the point in the forward-voltage region at which the degradation mechanism of gallium arsenide becomes active.
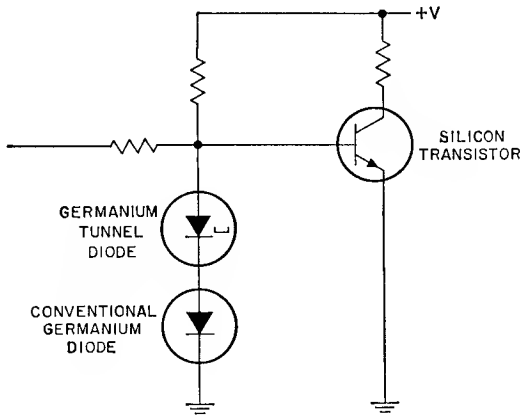
Fig. 104.   Method for "biasing-up" tunnel diodes.

Fig. 105 shows an example of a tunnel-diode overload-sensor circuit. This circuit uses high-current tunnel diodes and provides a fast-acting sensitive over-current detector which can be used to protect sensitive loads from current surges or overloads. Other circuit arrangements are possible if the power supply is to be protected rather than the load.
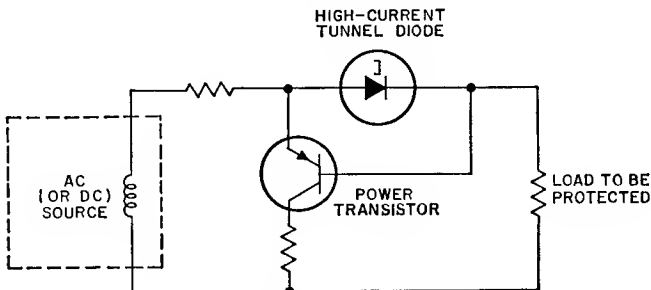
Fig. 105.   Tunnel-diode overload sensor.

REFERENCES

39. F. M. Carlson and P. D. Gardner, "High-Current Germanium Tunnel Diodes", presented at 1962 IRE Electron Devices Conference.

40. J. M. Marzolf, Tunnel-Diode Static Inverter, *USNRL Report* 5706, October 1961.

41. Gevert, Wang, and Broze, "Heat-to-AC Conversion Using Thermoelectric Generators and Tunnel Diodes, *Solid-State Electronics*, Vol. 3, 1961. In this paper, the equation for efficiency is given as

$$n = \frac{7}{8} \left[\frac{(I_P - I_V)\,(V_V - V_P)}{(I_P + I_V)\,(V_V + V_P)} \right]$$

42. A. M. Goodman, "A Test Set for Displaying the V-I Characteristic of a Tunnel Diode", *Review of Sci. Inst.*, March, 1960.

43. H. F. Storm and D. P. Shattuck, "Tunnel-Diode DC Power Converter", *Communications and Electronics* (AIEE), July, 1961.

44. A. C. Scott, "Symmetrical DC Converter Using Six-ampere Tunnel Diodes", *Proc. IRE*, p. 1851, August 1962.

45. A. C. Scott, "Design and Oscillator Applications of High-Current Tunnel Diode", Doctoral Thesis at MIT, September 1961.

46. J. M. Marzolf, "Tunnel-Diode Static Inverter", *Electronic Design*, Nov. 1961.

47. D. J. Hanrahan, "Analysis of Tunnel-Diode Converter Performance", *USNRL Report* No. 5722, US, Dec. 1961 (Also *IRE Transactions on Electron Devices*, July 1962).
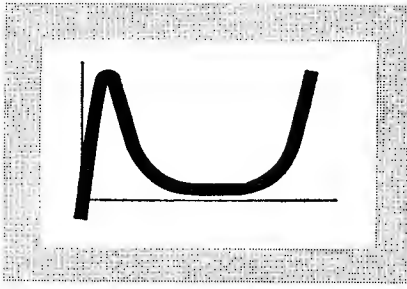
NOVEL DEVICES
AND CIRCUITS

THE tunnel resistor is basically a parallel combination of a tunnel diode and a resistor, integrated and miniaturized to fit in the same package as a tunnel diode. The voltage-current characteristic for this device is shown in Fig. 106. The
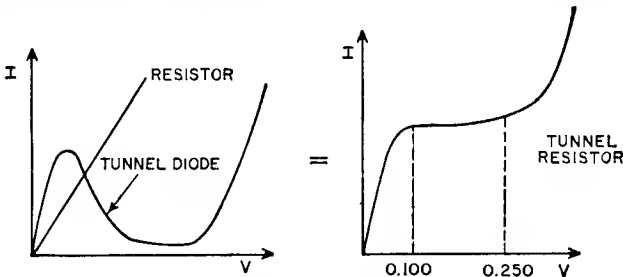
Fig. 106.   Tunnel-resistor characteristic.

resistor used is a special ultra-low inductance type. The inductance must be kept extremely low to prevent oscillations due to the tunnel-diode negative-resistance region. The flat portion of the resistor characteristic is formed by matching the positive resistance of the resistor to the steepest part of the negative-resistance portion of the tunnel-diode characteristic. The important parameters of the tunnel resistor include the current level of the plateau (high resistance region), the voltage at either end of the plateau, and the degree of flatness of the plateau.

The tunnel resistor is used primarily as a non-linear biasing element in tunnel-diode logic circuits, especially in monostable stages. In such applications, tunnel resistors offer faster tunnel-diode recovery time and require less current for triggering a stage than does a purely ohmic resistor. However, the principal advantage of the tunnel resistor is that it

118

reduces the power dissipation. As shown in Fig. 107, the load line of the tunnel resistor is nearly flat at operating point A compared to the dashed line of a conventional resistor using the same bias. As a result, the precise value of the bias voltage has much less effect on the operating current level of tunnel resistors. Thus a simulated constant-current load line can be obtained by use of a tunnel resistor and a low-voltage source, rather than a power-consuming current source. In the case of an ohmic resistor, the same load line at operating point A could only be achieved with a higher voltage source and, hence, a much greater power dissipation.
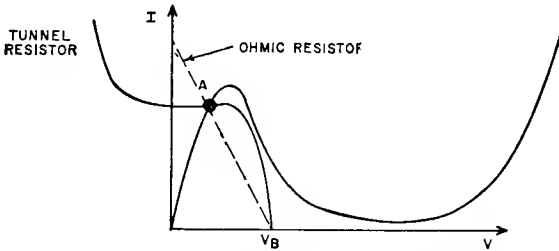
Fig. 107. Tunnel-diode having tunnel-resistor load.

HIGH-FREQUENCY SYNCHRONIZER

Many sampling oscilloscopes have inherent bandwidths much greater than the trigger (sync) circuits of the scope can handle. For example, although some sampling scopes have a 500-megacycle bandwidth, their trigger circuits cannot sync on frequencies greater than 50 megacycles. Thus, if a 500-megacycle signal is to be displayed, exact subharmonics of the input signal must be generated to trigger the scope sweep circuits. The tunnel diode is the only known device capable of triggering scopes over such a wide frequency range. The simple tunnel-diode counter shown in Fig. 108 can achieve
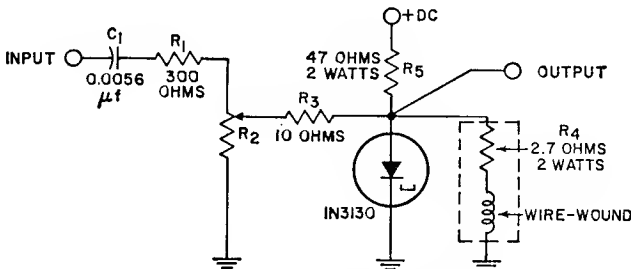
Fig. 108. Tunnel-diode synchronizer.

"countdowns" greater than 50 to 1, and can be used at frequencies higher than 500 megacycles. The upper usable limit is not known, but sine waves have been successfully displayed up to 1.2 gigacycles on a sampling scope capable of handling a maximum sync signal of only 100 megacycles.

Because of the high frequencies involved, loads should be kept as short as possible in the circuit of Fig. 108. The input combination of C_1R_1 blocks dc and the ac output from the input. (A small fraction of output signal, in the order of a few millivolts, does appear at the input, however.) After the circuit is assembled, it may be quickly checked out by application of a dc voltage of five to seven volts and observation of the output on a standard 30-megacycle scope. A trapezoidal-shaped wave having a frequency of five to thirty megacycles should be observed.

Operation of the counter is as follows: First, the output is connected directly to the scope trigger input socket, and then the input is connected to the signal source or trigger takeoff. (A minimum input signal of about ten millivolts is required.) At this point, a dc voltage of approximately five to seven volts is applied, and the voltage, resistor R_2, and the scope trigger controls are slightly adjusted until a stable display appears. These adjustments must be made slowly and very carefully. If the display drifts (becomes unstable), readjustment of the dc voltage is usually the quickest way to make the display stable again.

A more sophisticated synchronizer circuit which can be used at frequencies of more than 3000 megacycles is shown in Fig. 109. In this circuit, TD_1 is a 150-megacycle free-running relaxation oscillator; TD_2 is a monostably biased tunnel
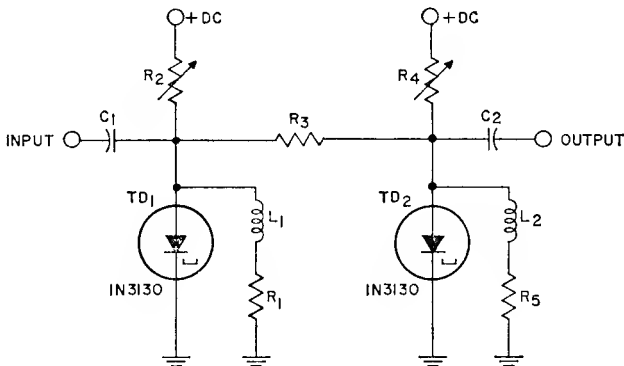
Fig. 109.   Five-gigacycle synchronizer circuit.

diode. The loadlines for these diodes are shown in Fig. 110. The output is at a frequency of approximately 50 to 100 kilocycles. Peak-to-peak voltage up to one volt can be provided at the output by use of a gallium arsenide 50-milliampere tunnel diode for TD_2. The input and coupling elements (C_1 and R_3) also may be replaced by high-speed diodes to reduce the feedback of the output into the input. The voltage developed across TD_1 must be held to a maximum of 500 to 600 millivolts; otherwise an input attenuator is needed.

The inductance L_1 must be kept to an extremely low value (approximately 1 to 10 nanohenries) for TD_1 to run freely at more than 100 megacycles. R_1 and R_5 may be one to two ohms.
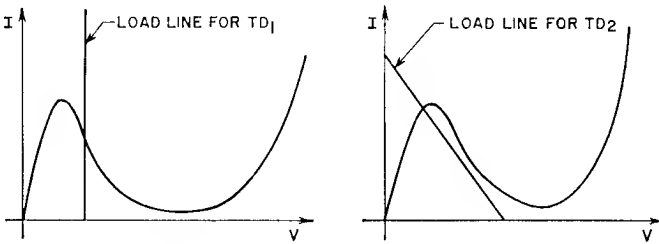
Fig. 110.   Tunnel-diode load lines.

TUNNEL-DIODE INDICATOR

Figs. 111 and 112 show two circuits which can be used to provide a visual indication of whether the tunnel diode is in the high or low state. Because the input impedance of either
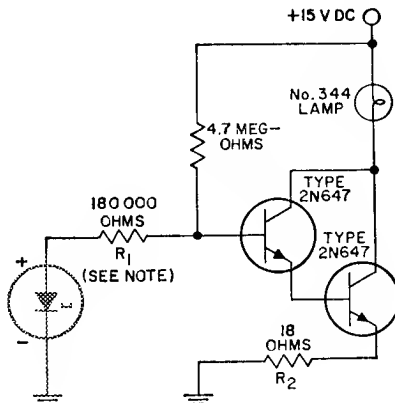
Fig. 111.   Tunnel-diode indicator for grounded anodes
(R_1 should be physically close to the diode).

circuit is greater than 100,000 ohms, negligible current is drawn from the diode under observation.
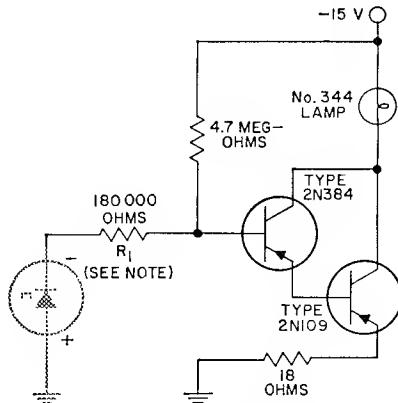
Fig. 112.   Tunnel-diode indicator for grounded cath-odes (R_1 should be physically close to the diode).

SCALE EXPANDER

A useful circuit which permits tunnel-diode peak current to be measured on a curve tracer with discrimination better than 0.1 per cent and accuracy better than 0.5 per cent is shown in Fig. 113. This simple attachment effectively magnifies the top portion of the tunnel-diode characteristic ten times. Thus, a one-per cent current deviation represents one major division instead of one-half of a minor division as on a conventional curve tracer graticule.
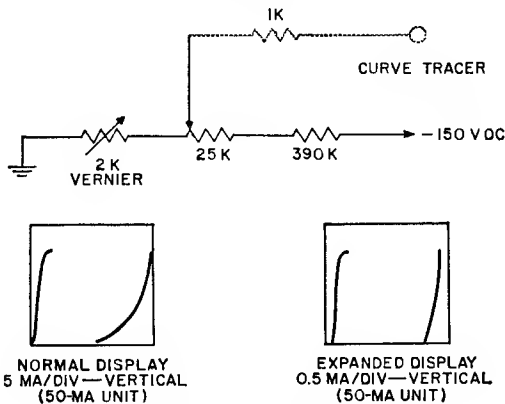
Fig. 113.   Scale expander.

This attachment basically expands the range of the vertical-positioning control so that the top portion of the characteristic can be seen on an expanded scale. Calibration is most easily obtained by use of a diode having a known peak current. (This calibration unit may have been measured on the precision-measurement equipment described in the section on Measuring Circuits.) Once the set is calibrated, the vertical-positioning controls must not be disturbed.

OTHER USES

Some other novel uses of tunnel diodes are found in decade counters or ring counters. Under certain conditions, for example, a "count-by-10" circuit can be designed by use of ten tunnel diodes in series. Tunnel diodes in conjunction with transistors have been used in ring counters having 100-mega-cycle repetition rates. Full adders using tunnel diodes with and without transistors have been described in the literature. (See reference in the section on Switching.) The use of tunnel diodes generally permits simpler full-adder circuitry than all-transistorized circuits.
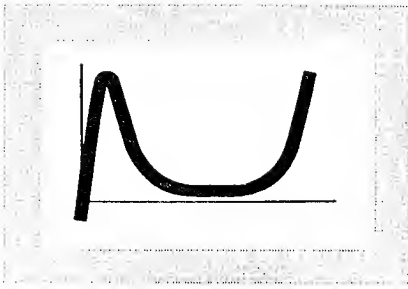
MEASURING CIRCUITS

TUNNEL-DIODE parameters are easily measured by display of their characteristics on a curve tracer. When a conventional curve tracer is used, a trace similar to that shown in Fig. 114 appears. The negative-resistance portion of the characteristic is not visible because of the speed with which the diode switches from the low-voltage positive-resistance portion
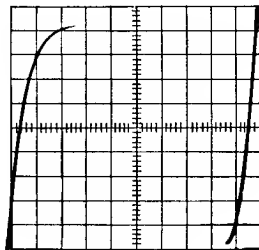
Fig. 114.   Tunnel-diode characteristic.

of the curve directly to the high-voltage positive-resistance region. The rapid switching occurs because the curve tracer has a total internal series resistance greater than the absolute value of the diode negative resistance. As a result, the diode load line is similar to that shown in Fig. 115, line A. As the sweep current exceeds the peak current (line B) of the diode, the diode immediately switches to its high state.

One of the requirements for display of the complete characteristic is that the total circuit series resistance R_T be less than the absolute value of the tunnel-diode negative resistance R_j, as follows:

$$R_T \ < \ |R_j| \tag{79}$$

124
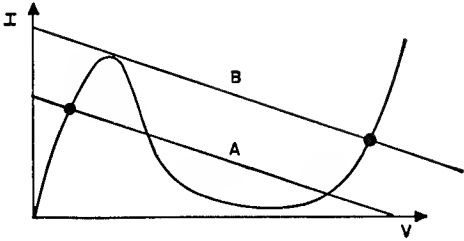
Fig. 115.   Tunnel-diode load lines.

When this condition is satisfied, the diode load line is similar to that shown in Fig. 116. In this case, when the curve-tracer sweep current exceeds the peak current, the diode does not switch directly to the high state, but instead travels through the negative-resistance region continuously. However, the
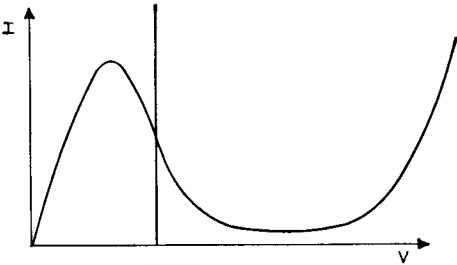
Fig. 116.   Load-line conditions for display of complete characteristic.

curve tracer may display characteristics such as those shown in Fig. 117. The presence of such "bumps" or "fuzz" in the

(a)   (b)
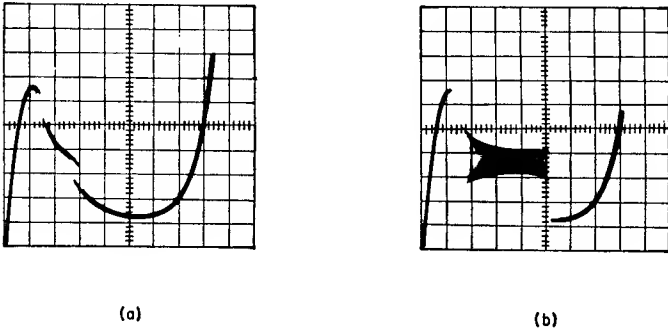
Fig. 117.   Presence of imperfections in diode charac-
teristic.

negative-resistance region indicates that the diode is oscillating as it is swept through this region. This effect can be prevented by use of a total circuit series inductance L_T (including case inductance) which is less than the product of the total circuit series resistance, the minimum negative resistance of the diode, and the juncton capacitance as shown by the following expression[48]:

$$L_T < R_T \times |R|_{Min} \times C_j \qquad (80)$$

Eqs. (79) and (80) represent the two stability conditions that must be met if the complete tunnel-diode characteristic is to be stably displayed.

For low-peak-current units, the circuit shown in Fig. 118 may be used to display the complete characteristic. In this circuit, resistor R_1 serves to bypass the power source so that only the resistance and inductance of resistors R_1 and R_2 are presented to the tunnel diode. R_2 is the current-sampling resistor, and R_3 is the current-limiting resistor. R_1 and R_2 may
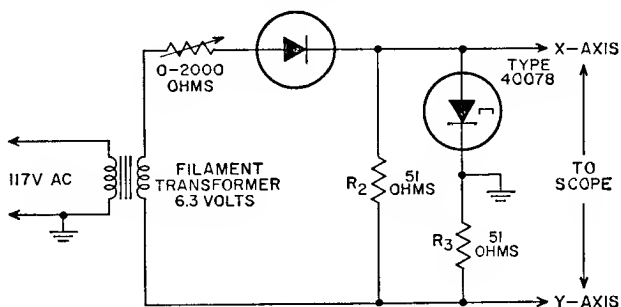
Fig. 118.   Tunnel-diode curve tracer.

be any values as long as their sum is less than $|R_j|$. It is a mistake to assume that the stability of the circuit is increased if R_1 and R_2 are very low. If the resistance $(R_1 + R_2)$ is lower than necessary, it is harder to stabilize the diode, as shown by Eq. (80).

For medium-peak-current units, the total inductance of two resistors in series may be too large to satisfy Eq. (80). In this case, the circuit shown in Fig. 119 can be used to reduce the circuit inductance by more than 50 per cent.[42] This circuit is basically a form of the familiar Wheatstone bridge. Resistor R_2 is used to obtain a "null" on the bridge without a diode in the circuit. Null is indicated on the scope by a perfectly horizontal line. The diode is then inserted, and the complete curve is traced out. Current through the tunnel diode is measured by the unbalanced condition it causes in the bridge. Methods
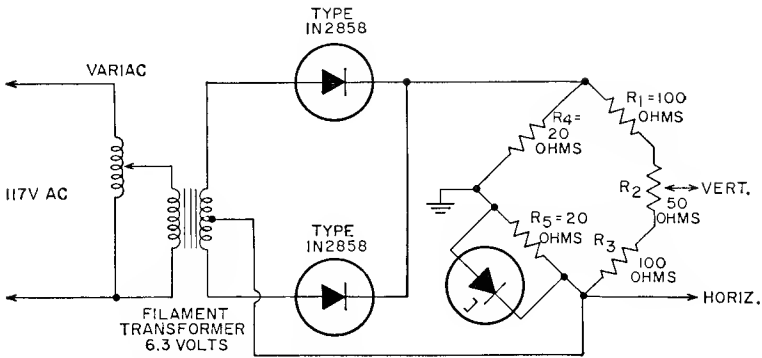
Fig. 119.   Tunnel-diode curve tracer.

for the reduction of the inductance of the critical section (R_5 plus tunnel-diode unit) are described in reference 42.

Medium-current units (50 milliamperes or more) generally have too much case inductance to be stabilized completely. For example, a 50-milliampere diode may have a case inductance of 0.4 nanohenry, a negative resistance of two ohms, and a capacitance of 10 picofarads. Substitution of these values in Eq. (80) produces the following impossible inequality:

$$4 \times 10^{-10} < (2)\ (2)\ (10^{-11}) = 0.40 \times 10^{-10}$$

HIGH-CURRENT UNITS

Most commercial curve tracers are limited to an average collector sweep current of 10 amperes or a peak current of 20 amperes for short durations. Although heavy-duty attachments are available, they are generally quite expensive. Because complicated and costly circuits such as staircase-waveform generators are not needed for the tracing of tunnel-diode curves, a high-current adapter may be easily built at low cost. The adaptor shown in Fig. 120 can extend the range of commercial curve tracers to a peak current of approximately 60 amperes. Provided properly rated components are used, this basic circuit can be used to build curve tracers usable up to 1000 amperes. (Although the transformer specified in Fig. 120 is rated at only 30 amperes, it is possible to trace curves of diodes having peak currents up to 60 amperes because current flows only every half-cycle, and the rms value of a half-rectified sine wave is one-half of the peak current.)

In Fig. 120, two of the four leads connected to the tunnel diode are voltage-sensing leads which measure the voltage
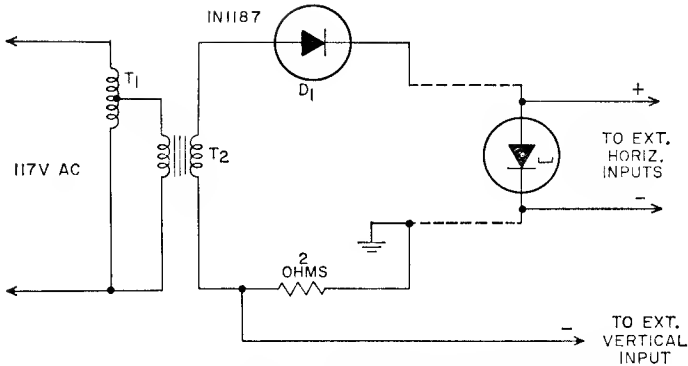
Fig. 120.   High-current adaptor (T_1 is a variable auto-
transformer and T_2 is a 5-volt filament
transformer).

appearing directly across the diode. As a result, all voltage
drops caused by contact resistance and connecting leads are
bypassed. Considerable errors may result in measurement of
peak voltage if the voltage and current leads are not kept
separate. Because most commercial curve tracers measure the
voltage appearing across their front-panel terminals, any ex-
ternal connecting-lead voltage drop appears in series with the
diode being measured and causes large errors at high currents.
All RCA high-current tunnel diodes are measured by applica-
tion of the signal from the voltage leads to the external differ-
ential voltage inputs available on the rear panel of most curve
tracers. This procedure eliminates errors due to lead drops.

The external voltage inputs of most commercial curve
tracers have a fixed sensitivity in the order of 100 millivolts
per dial division. Although this scale is not sensitive enough
to provide accurate measurement of peak voltage, the hori-
zontal-amplifier section of the circuit can be modified to pro-
vide variable gain when the external inputs are used.

Fig. 121a shows the horizontal-amplifier circuit of a con-
ventional curve tracer. As shown, the gain of this amplifier can
be verified by adjustment of switch 4R. However, this switch
is ganged to several other switches in the curve tracer, and
cannot be moved from the "EXT" position when the external
inputs are being used. In the modified circuit of Fig. 121b,
therefore, switch 4R is bypassed when the external inputs are
used, and switch S_1 is added to obtain horizontal sensitivities
of 10, 20, 50 or 100 millivolts per dial division.

An important change in the modified circuit of Fig. 121b
is the relocation of the 60,000-ohm resistor. If this resistor
were to remain in its original location, it would not be con-
nected to the cathode of the tube V354 when S_1 was in the 10,
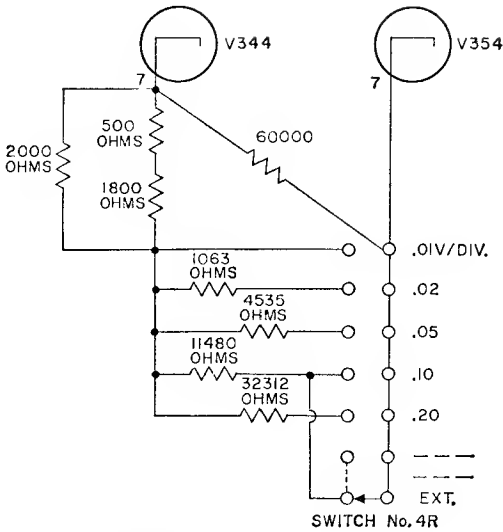
Fig. 121a. Simplified circuit for horizontal amplifier
switching.

20, or 50 millivolt per dial division positions. As a result, er-
rors in the order of five per cent might be introduced.

The entire modification described above does not interfere
with normal operation of the curve tracer, provided switch S_1
is connected in the 0.1 volt per dial division position when the
external inputs are not used.
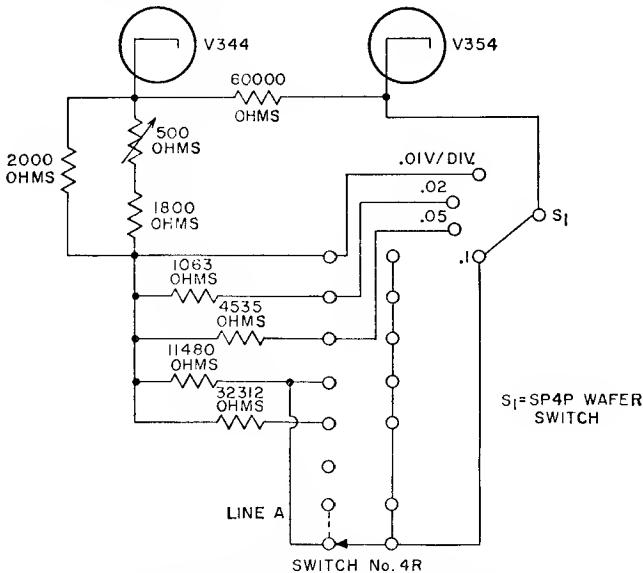
Fig. 121b. Modified circuit for horizontal amplifier
switching.

CAPACITANCE

Junction-capacitance measurements at RCA are made on a Wayne Kerr Model B801 admittance bridge, as shown in Fig. 122. Resistor R_1 is used to develop a bias voltage across the tunnel diode. The "unknown" terminals of the bridge appear as a dc short. Capacitance is measured at the valley point with an accuracy of approximately $\pm$ 0.2 picofarad or $\pm$ 2 per cent, whichever is greater.
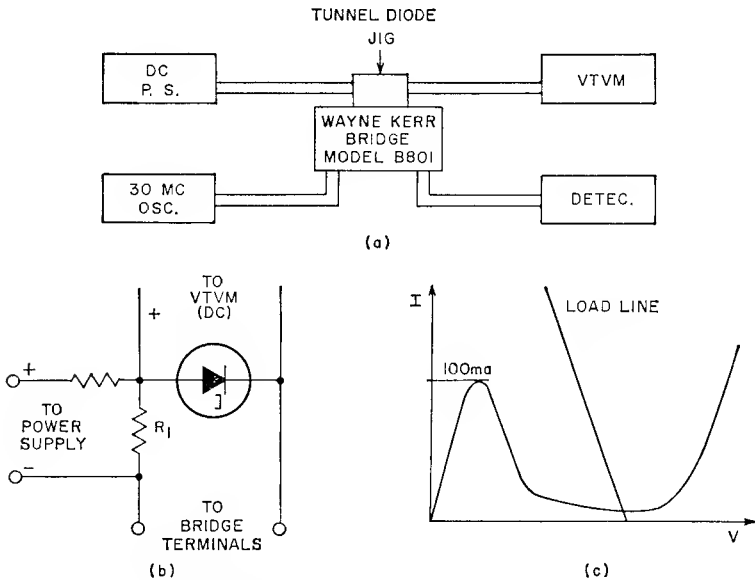
Fig. 122.   (a) Block diagram for capacitance test set, (b) tunnel-diode jig, and (c) required load line.

Operation of the circuit of Fig. 122 is as follows: The power-supply output is increased until the VTVM indicates that the tunnel diode is operating in the valley region. The bridge capacitance dials and the power supply are then successively adjusted until a null is obtained at the valley point. Capacitance is read directly from the bridge dials. The conductance dial is kept at zero during measurement of junction capacitance.

The 30-megacycle measuring signal should be kept as small as possible, preferably under 10 millivolts rms. In addition, the dc supply should be well regulated to minimize ripple. Shielding may be necessary when high-speed units are measured; otherwise, transients may momentarily push the bias point into the negative-resistance region, thus causing oscillations. The loop inductance (R_1 plus diode socket and corrections) should

be made as small as possible.

If it is desired to measure the capacitance of a tunnel diode at points other than in the valley, a rather lengthy procedure must be used. First, the bridge is balanced without any diode in the jig. A shorting strap is then substituted for the diode, and the constant loop impedance is measured. The diode is then inserted, and the admittance of the circuit is measured for various bias voltages. By initial balancing of the bridge at a small positive conductance, the conductance and capacitance in the negative-slope region can be measured, provided the conductance is not too large. From these measurements, the true diode junction capacitance can be computed by means of the following equations:

$$C_j = \frac{L_T + \dfrac{C_B}{G_B{}^2 + \omega^2 C_B{}^2}}{\left(\dfrac{G_B}{G_B{}^2 + \omega^2 C_B{}^2} - R_T\right)^2 + \omega^2 \left(L_T + \dfrac{C_B}{G_B{}^2 + \omega^2 C_B{}^2}\right)^2}$$

(81)

$$g_D = \frac{\dfrac{G_B}{G_B{}^2 + \omega^2 C_B{}^2} - R_T}{\left(\dfrac{G_B}{G_B{}^2 + \omega^2 C_B{}^2} - R_T\right)^2 + \omega^2 \left(L_T + \dfrac{C_B}{G_B{}^2 + \omega^2 C_B{}^2}\right)^2}$$

(82)

where C_J is the true junction capacitance, g_D is the diode conductance, $R_T = R_1 + R_S$; $L_T = L_1 + L_S$, and G_B and C_B are values indicated in Fig. 123.

The impedance $Z_1 = R_1 + j\omega L_1$ is the impedance measured when the diode holder is shorted. Fig. 123 shows the variation
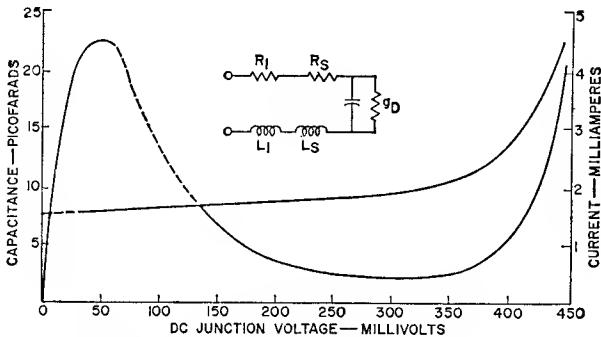
Fig. 123.   Capacitance characteristic for five-milli-ampere tunnel diode.

in capacitance as a function of bias voltage for a five-milli-ampere tunnel diode.

PRECISION MEASUREMENTS

The conventional curve-tracer methods for the measurement of parameters I_P, V_P, I_V, V_V and V_F are simple and rapid, but are not accurate enough for all applications. Better than one per cent accuracy on a curve tracer is almost impossible even if perfect calibration is assumed. Because RCA produces tunnel diodes having a ± 1-per-cent tolerance on peak current, a method more accurate than that of the curve tracer is necessary. This required accuracy is provided by the circuit shown in Fig. 124a. This method was selected for several reasons: (1.) the diode can be stably biased at the peak; (2.) the circuit is not transient or noise-sensitive; (3.) the use of a digital voltmeter for display of the measured parameter reduces the chances of operator error; and, (4.) both peak current and peak voltage are easily measured.

Resistors R_1 and R_2 form a low-inductance monostable load-line for the tunnel diode, as shown in Fig. 124b. The amplifier A' senses the voltage across R_2, amplifies it, inverts it, and feeds it back through R_3. The current generated by this process thus cancels out the current originally flowing in R_2. When the voltage across R_2 drops to zero (ideally), all current flowing through the tunnel diode is diverted through precision resistor R_3 to ground. Therefore, when switch S_1 is in the peak-current position, the digital voltmeter monitors the voltage across R_3 and provides a direct indication of diode current. For measurement of peak current, the power-supply voltage is increased until the diode current reaches a maximum peak. Valley current is measured by continued increase of power-supply voltage until minimum diode current is obtained. When the switch S_1 is placed in the peak-voltage position, the digital voltmeter B' provides a direct indication of diode voltage. Both peak voltage and valley voltage can then be measured by adjustment of the power supply.

With this circuit, accuracies to 0.1 per cent can be achieved. Short-term repeatibility of results is better than ± 0.1 per cent. The sensitivity of the system is sufficient to detect the small changes in tunnel-diode parameters caused by normal variations in room temperature from day to day. Factors affecting accuracy include the tolerance of precision resistor R_3, the voltmeter accuracy, the null voltage across R_2, and the type of jig used to hold the diode.

(a)

(b)
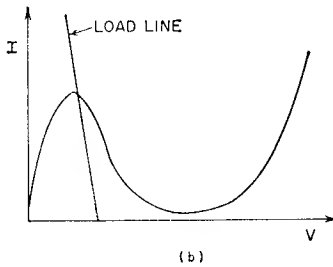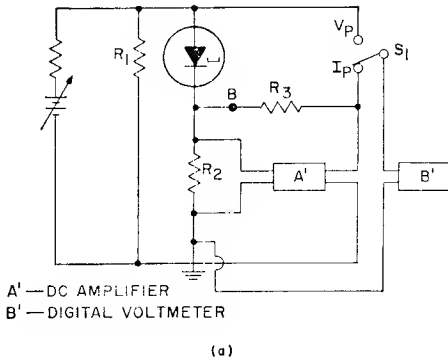
Fig. 124.   (a) Precision measurement circuit, and (b)
tunnel-diode load line.

In the test circuit shown in Fig. 124a, the precision re-
sistor R_3 has a tolerance of 0.01 per cent. The digital volt-
meter B′, which is a four-digit high-speed semiconductor type,
has an accuracy of 0.01 per cent. The voltage across resistor
R_2, which was measured to be less than 20 millivolts, corre-
sponds to an error of less than 0.04 per cent for a 50-milli-
ampere diode. The possible stray potential differences caused
by the contact of two dissimilar metals in the amplifier input
leads may be another source of error.

The type of diode holder or jig required depends upon
individual needs. A jig for use by circuit design engineers need
not be as elaborate as one for production usage. Examples of
RCA holding jigs are shown in Fig. 125. Any holder (together

with resistors R_1 and R_2) meeting the following requirements is satisfactory, provided R_1 has adequate power-handling capacity. First, the sum of resistances R_1 and R_2 and the tunnel-diode series resistance R_s must be less than the absolute value

(a)

(b)
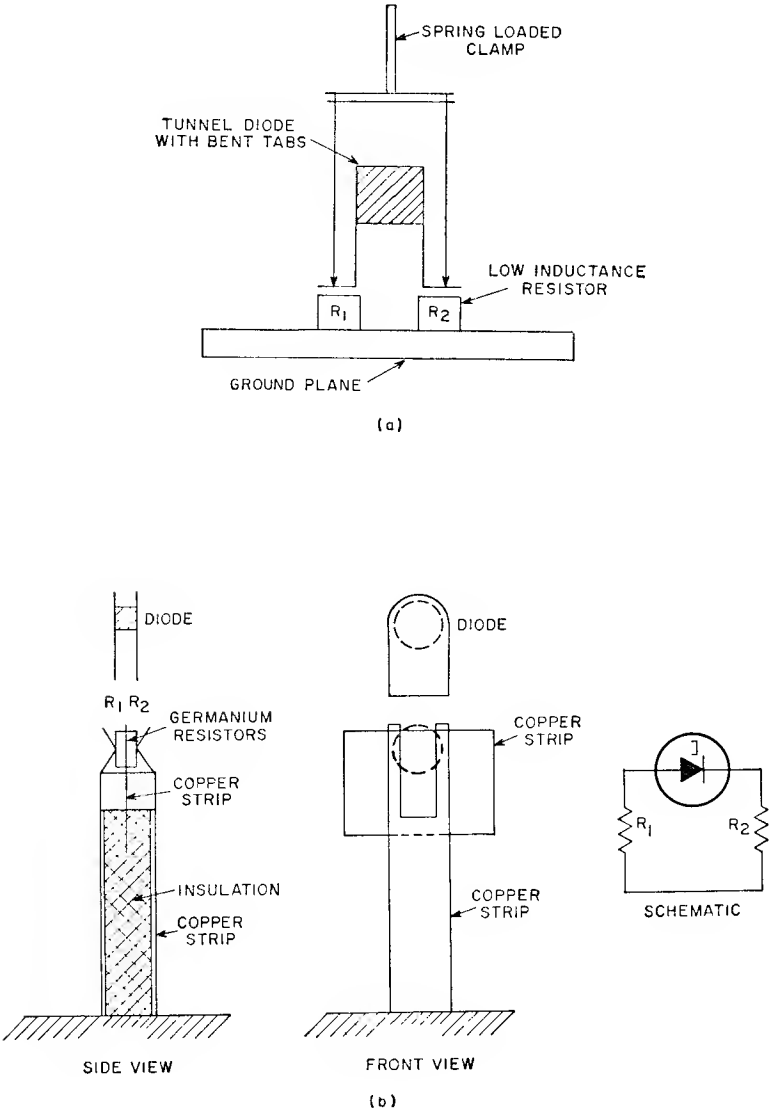
Fig. 125. Typical tunnel-diode holders.

of the negative resistance, or

$$R_T = R_1 + R_2 + R_S \leq |R_j| \qquad (83)$$

Second, the total inductance L_T presented to the diode must be kept below the following limit:

$$L_T \leq R_T \times |R_j| \times (C_j) \qquad (84)$$

Third, the holder for the tunnel diode must not grip the unit in any way which would cause excessive pressure to be applied to the tunneling junction. Finally, the amplifier input leads must be kept separate from the current-carrying leads. If this precaution is not observed, considerable errors may result. For example, it is not permissible to connect the amplifier input lead to point B of Fig. 125a instead of point A.

The conditions of Eqs. (83) and (84) represent the stability criteria for a tunnel diode. For high-current units, the second requirement is often impossible to meet. However, if the total inductance is kept to an extremely low value, even 50-milliampere low-capacitance units (I_p/C_j greater than or equal to 5:1) can be stabilized slightly past the peak of the diode characteristic.

In both holders shown in Fig. 125, resistors R_1 and R_2 are small cubes of germanium, because conventional carbon resistors are too inductive for this application. However, low-inductance resistors, such as carbon-disc resistors, may also be used in place of the germanium cubes. Both holders accept the RCA tunnel-diode package shown in Fig. 8 in the first section on Theory. The holder in Fig. 125a requires bending of the package tabs; the one shown in Fig. 125b receives straight tabs.

Although forward voltage could be measured with the test circuit shown in Fig. 124, it is much easier and quicker to measure this parameter with the circuit shown in Fig. 126. This circuit consists of a constant-current supply and a digital voltmeter.
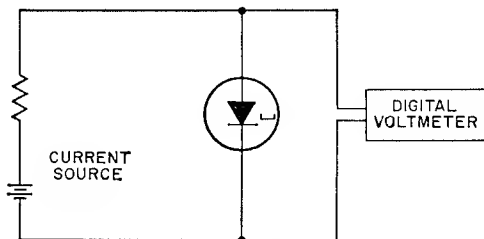
Fig. 126.   Forward-voltage measuring circuit.

OTHER METHODS FOR MEASURING PEAK CURRENT

The method shown in Fig. 127 uses a precision ammeter in series with the tunnel diode. Resistor R_2 stabilizes the diode to prevent switching. This method is not suitable for high-speed units because the ammeter inductance makes it very difficult to stabilize the unit at the peak. Noise from the power supply, or rf pickup, tends to push the bias point slightly into the negative-resistance region. If the inductance in series with the diode is not small enough to meet the stability requirements, then oscillations occur in the negative-resistance region.
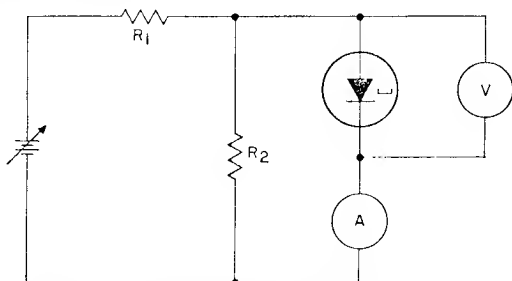
Fig. 127. Peak-current measuring circuit using ammeter in series.

Fig. 128 shows another method for measuring peak current. In this method pulses of current are used to switch the diode. The peak current equals the pulse current (ideally) when the pulse current is increased until the diode is just barely switching, as observed on the scope. However, there are two disadvantages to this method. First, random noise may switch the diode prematurely, and secondly, it is very difficult to measure either peak or valley voltage. In addition to these disadvantages, a method is needed for measuring the input-pulse amplitude to an accuracy of ± 0.1 per cent.
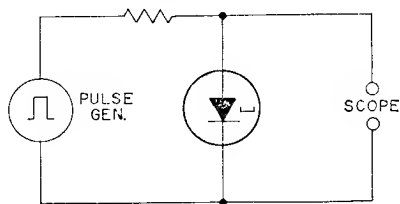
Fig. 128. Peak-current measuring circuit using pulse generator.

The third method, shown in Fig. 129, is similar to that of Fig. 128 except that a rectified 60-cps sine wave is used to drive the diode past the peak on a load-line. The peak-reading digital voltmeter registers the maximum current passed through the diode (peak current). This method has the same two disadvantages of the method shown in Fig. 128, but offers a rapid method for measuring peak current.
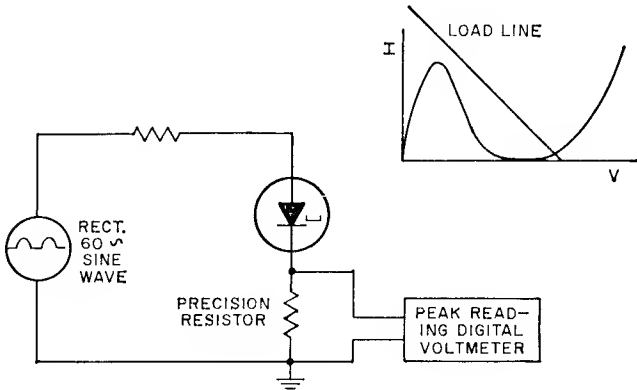
Fig. 129.   Peak-current measuring circuit using 60 cps sine wave.

The fourth method, shown in Fig. 130, is similar to the method of Fig. 124a except that the amplifier feedback loop is omitted. In this circuit, the voltage across resistor R_2 is in direct proportion to the current flowing through the diode. Provided the resistance of R_2 is accurately determined, the peak-current reading may be obtained by "peaking" this voltage. However, it is very difficult to obtain a non-inductive temperature-stable one-ohm resistor having a tolerance of
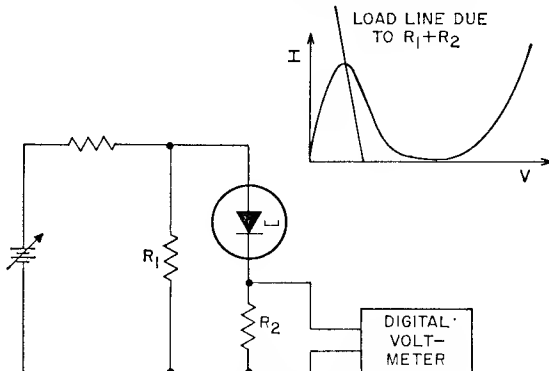
Fig. 130.   Peak-current measuring circuit.

±0.1 per cent. It is desirable to use a resistance of exactly one ohm for R_2 and thus avoid a cumbersome conversion factor when the digital voltmeter is read. Another problem with this circuit involves accurate measurement of the low voltage appearing across resistor R_2.

SERIES RESISTANCE

The series resistance of tunnel diodes is normally measured by the curve-tracer method because close accuracy is not required. The tunnel diode is swept out to 200 milliamperes in the reverse direction. The slope of the characteristic between the 100- and 200-milliampere intercepts is considered to be the series resistance for a 50-milliampere unit; lower-peak-current units require lower-current intercepts which are determined by the maximum current ratings of the units ($1.4 \times dc_{max} = ac_{peak}$). In this region, the reverse characteristic is approximately linear.

Series resistance of tunnel rectifiers may also be measured by this technique. However, it may be advisable to measure the slope between the 50- and 100-milliampere points (or lower) to prevent damage to the units.

Some tunnel-rectifier data do not specify series resistance but instead give a voltage maximum for a given current. This information is more useful in nonlinear (switching) applications than data on series resistance. Conversely, for linear (amplifier, oscillator) applications, series resistance is the more useful parameter.

Several other methods for the measurement of series resistance have been proposed. The method shown in Fig. 131 uses the Wheatstone bridge principle.[48] (In this circuit, line
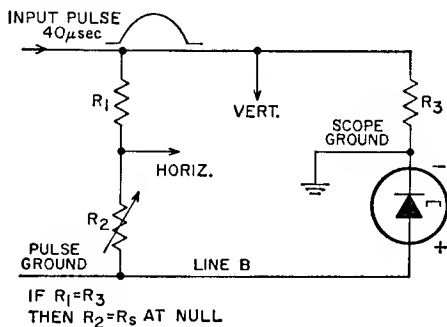
Fig. 131.   Series-resistance measuring circuit.

B should be grounded and differential scope units used to simu-
late the scope ground indicated.) The diode is inserted into
one arm of the bridge and a pulse is applied to the bridge.
When resistor R_2 equals the series resistance at a given bias
current, the trace on the scope becomes vertical (perpendicular
to the x-axis) at that bias point, as shown by Fig. 132. Be-
cause this method tests diodes at larger reverse currents than
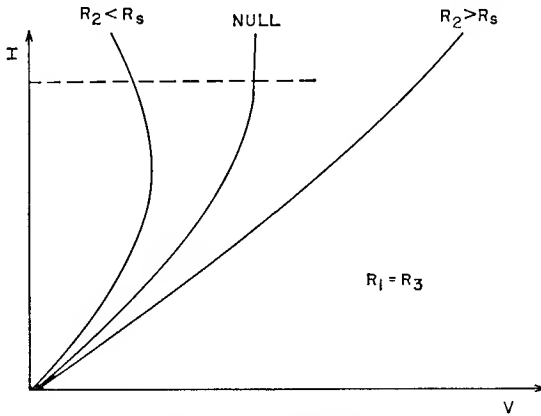
Fig. 132.   Scope display.

possible with steady-state methods, the value of series re-
sistance read is lower and closer to the true value than that
obtained with the previous method.

Another method is to apply a large pulse of current and
a low-level sine wave to the diode simultaneously. The pulse
serves to bias the unit at a large reverse current; the ratio of
the superimposed ac-signal voltage to the ac current is the
series resistance at this bias level.

INDUCTANCE

The inductance of a tunnel diode is a difficult electrical
parameter to measure, primarily because it is so small. As a
result, it is necessary to use microwave frequencies to measure
the inductance of the diode. Fig. 133 shows the test setup
used. All connecting cables have a characteristic impedance of
50 ohms, except for the four-ohm line in the dc branch of the
circuit. This low-impedance line is used to filter out high-
frequency disturbances which may pass down from the rf
stages. The variable delay line is adjusted to present an open
circuit to rf current from the signal generator. The dc block-
ing capacitor prevents dc from flowing in the rf signal genera-
tor. The VSWR meter is tuned to one kilocycle to pick up the

modulating signal generated by the square-wave generator. The dc power supply is used to bias the tunnel diode in its valley region where the junction capacitance of the tunnel diode is known and the dynamic conductance of the tunnel diode is approximately zero.
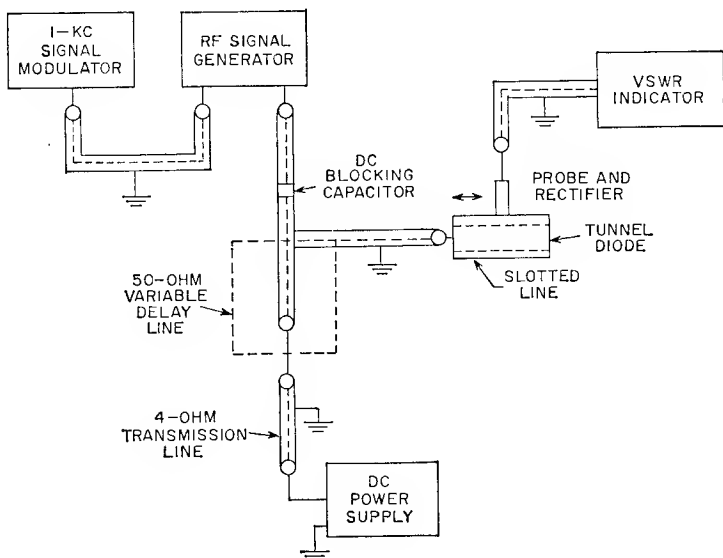
Fig. 133.   Test setup for measuring inductance.

The inductance is determined from the VSWR of a tunnel diode, the shift away from a short-circuit reference null, and a Smith chart. By means of the equivalent circuit for tunnel diodes, the input impedance Z of the device is found to be

$$Z \,=\, R_s \,+\, \frac{g_D}{g_D{}^2 \,+\, \omega^2 C_j{}^2} \,+\, j \left[\omega L_s \,-\, \frac{\omega C_j}{g_D{}^2 \,+\, \omega^2 C_j{}^2} \right] \quad (85)$$

Under valley-region bias conditions, g_D becomes approximately zero and Eq. (85) becomes

$$Z \,=\, R_s \,+\, j \left[\omega L_s \,-\, \frac{1}{\omega C_j} \right] \,=\, R_s \,+\, jX \qquad (86)$$

The value of X is obtained from the previously mentioned Smith chart. Because the diode capacitance is known accurately in the valley region, the term $1/\omega C_j$ can be computed and added to X to determine ωL_s. When ωL_s is known, L_s can be determined. For the dynamic conductance in the valley to remain

essentially zero, a small rf signal must be used to drive the
tunnel diode. In these tests, a peak-to-peak amplitude of five
millivolts is used. With this signal level, the VSWR indicator
must be operated in its most sensitive range. At this sensitivity,
the background noise level makes it difficult to locate the null
and peak of the standing wave. A typical tunnel diode VSWR
is about 32 decibels. Another area of difficulty is the connec-
tion of the tunnel diode to the slotted line. The repeatability
of measurements is only about 20 per cent.

Typical value of the inductance measured for the RCA
standard packages is in the order of 0.4 nanohenry.

SWITCHING SPEED

The switching speed, or rise time, of a tunnel diode is
directly proportional to the ratio between the peak current I_p
and the junction capacitance C_j. This "speed ratio" may vary
from about 0.005 to 10.0 or more, depending upon the type of
diode. RCA tunneling devices shown in this manual have
speed ratios in the range from 0.1 to 10.0 or more. An appro-
priate "rule of thumb" which relates rise time to the "speed
ratio" is that a speed ratio of 0.5 results in a rise time of ap-
proximately one nanosecond for a germanium tunnel diode, or
two nanoseconds for a gallium arsenide diode. A more accurate
estimate of rise time t_r may be obtained from the following
equation:

$$t_r = C_j \left(\frac{V_F - V_P}{I_P - I_V} \right) \tag{87}$$

Rise time is generally measured on high-frequency sampling
scopes. Conventional scopes lack adequate bandpass, and
"traveling-wave" scopes have insufficient vertical (amplitude)
sensitivity. A convenient circuit for the measurment of rise
times without delay lines is shown in Fig. 134.
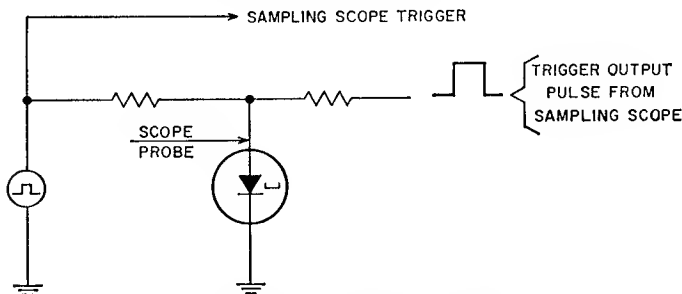
Fig. 134.   Rise-time measurement circuit.

An alternate method for measuring rise time, which is quite useful for multiampere units, is to apply a dc bias of approximately 0.2 volt to the diode. At this bias level, the diode automatically begins to operate as a relaxation oscillator, and has a waveform as shown in Fig. 135. The rise time of these pulses closely approximates the rise time obtained by the pulse method (Fig. 134).

VERTICAL: 0.2 V/DIV.
HORIZONTAL: 10 μSEC/DIV.
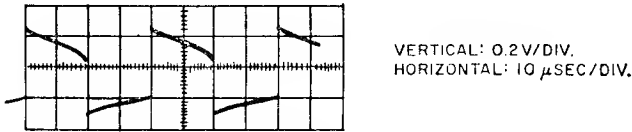
Fig. 135.   Output waveform for ten-ampere tunnel diode operated as relaxation oscillator.

Because most commercially available sampling scopes have a maximum response of approximately 0.4 nanosecond, tunnel diodes having a "speed ratio" greater than 1.0 are difficult to measure directly. For this reason, junction capacitance, rather than rise time, is usually specified on tunnel-diode data sheets. When the capacitance is known, the approximate rise time may be computed.

REFERENCES

48. D. S. Cleverly, "Proposal for the Measurement of Tunnel-Diode Series Resistance", JEDEC Committee, JS-9.
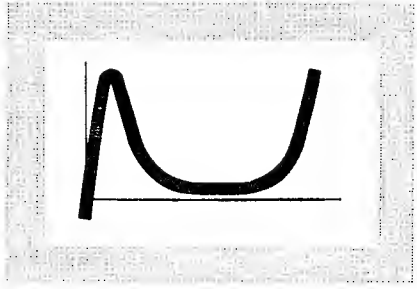
TECHNICAL
DATA

In addition to the devices listed in the following charts, RCA can supply a wide range of tunneling devices to meet customer specifications. These devices include germanium and gallium arsenide tunnel diodes for switching applications with rise times less than 50 picoseconds, tunnel diodes for microwave power generation and amplification with cutoff frequencies well above X-band, very-high-current tunnel diodes for power conversion, and also tunnel rectifiers and tunnel resistors.

For developmental data sheets and for information about these devices, contact your RCA local representative or the Special Products Department, RCA Semiconductor and Materials Division, Somerville, N. J.

M A X I M U M   R A T I N G S (at 25°C Free-air Temperature)

TUNNEL DIODES

Type	Material	Out-line	DC Current (ma) Forward	Reverse	Dissipation[1] (mw)	Ambient Temperature (°C) Range Operating and Storage	Lead Temperature (3 seconds maximum)
1N3128	Ge	1	40	70	20	−35 to 100	175
1N3129	Ge	1	55	85	30	−35 to 100	175
1N3130	Ge	1	70	100	40	−35 to 100	175
1N3847	Ge	1	10	15	5	−35 to 100	175
1N3848	Ge	1	18	25	10	−35 to 100	175
1N3849	Ge	1	35	50	20	−35 to 100	175
1N3850	Ge	1	85	125	50	−35 to 100	175
1N3851	Ge	1	170	250	100	−35 to 100	175
1N3852	Ge	1	10	15	5	−35 to 100	175
1N3853	Ge	1	18	25	10	−35 to 100	175
1N3854	Ge	1	35	50	20	−35 to 100	175
1N3855	Ge	1	85	125	50	−35 to 100	175
1N3856	Ge	1	170	250	100	−35 to 100	175
1N3857	Ge	1	10	15	5	−35 to 100	175
1N3858	Ge	1	18	25	10	−35 to 100	175
1N3859	Ge	1	35	50	20	−35 to 100	175
1N3860	Ge	1	85	125	50	−35 to 100	175
TUNNEL RECTIFIERS							
1N3861	Ge	2	10	30	10	−35 to 100	175
1N3862	Ge	2	10	30	10	−35 to 100	175
1N3863	Ge	2	10	30	10	−35 to 100	175

[1] Above 25°C, derate linearly to 0 mw at 100°C.

ELECTRICAL CHARACTERISTICS (at 25°C Free-air Temperature)

TUNNEL DIODES

Type	I_P (ma)	I_v (ma) max	I_P/I_v min	V_P (mv)	V_v (mv) min	V_F' (mv)	C'' (pf) max	R_s (ohms) max	t_r (psec) max	t_r (psec) typ.
1N3128	4.75-5.25	0.6	8/1	40- 80	280	445-530	15	3	5000	1000
1N3129	19-21	2.4	8/1	50-100	300	475-575	20	2.5	2000	300
1N3130	47.5-52.5	6	8/1	70-120	350	520-620	25	1.5	500	160
1N3847	4.5-5.5	0.75	6/1	—	—	430-590	25	3	—	1800
1N3848	9-11	1.5	6/1	—	—	440-600	25	2.5	—	900
1N3849	18-22	3	6/1	—	—	460-620	30	2	—	600
1N3850	45-55	7.5	6/1	—	—	530-640	40	1.5	—	350
1N3851	90-110	15	6/1	—	—	540-650	40	1	—	125
1N3852	4.75-5.25	0.6	8/1	50- 90	330	490-560	15	3	—	1200
1N3853	9.5-10.5	1.2	8/1	55- 95	350	510-580	15	2.5	—	600
1N3854	19-21	2.4	8/1	65-105	365	530-600	20	2	—	400
1N3855	47.5-52.5	6	8/1	80-130	380	550-620	25	1.5	—	200
1N3856	95-105	12	8/1	90-140	390	560-630	25	1	—	75
1N3857	4.75-5.25	0.6	8/1	50- 90	330	490-560	8	3	—	600
1N3858	9.5-10.5	1.2	8/1	55- 95	350	510-580	8	2.5	—	300
1N3859	19-21	2.4	8/1	65-105	365	530-600	10	2	—	200
1N3860	47.5-52.5	6	8/1	80-130	380	550-620	12	1.5	—	150

TUNNEL RECTIFIERS

Type	I_P (ma)	C'' (pf) max	V_R (mv) at $I_R = 10$ ma max	V_R (mv) at $I_R = 30$ ma max	V_F (mv) at $I_F = 1$ ma min
1N3861	0.1-1	6	170	—	400
1N3862	0.1-1	4	150	300	420
1N3863	0.1-0.5	4	150	300	435

[2] Includes case capacitance of 0.8 pf. [3] Includes case capacitance of 0.4 pf.

MAXIMUM RATINGS (at 25°C Free-air Temperature)

TUNNEL DIODES

RCA Type	Former Developmental Designation	Material	Outline	DC Current (ma) Forward[4]	Reverse	Ambient Temperature (°C) Range Operating and Storage
40058	TD169	GaAs	3	0.5 ma/pf	250	—30 to 85
40059	TD170	GaAs	3	0.5 ma/pf	250	—30 to 85
40060	TD171	GaAs	3	0.5 ma/pf	100	—30 to 85
40061	TD172	GaAs	3	0.5 ma/pf	100	—30 to 85
40062	TD173	GaAs	3	0.5 ma/pf	50	—30 to 85
40063	TD174	GaAs	3	0.5 ma/pf	50	—30 to 85
40064	TD175	GaAs	3	0.5 ma/pf	25	—30 to 85
40065	TD176	GaAs	3	0.5 ma/pf	25	—30 to 85
40076	TD219	GaAs	4	0.5 ma/pf	400	—30 to 85
40077	TD213	Ge	3	1.6	2.5	—30 to 85
40078	TD211	Ge	3	1.6	2.5	—30 to 85

HIGH-CURRENT TUNNEL DIODES

RCA Type	Former Developmental Designation	Material	Outline	Dissipation[5] (watts)	Ambient Temperature (°C) Range Operating and Storage
40066	TD189	Ge	5	0.5	—55 to 85
40067	TD190	Ge	5	1.7	—55 to 85
40068	TD191	Ge	6	3.5	—55 to 85
40069	TD192	Ge	6	7.0	—55 to 85
40070	TD225	Ge	7	30.0	—55 to 85
40079	TD236	GaAs	7	50.0	—55 to 85

4 Above 25°C ambient, derate linearly to valley current at 75°C.
5 Measured at 25°C case temperature; derate linearly to 0 watt at 85°C.

ELECTRICAL CHARACTERISTICS (at 25°C Free-air Temperature)
TUNNEL DIODES

Type	I_P (ma)	I_v (ma) max	I_P/I_v min	V_P (mv) max	V_v (mv) min typ	V_F' (mv) min	V_F' (mv) max	$C^{a,7}$ (pf) max	R_s (ohms) max	t_r (psecs) max	t_r (psecs) typ	f_{ro} (kmc) typ
40058	47.5-52.5	—	12/1	200	500-570	1050	—	20	3	500	333	5
40059	45-55	—	10/1	200	450-570	1080	—	40	2.5	1000	667	—
40060	19-21	—	11/1	180	500-570	1000	—	15	8	1000	600	3
40061	18-22	—	9/1	180	450-530	900	—	30	5	2000	1250	—
40062	9.5-10.5	—	10/1	180	500-570	1000	—	10	9	1250	1000	2
40063	9-11	—	8/1	180	450-530	900	—	25	5	3000	2000	—
40064	4.75-5.25	—	8/1	170	560-550	950	—	8	18	2000	1250	1.2
40065	4.5-5.5	—	7/1	170	420-520	900	—	20	12	6000	3000	—
40076	180-220	—	15/1	240(typ)	— 600	—	—	25	0.9	—	—	8
40077	0.9-1.1	.15	6/1	60(typ)	— 335	—	550	5	6	—	—	6
40078	0.9-1.1	.18	5/1	60(typ)	— 330	400	550	10	4	—	—	—

HIGH-CURRENT TUNNEL DIODES

Type	I_P (amp)	I_P/I_v min	V_P (mv) max	V_v (mv) min	V_F' (mv) min	C (μfd) typ	R_s (ohms) typ	t_r (nsec) typ	R_1 (ohms) typ
40066	.9-1.1	8/1	125	300	490	.002	.055	1	.12
40067	4.5-5.5	8/1	130	300	490	.016	.014	1.5	.024
40068	9.0-11.0	8/1	130	300	490	.045	.007	2	.012
40069	18-22	8/1	130	300	490	.090	.0035	2	.006
40070	90-110	8/1	130	300	430	.5	.0006	2	.0012
40079	180-220	10/1	180	550	—	1.25	.0002	4	.001

6 $C_i = C - 0.8$ pf.

7 Actual recorded capacitance readings are provided with each diode.

TUNNEL RECTIFIERS

MAXIMUM RATINGS (at 25°C Free-air Temperature)

RCA Type	Former Developmental Designation	Material	Outline	DC Current (ma) Forward	Reverse	Ambient Temperature (°C) Range Operating and Storage
40054	TD177	GaAs	3	0.5 ma/pf	15	−30 to 85
40055	TD178	GaAs	3	0.5 ma/pf	15	−30 to 85
40056	TD216	GaAs	3	0.5 ma/pf	15	−30 to 85
40057	TD217	GaAs	3	0.5 ma/pf	15	−30 to 85

ELECTRICAL CHARACTERISTICS (at 25°C Free-air Temperature)

RCA Type	I_P (max mv)	V_F (mv) at 1 ma min	V_R (mv) at 5 ma max	V_R (mv) at 10 ma max	C[8,9] (max pf)
40054	1	950	200	300	6
40055	0.5	950	250	350	6
40056	1	950	160	225	6
40057	0.5	950	180	275	6

[8] $Cj = C - 0.8$ pf.

[9] Actual recorded capacitance readings are provided with each diode.

— OUTLINES —
All dimensions in inches
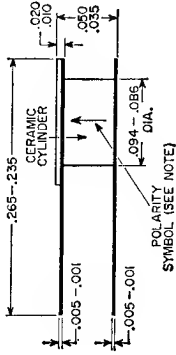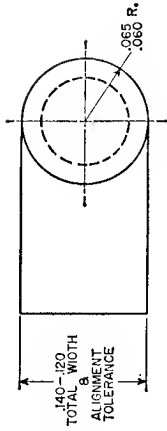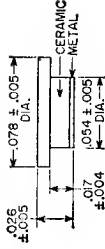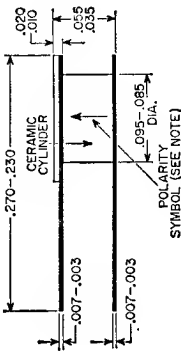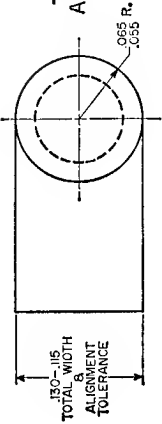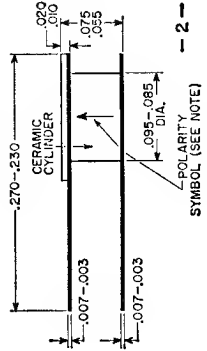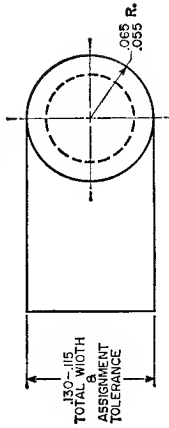
Note: Arrow shows the direction of forward current flow as indicated by dc ammeter.
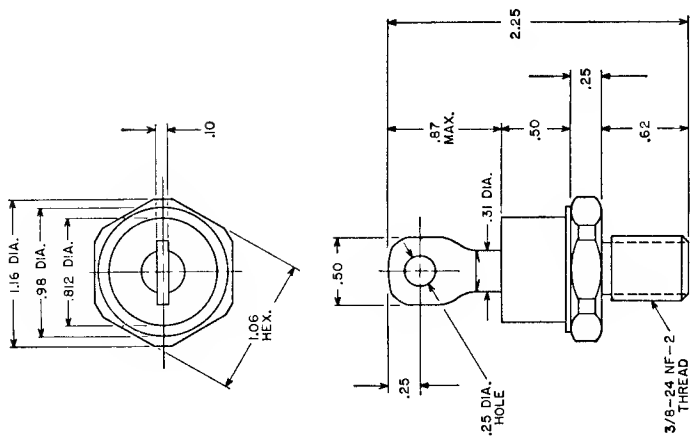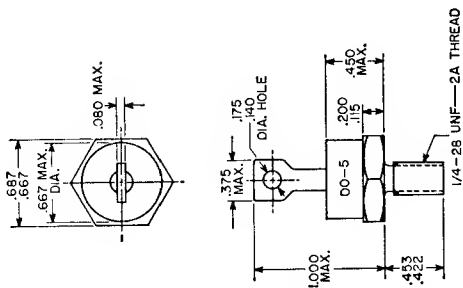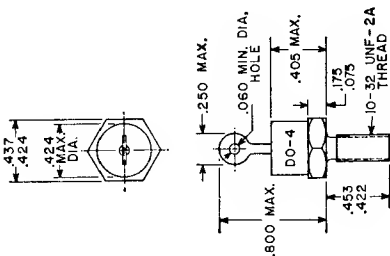
DEFINITIONS

The following terms and symbols are, for the most part, defined with respect to either the tunnel diode characteristic curve or the equivalent circuit shown below.
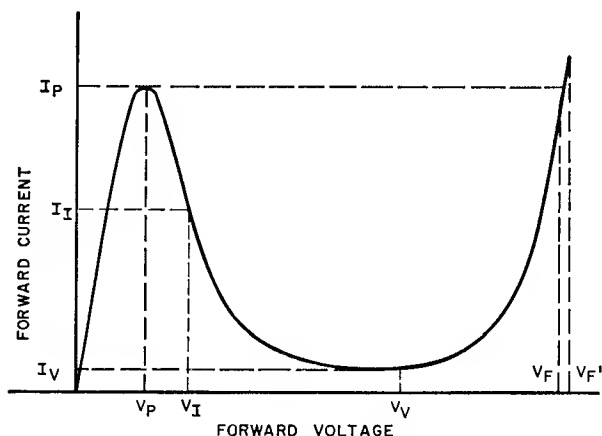
Static forward characteristic of tunnel diode.
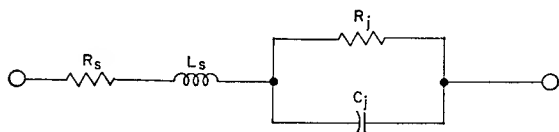
Equivalent circuit of tunnel diode.

Fall time (t_r)—The time required for the tunnel diode to switch from a high-voltage state to a low-voltage state.

Figure-of-merit frequency (f_c)—The frequency equal to the reciprocal of $2\pi R_{min} C_j$ at a specified bias in the negative-resistance region.

Forward voltage point (V_F')—The forward voltage, greater than peak voltage, for which the current is equal to the maximum peak current.

Junction capacitance (C_j)—The small-signal capacitance associated with the pn junction alone at a specified bias and frequency.

Junction resistance (R_j)—The incremental resistance reduced by the series resistance of the diode, or $dV/dI - R_s$.

Incremental resistance (dV/dI)—The reciprocal of the slope of the current-voltage characteristic.

Inflection point current (I_i)—The current corresponding to the inflection point voltage on the static characteristic curve.

Inflection point voltage (V_i)—The voltage at which the slope of the current-voltage characteristic reaches its most negative value.

Peak current (I_p)—The current at which the slope of the current-voltage characteristic changes from positive to negative as the forward voltage is increased.

Peak voltage (V_p)—The voltage at which the peak current occurs.

Resistive cutoff frequency (f_{ro})—The frequency at which the diode no longer exhibits negative resistance for a specified bias. This frequency is equal to

$$f_{ro} = \frac{1}{2\pi R_j C_j} \sqrt{\frac{R_j}{R_s} - 1}$$

Rise time (t_r)—The time required for the tunnel diode to switch from a low-voltage state to a high-voltage state.

Self-resonant frequency (f_{xo})—The frequency below which the reactance of the diode is capacitive; above this frequency, the reactance is inductive. This frequency is equal to

$$f_{xo} = \frac{1}{2\pi R_j C_j} \sqrt{\frac{R_j^2 C_j}{L_s} - 1}$$

Series inductance (L_s)—The self-inductance of a diode in a specified circuit configuration.

Series resistance (R_s)—That portion of the small-signal terminal resistance of a pn-junction diode which is external to the junction.

Speed index $(I_p : C_j)$—The ratio of the peak current to the junction capacitance. This index determines the speed capability of the device.

Valley current (I_v)—The current at which the slope of the current-voltage characteristic changes from negative to positive as the forward voltage is increased.

Valley voltage (V_v)—The voltage at which valley current occurs.

INDEX

RCA TECHNICAL PUBLICATIONS

Semiconductor Products

RCA SEMICONDUCTOR PRODUCTS HANDBOOK—HB-10. Two binders, each 7⅜″ L x 5⅝″ W x 2⅞″ D. Contains over 1000 pages of loose-leaf data and curves on RCA semiconductor devices such as transistors, silicon rectifiers, and semiconductor diodes. Available on a subscription basis. Price $10.00 including service for first year. (Also available with RCA Electron Tube Handbook HB-3 at special combination price of $25.00)

RCA TRANSISTOR MANUAL—SC-10 (8⅜″ x 5⅜″)—304 pages. New manual contains detailed technical data on RCA semiconductor devices. Easy-to-read text contains information on basic theory, application, and installation of transistors, silicon rectifiers, and semiconductor diodes. Includes circuit diagrams and parts lists for many typical applications. Features lie-flat binding. Price $1.50.

RCA SEMICONDUCTOR PRODUCTS GUIDE—60S16R4 (10⅞″ x 8⅜″)—12 pages. Contains classification chart, index, and ratings and characteristics on RCA's line of transistors, silicon rectifiers, semiconductor diodes, and photocells. Single copy free on request.

RCA SILICON POWER TRANSISTORS APPLICATION GUIDE —1CE-215 (10⅞″ x 8⅜″)—28 pages. Describes outstanding features of RCA silicon power transistors and their use in many critical industrial and military applications. Includes construction details, discussion of voltage ratings, thermal stability conditions, and equivalent circuits for power transistors. Price 50 cents.

RCA SILICON VHF TRANSISTORS APPLICATIONS GUIDE —1CE-228 (10⅞″ x 8⅜″)—20 pages. Describes unique capabilities of RCA silicon vhf transistors and their use in critical industrial and military applications up to 300 megacycles. Price 50 cents.

TRANSISTORIZED VOLTAGE REGULATORS APPLICATION GUIDE—1CE-254 (10⅞″ x 8⅜″)—12 pages. Describes and discusses transistorized voltage regulators of the series and

shunt types. Included are design considerations, step-by-step design procedures, and the solutions to sample design problems. An Appendix contains the derivations of design equations. Price 25 cents.

TECHNICAL BULLETINS—Authorized information on RCA semiconductor products. Bulletins contain characteristics and performance curves. Be sure to mention transistor or rectifier type desired. Single copy on any type free on request.

RCA TRANSISTOR REPLACEMENT GUIDE—1L1115—36 pages. Listing of RCA transistors and semiconductor diodes intended to serve as replacements in entertainment-type electronic equipment. This booklet includes replacement information on more than 1000 models of portable and table radio receivers, tape recorders, and portable equipment of 145 domestic and foreign manufacturers. Price 35 cents.

RCA SILICON RECTIFIER INTERCHANGEABILITY GUIDE —1CE-229A—16 pages. Lists RCA silicon rectifier replacements for a majority of industry types. The guide also includes a list of 125-milliampere selenium rectifiers and the RCA single-ended T0-1-case silicon rectifiers which can be used as replacements for these types. Price 25 cents.

Electron Tubes

RCA ELECTRON TUBE HANDBOOK—HB-3 ($7\frac{3}{8}''$ x $5\frac{5}{8}''$). Five $2\frac{1}{4}$-inch-capacity binders. Contains over 5000 pages of looseleaf data and curves on RCA receiving tubes, transmitting tubes, cathode-ray tubes, picture tubes, photocells, phototubes, camera tubes, ignitrons, vacuum gas rectifiers, traveling-wave tubes, premium tubes, pencil tubes, and other miscellaneous types for special applications. Available on subscription basis. Price $20.00 including service for first year. Also available with RCA Semiconductor Products Handbook HB-10 at special combination price of $25.00.

RCA RECEIVING TUBE MANUAL—RC-21 ($8\frac{1}{4}''$ x $5\frac{3}{8}''$)— 480 pages. Contains technical data on 903 receiving tubes and 106 picture tubes for black-and-white and color television. Features tube theory written for the layman, application data for radio and television circuits, new receiving-tube and picture-charts, and several circuits for high-fidelity audio amplifiers. Features lie-flat binding. Price $1.00.

RCA TRANSMITTING TUBES—TT-5 ($8\frac{1}{4}''$ x $5\frac{3}{8}''$)—320 pages. Gives data on over 180 power tubes having plate-input ratings up to 4 kw and on associated rectifier tubes. Provides basic information on generic types, parts and materials, installation and application, and interpretation of data. Contains circuit diagrams for transmitting and industrial applications. Features lie-flat binding. Price $1.00.

RADIOTRON DESIGNER'S HANDBOOK—4th Edition (8¾" x 5½")—1500 pages. Comprehensive reference covering the design of radio and audio circuits and equipment. Written for the design engineer, student, and experimenter. Contains 1000 illustrations, 2500 references, and cross-referenced index of 7000 entries. Edited by F. Langford-Smith.

Batteries

RCA BATTERY MANUAL—BDG-111 (10⅞" x 8¾")—64 pages. Contains information on dry cells and batteries (carbon zinc (Leclanché), mercury, and alkaline types). Includes battery theory and applications, detailed electrical and mechanical characteristics, a classification chart, dimensional outlines, and terminal connections on each battery type. Price 50 cents.

RCA BATTERIES—BAT-134F—24 pages. Contains new classification charts and data charts on more than 100 RCA battery types, contains interchangeability directory listing RCA replacements for battery types of 11 manufacturers, and a replacement guide giving the RCA battery complement for more than 3000 portable radio models of 300 domestic and foreign manufacturers. Price 35 cents.

RCA BATTERIES FOR TRANSISTOR APPLICATIONS—TBA-107A (10⅞" x 8⅜")—12 pages. Technical data and curves on 25 RCA Leclanché and mercury-type dry batteries designed for use in applications utilizing transistors. Price 25 cents.

Test and Measuring Equipment

INSTRUCTION BOOKLETS—Illustrated instruction booklets, containing specifications, operating and maintenance data, application information, schematic diagrams, and replacement parts lists, are available for all RCA test instruments. Prices for booklets on individual instruments are available on request.

In addition to the tunnel diodes described in this manual, the RCA Semiconductor and Materials Division offers many other semiconductor devices for military, industrial, and consumer applications:

> silicon and germanium transistors
> silicon rectifiers
> silicon controlled rectifiers
> thyristors
> varactor diodes
> magnetic memory components, devices, and systems
> micromodules
> digital microcircuits
> electro-optical devices
>> laser crystals
>> optical diodes
>> laser modulator crystals

Requests for technical information should be addressed to Commercial Engineering, RCA Semiconductor and Materials Division, Somerville, N.J.
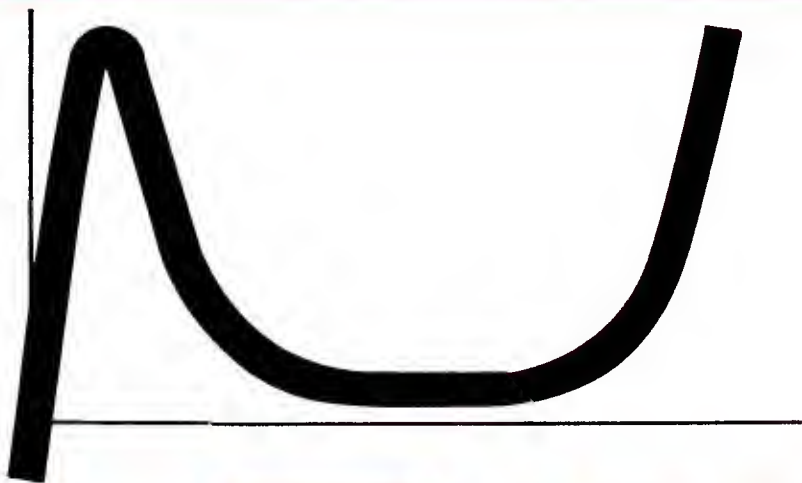
Requests for information on packaged solid-state microwave assemblies, photocells, and other products manufactured by the RCA Electron Tube Division should be addressed to Commercial Engineering, Radio Corporation of America, Harrison, N.J.

Contents
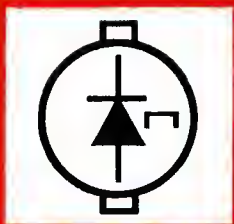
RCA TUNNEL DIODE MANUAL

The RCA Tunnel Diode Manual represents the industry's most up-to-date reference source for tunnel-diode theory and applications. This publication was prepared for circuit designers by RCA device-design and circuit-application engineers. It includes theory, device characteristics, circuit diagrams, and detailed design data on these important new semiconductor devices.